The role of conserved residues in African horsesickness virus protein NS3 in intracellular localisation and cytotoxicity

by

Etienne van de Merwe

Submitted in partial fulfilment of the requirements for the degree
Magister Scientiae

In the Faculty of Natural & Agricultural Science
University of Pretoria
Pretoria

Under supervision of Dr Vida van Staden, and Prof Henk Huismans

2010-11-25

DECLARATION

I, Etienne van de Merwe, declare that the thesis/dissertation, which I hereby submit for the degree *Magister Scientiae* at the University of Pretoria, is my own work and has not previously been submitted by me for a degree at this or any other tertiary institution.

Signature: _____ Date: _____

Etienne van de Merwe

ACKNOWLEDGEMENTS

My Mentor

Dr V. van Staden

My family

Dr. T.J van de Merwe
Dr. C Erasmus
T.J. van de Merwe
C. Y. van de Merwe

My colleagues

R. van der Sluis
A. N. Hall
P. Wege
S. L. Ungerer

My best friend

T. Berelowitz

Aan God
Dankie vir Jou genade en krag

RESEARCH OUTPUTS

Parts of this study have been presented at the following scientific meetings:

Van de Merwe, E., Van der Sluis, R., Meiring, T.L., Hall, A.N., Huismans, H., Van Staden, V. 2008. Conserved residues in nonstructural protein NS3 of African Horsesickness Virus influence subcellular localisation. Microscopy Society Southern Africa Congress 2008, 23-25 July 2008, Gaborone, Botswana.
(*Leica* Systems Prize for Best Presentation Confocal Microscopy)

Van der Sluis, R., Van de Merwe, E., , Hall, A.N., Huismans, H., Van Staden, V. 2008. The role of conserved residues in the transmembrane domains and flanking regions of AHSV nonstructural protein NS3. 20th South African Genetics Symposium 2008. 27 - 29 March 2008, Pretoria, South Africa.

Ungerer, S. L., Van de Merwe, E., Hall, A.N., Huismans, H., Van Staden, V. 2009. Using eGFP for investigating the subcellular localisation of African Horsesickness virus non-structural protein NS3. Microscopy Society Southern Africa Congress 2009, Durban, South Africa.
(*Leica* Systems Prize for Best Presentation Confocal Microscopy)

Huismans, H., Ungerer, S. L., Van de Merwe, E., Van Staden, V., 2009. Localisation and trafficking of recombinant baculovirus expressed African horsesickness virus nonstructural protein NS3. 10th International Symposium on Double-Stranded RNA Viruses 2009. 21 – 25 June 2009, Hamilton Island, Great Barrier Reef, Australia.

Van de Merwe, E., Hall, A.N., Huismans, H., Van Staden V. 2010. AHSV non-structural protein NS3 associated intranuclear bodies; a possible role in eliciting cytotoxicity. 21th South African Genetics Symposium 2010, 9 – 10 April 2010, Bloemfontein, South Africa.

SUMMARY

Project title: The role of conserved residues in African horsesickness virus protein NS3 in intracellular localisation and cytotoxicity

Student: Etienne van de Merwe

Supervisor: Dr. V. van Staden
Department of Genetics
University of Pretoria
Pretoria

Co-supervisor: Prof. H. Huismans
Department of Genetics
University of Pretoria
Pretoria

For the degree: *Magister Scientiae*

The role of the non-structural protein NS3 in the viral life cycle of African horsesickness virus (AHSV) is an active area of research. It has been shown to be involved in the lytic and non-lytic mechanisms of viral release. How the NS3 protein acts in the lytic release of viral progeny has not yet been clarified. When expressed in a baculovirus system in insect cells the protein causes cell lysis. This phenomenon could be related to the lytic activity of the NS3 protein that facilitates viral release. It has been proposed that the AHSV NS3 protein may function as a viroporin at the plasma membrane causing damage and in this way facilitates viral release.

Several residues of unknown function had been identified previously that are highly conserved in the NS3 protein of AHSV and the cognate proteins of other closely related viruses. The nature and characteristics of these residues and the motifs, which they resemble, were predicted to be important in protein folding and protein-protein interaction. Thus, they may be required for the function of NS3 and possibly for the viroporin-like activity of NS3. This study set out to characterise the functions of these residues by mutational studies.

Targets for mutation were selected and mutations were designed that involved either the hydrophobic domain 1 (HD1), hydrophobic domain 2 (HD2) or the intervening spacer region (ISR). Eight mutant constructs were produced during the course of this project and three constructs, produced previously, were included in the various assays. These mutant

versions of the NS3 proteins were expressed using the baculovirus expression system and assayed for membrane association, sucellular localisation, intracellular trafficking and their effects on cell viability.

The mutations had various effects on membrane association of the proteins, as well as on their subcellular localisation, intracellular trafficking. There were intrinsic differences in the reponses of the AHSV-2 NS3 and AHSV-3 NS3 proteins to the introduced mutations. The tendency of the AHSV-2 NS3 mutant proteins to retain their nuclear localisation may be due to the presence of a nuclear localisation signal which is not present in AHSV-3 NS3. The intrinsic characteristics of the proteins can influence possible responses of proteins to modifications, thus generalised conclusions relating to mutagenesis could not be made. The modifications had varying effects on the cytotoxic effect on insect cells. Mutation of the HD domains seemed to interfere with plasma membrane trafficking, but this did not always correlate with a loss of cytotoxic ability. There were however intranuclear bodies observed, of which the functions still remain unclear. When the formation of the intranuclear bodies were lost there was a significant reduction in cell death. This may indicate that the intranuclear bodies have a role in AHSV NS3 induced cell death.

ABBREVIATIONS

µg	micrograms
µl	microlitres
µm	micrometers
aa	amino acid
AHS	African horsesickness
AHSV	African horsesickness virus
amp	ampicillin
Bac	baculovirus
bp	base pairs
BTV	bluetongue virus
cm2	centimetre squared
D	aspartic acid
Dept	Department
DNA	deoxyribonucleic acid
dNTP	deoxyribonucleotide triphosphate
ds	double-stranded
EDTA	ethylenediaminetetra-acetic acid
eGFP	enhanced green fluorescent protein
ER	endoplasmic reticulum
et al.	et alibi
Fig.	figure
gal	galactosidase
gent	gentamycin
h	hours
h.p.i.	hours post infection
HD	hydrophobic domain
HDF	high density fraction
HIV	human immunodeficiency virus
I	isoleucine
IPTG	isopropyl-β-D thiogalactopyranoside
ISR	intervening spacer region
k	kilo
kan	kanamycin
L	leucine
L1-L3	large segment 1 to 3
LB	Luria-Bertani medium
LDF	low density fraction
M	molal
M.O.I.	multiplicity of infection
M4-M8	medium segment 4 to 8
min	minutes
mM	millimolal
N	asparagine
N fraction	nuclear fraction
NaCl	sodium chloride
ng	nanograms
nm	nanometers
NS	non-structural
oC	degrees Celsius
OD600	optical density at 600 nm
OIE	Office International des Epizooties
ORF	open reading frame
OVI	Onderstepoort Veterinary Institute
P	particulate
p.i.	post infection
PAGE	polyacrylamide gel electrophoresis
PCR	polymerase chain reaction
RdRp	RNA dependant RNA polymerase

RNA	ribonucleic acid
rpm	revolutions per minute
S	soluble
S9-S10	small segment 1 to 10
SD	standard deviation
sec	second/s
Sf9	*Spodoptera frugiperda* insect cells
SNAREs	soluble NSF attachment receptor proteins
SRP	signal recognition peptide
TEMED	N,N,N',N'-tetramethylethylene diamine
TOPO	PCR8/GW/TOPO plasmid vector
TS	threonine serine motif
UHQ	ultra high quality water
UP	University of Pretoria
UV	ultraviolet
V	volts
v/v	volume per volume
v/w	volume per weight
VIB	viral inclusion body
VLP	virus-like particle
VP	virus protein
X-gal	5-bromo-4-chloro-3-indolyl-β-D-galactopyranoside

LIST OF BUFFERS

Hypotonic buffer:	10 mM Tris, 0.2 mM $MgCl_2$, 1mg/ml Pefabloc (Roche) [pH 7.4]
NTE:	100 mM NaCl, 10 mM Tris, 1 mM EDTA [pH 7.4]
PBS:	137 mM NaCl, 2.7 mM KCl, 4.3 mM $Na_2HPO_4.7H_20$, 1.4 mM KH_2PO_4 [pH 7.3]
PSB (2x):	125 mM Tris-HCl 4% SDS, 20% glycerol, 10% 2-mercaptoethanol [pH 6.8],
TAE buffer	40 mM Tris-HCl, 20 mM Na-Acetate, 1 mM EDTA
TGS:	25 mM Tris-HCl, 192 mM glycine, 0.1% SDS [pH 8.3]
Transfer buffer:	0.025 M Tris, 0.15 M glycine, 20% methanol [pH 8.3]

Contents

CHAPTER 1: LITERATURE REVIEW

1.1. Introduction

Orbivirus infection causes disease in wild and domestic ruminants as well as a variety of other economically important animals. African horsesickness virus (AHSV) and Bluetongue virus (BTV) are two of the 19 species of viruses classified in the *Orbivirus* genus, family *Reoviridae* (Calisher & Mertens, 1998). These virus species are further sub-classed into different serotypes based on cross-neutralisation studies of the major outer capsid protein VP2. AHSV has nine serotypic groups and BTV has 24 (Calisher & Mertens, 1998; Huismans & Cloete, 1987). BTV is the prototype virus of the genus and has been very well characterized. AHSV is the aetiological agent of African horsesickness (AHS) in members of the *Equidae* family (Mellor, 1993). For the family *Equidae*, infection with AHSV is usually fatal, with the exception of *Equus burchellii,* the zebra, which barely ever shows symptoms. Zebras may be considered the natural vertebrate reservoir or natural cycling host for AHSV and it is not yet clear why they aren't negatively affected (Lord *et al.*, 1997; Venter *et al.*, 2006). Trade and export of horses contributes greatly to the South African economy and is responsible for an estimated R60 million annually (Venter *et al.*, 2006). AHSV outbreaks in equids are often accompanied by a two year embargo on export (Venter *et al.*, 2006).

The transmission of orbiviruses occurs by haematophagous arthropods. Orbiviruses are able to replicate in the insect vector and the primary vertebrate host. The *Culicoides* genus of biting midges are vector to nine *Orbivirus* species (Calisher & Mertens, 1998). AHSV is non-contagious and spreads only by means of the vector species *Culicoides* (Du Toit, 1944). Due to the effects of temperature on *Culicoides* and the great dispersive potential on the wind, the occurrence of future pandemics is almost guaranteed (Mellor & Leake, 2000; Paweska *et al.*, 2002; Wittmann *et al.*, 2002).

This study is aimed enhancing the understanding of AHSV virulence and pathogenesis by specifically evaluating the functions of one of its genes, NS3. This gene functions in viral release from infected cells and may well contribute to the pathogenesis and clinical picture seen in infected horses.

1.2. AHSV Epidemiology

African horsesickness is a listed disease of the Office Internationale des Epizooties (Website: http://www.oie.int, 24-04-2008). The disease occurs mainly in sub-Saharan Africa, with sporadic outbreaks of the disease in North Africa, the Middle East and Southern Europe (Mellor & Boorman, 1995). The disease emerges periodically in Southern Africa (Baylis *et al.*, 1999; Bosman *et al.*, 1995; Venter *et al.*, 2006). It was first noted in the Cape of Good

Hope in 1652 with the arrival of horses from Europe and the Far East (Venter *et al.*, 2006). In 1854 an AHS epidemic, in the Cape of Good Hope Colony in South Africa, killed an estimated 70 000 horses (European Food Safety Authority, 2007). In 1959/60, AHS made its way through the near and middle East and caused an estimated 300 000 deaths. There have been 14 such major AHS epizootics from 1803 (Baylis *et al.*, 1999).

Events that are more recent include the period between May and November 2007, with 40 outbreaks of AHSV-2 in Senegal. Of the estimated 1472 susceptible horses, a reported 475 horses were infected and of these 459 died. In order to manage the epidemic, 110 000 horses were vaccinated and a state of quarantine was instated (Website: http://www.oie.int, reported=6547, 22-04-2008). The Eastern Cape has suffered AHSV-2 infections every year since 2003. Between January 2008 and March 2008 more than 180 cases of AHS were reported in the Eastern Cape, of these cases at least 130 horses died (Website: http://www.promedmail.org, archive nr=20080326.1135, 22-04-2008). Between March and September 2008, there were 15 outbreaks of AHSV-2 in Ethiopia. A reported 4000 horses were infected and of these 2185 died (Website: http://www.oie.int, reportid=7362, 15-12-2009).

The epidemiological potential of the disease is mostly a product of the vector's competence and distribution, as it is the only means for the spread of infection (Du Toit, 1944; Paweska *et al.*, 2002; Venter *et al.*, 2000; Wittmann *et al.*, 2002). There are physiological barriers, innate to the incompetent vector species, that may prevent the transfer of infection (Fu *et al.*, 1999). Vector competence may be the result of coevolutionary relationship between the virus and the vector, which means that non-vectors could potentially become competent. Eight species of *Culicoides* that are able to spread the virus have been identified thus far, however there are more than 1200 species of *Culicoides* (Meiswinkel & Paweska, 2003; Paweska *et al.*, 2003; Paweska *et al.*, 2002). The major AHSV vector is *C. imicola* and may represent up to 99% of the *Culicoides* population during an AHSV outbreak (Venter *et al.*, 2006). In areas where the environment is less supportive of the *C. imicola* species, the *C. bolitinos* species seems to be responsible for AHSV transmission (Venter *et al.*, 2000; Venter *et al.*, 2006).

The timing of the major AHSV epizootic emergences in South Africa corresponds to El Nino events, which is the warm phase of the El Nino /Southern Oscillation. El Nino events are also associated with drought and altered rainfall patterns which may stimulate competent vector species (Baylis *et al.*, 1999; Wittmann *et al.*, 2002). Virus distribution is directly related to biting midge distribution (Tabachnick, 2004). Global warming may therefore enhance the vector's ability to transmit the virus and thus increase the risk for major

epidemics (Gould & Higgs, 2009). BTV and AHSV are spread by the same *Culicoides* species (Purse *et al.*, 2005). The impacts of climate change are evident from the spread of BTV into Northern Europe by *Culicoides* (Tomley & Shirley, 2009). This provides a troubling illustration of how quickly a vector-borne disease can spread through new geographic regions. Since the arrival of BTV in Europe tens of thousands of animals have died (Tomley & Shirley, 2009).

Temperature affects the vector's life cycle and ability to transmit the virus in several ways (Purse *et al.*, 2005). The insect needs to feed on infected hosts during viraemia, which is prolonged at higher temperatures (Gard *et al.*, 1988). The gonadotropic cycle of the vector is affected, subsequently the rate of propagation and thus the number of potential vectors (Paweska *et al.*, 2002; Purse *et al.*, 2005). Temperature influences the *Culicoides* biting rate and as a result may determine how aggressively the vector spreads the infection (Mullens & Holbrook, 1991). The extrinsic incubation time, which is the time between the insect obtaining the virus and the time when it has sufficient viral titres in the required organs to transmit the virus, is affected (Paweska *et al.*, 2002; Wittmann *et al.*, 2002). It is evident from the literature that a higher temperature seems to increase the virus's spreading potential through the competent vector species. Additionally the virus is believed to have an over wintering ability through *Culicoides* and can survive freezing temperatures (European Food Safety Authority, 2007). Consequently, the virus can persist throughout the year and at suitable temperatures re-emerge.

1.3. AHSV Pathogenesis

AHS is a temporally relevant disease with impacts on animal trade, sport, breeding etc. Understanding the disease and its pathology may provide insights into the diagnosis and treatment of the disease. AHS is a respiratory disease and several factors influence its pathological presentation, symptomatic severity and disease progression. AHSV is highly pathogenic and depending on the type the mortality rate may reach 100% (Table 1). The virus targets and infects endothelial cells of the lymph nodes and lungs. Given in Table 1 is a summary of the four forms of AHSV, this data was compiled from several sources (Burrage & Laegreid, 1994; Laegreid *et al.*, 1993; Mellor & Hamblin, 2004). The clinical manifestation of the disease is determined by the virulence of the AHSV isolate and the susceptibility of the host. More specifically disease manifestation is directly related to the ability of the virus to infect specific organs of a susceptible host (Burrage & Laegreid, 1994). Factors like age, sex, condition and the relative immune naivety of the animal may affect the susceptibility of the host. Other important factors may include the initial viral dose, the host-virus genetic interaction and the route of infection (Burrage & Laegreid, 1994; Erasmus,

1973; Laegreid *et al.*, 1993). A clinically definable phenotype develops because of these complex interactions.

Table 1: Forms of disease caused by AHSV infection

Form	Status at time of exposure	Clinical signs	Mortality
Peracute pulmonary form: Dunkop	Usually naive	• Short incubation time of four to five days • High fever (41° C) • Sudden onset laboured breathing • Death often within few hours after occurrence • Paroxysms (violent attacks) of coughing • Discharge of frothy/serofibrinous fluid from nostrils often occurs *post mortem* (Fig. 2a) • Oedema of the head and neck • Bulging supraorbital (eye cavity) fossae (Fig. 2b)	100% mortality two to three days after first symptoms appear

Subacute cardiac form: Dikkop		• Incubation of 7 to 14 days
		• Oedema of the (earlier in infection indicating seriousness of infection)
		  ○ Neck
		  ○ Supraorbital fossae
		  ○ Eyelids
		  ○ Lips
		  ○ Intermandibular region
		  ○ Cervical region
		  ○ Sternal region
		  ○ Ventral abdomen
		• Fever reaches max at later stage of infection than dunkop
		  ○ remains for three to six days
			Mortality of 50% to 80% at four to eight days after onset of febrile reaction

Acute mixed form	May be due to dual infections with different serotypes	• Incubation of five to seven days • Most common • Intermediate between cardiac and pulmonary forms	Mortality of up to 80% three to six days after onset of fever

African horsesickness fever	Animals with immunity to one or more strains and some cross protection	• Five to 14 day incubation period
		• Mildest form of the disease
		• Often not diagnosed
		• Transient symptoms
		  ○ High body temperature of 40.5°C for 1 to 6 days followed by drop back to normal
		  ○ Partial loss of appetite
		  ○ Congestion of conjunctivae (Fig. 2c)
		  ○ Slightly laboured breathing
		  ○ Increased heart rate
			100% recovery

After a bite from an infected *Culicoides* biting midge that is able to transmit the disease, virus replication begins in the regional lymphoid tissue and the first peak in viraemia occurs. In the blood, the virus particles are closely associated with erythrocytes and spread to the primary susceptible target organs, the lungs and lymphoid tissues. Infection spreads to the spleen, lungs, caecum, pharynx, choroid plexus and most of the lymph nodes. Viral replication within the infected tissues gives onset to a secondary viraemia with a variable duration that generally does not exceed 21 days in horses. In fatal cases the following may be observed: effusion, haemorrhage, heart failure and pulmonary alveolar flooding accompanied by respiratory distress and finally asphyxiation (Coetzer & Erasmus, 1994).

The common features between the different disease phenotypes seem to be oedema, effusion and haemorrhage (Fig. 1). These are believed to be due to the loss of the endothelial cell barrier function and loss of membrane integrity, specifically of the endothelial cells of the capillaries (Gomez-Villamandos *et al.*, 1999; Laegreid *et al.*, 1992a; Skowronek *et al.*, 1995). The non-structural protein NS3 of BTV and AHSV has been shown to play a role in viral release, and variation within certain domains of the protein has been shown to influence the timing of virus particle release and virulence (Hyatt *et al.*, 1991; Martin *et al.*, 1998; O'Hara *et al.*, 1998). The AHSV NS3 protein is specifically associated with the plasma membrane and seems to be directly involved in viral release. When reassortant viruses were generated in which AHSV NS3 of one serotype was incorporated in the genetic background of another serotype, infection lead to increased membrane permeability and significantly increased viral titres as compared to the parental strains (Meiring *et al.*, 2009b). The study of the NS3 protein may therefore provide valuable insights into its function in the viral life cycle and into factors that may influence viral pathogenesis and epidemiological potential. In order to understand the role of the AHSV NS3 protein, it is first necessary to understand parts of the virus' molecular biology.

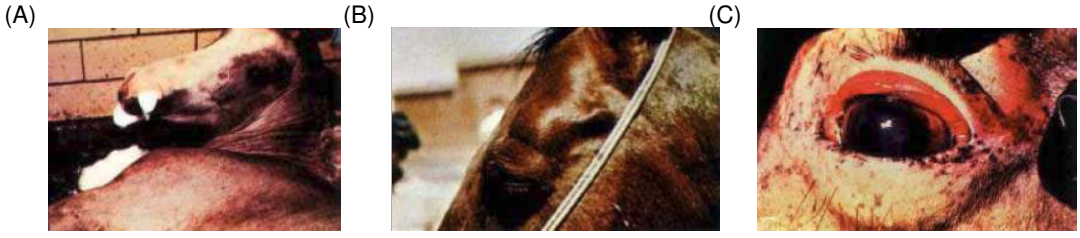

Figure 1: Some of the symptoms of AHS: (A) Dilated nostrils with frothy fluid effusion; (B) Oedema of the supraorbital fossa; (C) Congestion of conjunctivae (website: http://www.spc.int/rahs/Manual/images/african_horse_sickness.htm, 2008-04-22)).

1.4. Virus Molecular Biology

BTV is the prototype virus of the *Orbivirus* genus and has been extensively studied. BTV is also strikingly similar to AHSV in terms of its molecular biology and this is why it will be discussed in parallel with AHSV. BTV and AHSV have a 19 kb genome that is partitioned into ten dsRNA segments with sizes ranging from 822 bp to 3954 bp and 758 bp to 3965 bp respectively (website: http://www.ncbi.nlm.nih.gov, 28/04/2008)(Bremer *et al.*, 1990; Els, 1973; Roy, 1989; Verwoerd *et al.*, 1970). The segmented nature of the genome allows the possibility of reassortment during co-infection, which may have a strong effect on immune evasion and virus microevolution (Roy, 1989). The segments are numbered in order of dsRNA migration on polyacrylamide and agarose electrophoretic gels (Large = L1 to L3; Medium = M4 to M6; Small = S7 to S10)(Bremer *et al.*, 1990; Oellermann, 1970; Verwoerd *et al.*, 1970). With the exception of S10, all of the segments encode one protein product. S10 encodes two related proteins, NS3 and NS3A.

Depicted in Fig. 2 is a schematic representation of the double-layered particle of BTV. Like in BTV, the AHSV virion is non-enveloped with a dual layer capsid enclosing ten dsRNA genome segments. In brief, the BTV and AHSV capsids are composed of four major proteins. The outer capsid is composed of structural proteins VP2 and VP5 while the inner core is made of structural proteins VP3 and VP7 (Burroughs *et al.*, 1994; Mertens *et al.*, 1987; Prasad *et al.*, 1992; Verwoerd & Huismans, 1972; Verwoerd *et al.*, 1979). There are three proteins with enzymatic functions arranged specifically within the core and these form the transcription complex. There are also four non-structural proteins encoded by the viral genome, these do not form part of the mature virus particle, but function during virus particle formation and progeny release (Huismans & Van Dijk, 1990; Oellermann *et al.*, 1970; Verwoerd *et al.*, 1972). Proteins of BTV and AHSV are analogous in their functions, and each protein has a very specific and highly organized function. The functions of the respective protein products of each of the ten segments are given in Table 2. The protein constituents harmoniously cooperate to produce an efficient replicative production line, whose sole purpose is to crank out vast numbers of virus progeny.

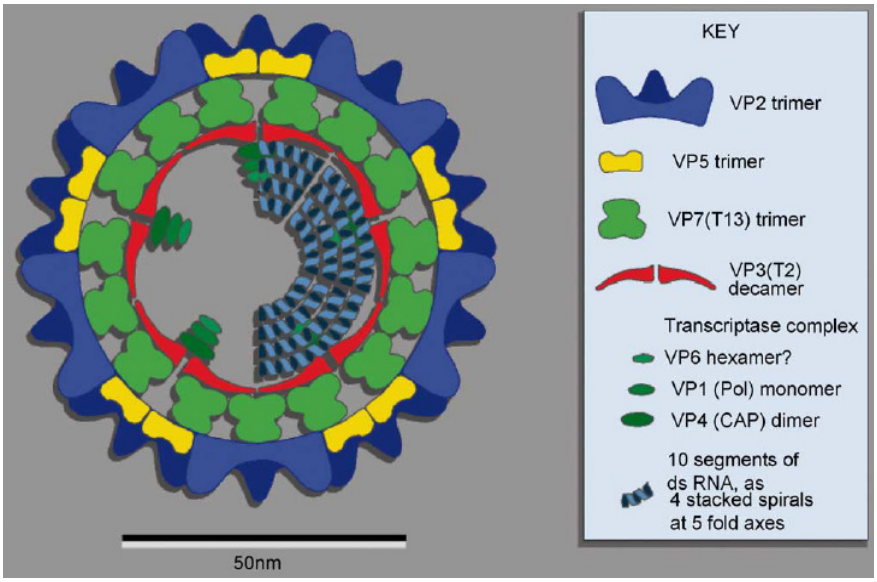

Figure 2: The non-enveloped virion particle of BTV with its double layered capsid (Taken from Mertens, 2004).

Table 2: Summary of BTV and AHSV genome segments and the molecular functions of various gene products (Website: www.ncbi.nlm.nih.gov/entrez, 28-04-2008)

Segment and size in bp	**Protein**	**Function and notes**
L1 BTV = 3944 (ORF = 3908) AHSV = 3965 (ORF = 3917)	VP1 BTV = 1302 amino acids (aa) = 149 kDa AHSV = 1305 aa = 150 kDa	RNA dependant RNA polymerase (Boyce *et al*., 2004; Roy *et al*., 1988; Urakawa *et al*., 1989) • mRNA as a template • De novo initiation • 5' to 3' Polymerase • Template dependant • Synthesis of positive strand for translation and negative strand to complete replication
L2 BTV = 2953 (ORF = 2870) AHSV = 3203 (ORF = 3155)	VP2 BTV = 956 aa = 111 kDa AHSV = 1051 aa = 122 kDa	VP2 sail-shaped spikes form 60 triskelion-type motifs and overlay most of the VP7 trimers (Hewat *et al*., 1992a; Hewat *et al*., 1992b) Directly involved in viral attachment to cell (Huismans et al., 1983; Roy, 2001) Elicits virus neutralising antibodies (Fukusho *et al*., 1987; Ghiasi *et al*., 1987; Inumaru & Roy, 1987) • Allows some cross protection • Responsible for serotype specificity (Huismans & Bremer, 1981; Huismans & Erasmus, 1981; Roy, 1990; Roy *et al*., 1996) • Responsible for hemagglutinin activity (Kahlon *et al*., 1983) Most variable of BTV proteins
L3 BTV = 2772 (ORF = 2705) AHSV = 2792 (ORF = 2717)	VP3 BTV = 901 aa = 103 kDa AHSV = 905 aa = 100 kDa	VP3 dimers are the building blocks for the inner icosahedral structure of the sub-core (Huismans *et al*., 1987b; Kar *et al*., 2005; Maree *et al*., 1998) Characteristics of the inside of the VP3 layer (Gouet *et al*., 1999; Mertens & Diprose, 2004; Verwoerd, 1969) • chemically featureless grooves • form tracks for the RNA • may facilitate the movement of the dsRNA segments during transcription Interacts with • surface layer of VP7 in the core • minor proteins (VP1,VP6,VP4) • RNA Determinant of • capsid morphology • genome organisation within core

M4 BTV = 1980 (ORF = 1934) AHSV = 1978 (ORF = 1928)	VP4 BTV = 644 aa = 76 kDa AHSV = 642 aa = 76 kDa	Capping enzyme (Martinez-Costas *et al.*, 1998; Ramadevi *et al.*, 1998; Ramadevi & Roy, 1998; Sutton *et al.*, 2007) • Guanylyltransferase • Methyltransferases 1 and 2 • RNA 5' triphosphatase • Inorganic pyrophosphatase • NTPase
M5 BTV = 1685 (ORF = 1658) AHSV = 1748 (ORF = 1646)	NS1 BTV = 552 aa = 64 kDa AHSV = 548 aa = 63 kDa	Most abundantly synthesized protein during BTV infection (Huismans & Els, 1979) Forms tubules during replication (Maree & Huismans, 1997; Urakawa & Roy, 1988) • Cytoskeleton associated (Eaton *et al.*, 1988) • Role in cellular pathogenesis and morphogenesis of BTV (Owens *et al.*, 2004) Major immunogen for cytotoxic T lymphocytes (Andrew *et al.*, 1995)
M6 BTV = 1638 (ORF = 1580) AHSV = 1564 (ORF = 1517)	VP5 BTV = 526 aa = 59 kDa AHSV = 505 aa = 57 kDa	VP5 molecules are arranged on six-membered rings of VP7 trimers Located in spaces formed by six membered VP7 rings (Mertens & Diprose, 2004) Function: (Diprose *et al.*, 2001; Forzan *et al.*, 2004; Hyatt *et al.*, 1989) • Role in penetration of endosomal membrane • May play a role in virus neutralization (in AHSV contains epitopes) • pH dependent conformational change of VP5 responsible for virus release into cytoplasm o When C-terminal globular domain attaches to endosomal membrane o Allowing N-terminal coiled-coil domain to extend o This likely destabilizes the endosomal membrane o Releases of transcriptionally active core VP5 can induce cytotoxicity by permeabilizing mammalian and *Culicoides* insect cells (Hassan *et al.*, 2001)
S7 BTV = 1156 (ORF = 1049) AHSV = 1179 (ORF = 1061)	VP7 BTV = 349 aa = 38 kDa AHSV = 353 aa = 38 kDa	Form trimers with relatively flat bases (Grimes *et al.*, 1995) BTV core outer layer with 690Å diameter is composed of 260 trimers of VP7 Organized on a T=13 icosahedral lattice VP7 layer interacts with the inner layer composed of 120 copies of VP3 (~103 kDa) arranged as 60 dimers on a T=2 icosahedral lattice (Grimes *et al.*, 1998). BTV outer capsid proteins interact extensively with the VP7 layer (Nason *et al.*, 2004).
S8 BTV = 1125 (ORF = 1064) AHSV = 1166 (ORF = 1097)	NS2 BTV = 354 aa = 40 kDa AHSV = 365 aa = 41 kDa	Only virus specific phosphoprotein (Huismans *et al.*, 1987a) Forms and is located in cytoplasmic viral inclusion bodies (VIB) (Modrof *et al.*, 2005) Recruits mRNA species into VIBs (Roy, 2005) Binds only ssRNA (Huismans *et al.*, 1987a) Sequence specific binding to +strand RNA (Lymperopoulos *et al.*, 2006; Lymperopoulos *et al.*, 2003) VIBs are sites for virion assembly
S9 BTV = 1049 (ORF = 989) AHSV = 1169 (ORF = 1109)	VP6 BTV = 329 aa = 35 kDa AHSV = 369 aa = 38 kDa	Binds ds and ssRNA (De Waal & Huismans, 2005) Acts as helicase enzyme which uses ATP and divalent cations (Mg^{2+})(Kar & Roy, 2003; Stauber *et al.*, 1997)
S10 BTV (ORF = 822) AHSV (ORF = 691) (ORF = 654 /657)	NS3	Proteins believed to function in viral release. NS3 will be discussed in detail in the text
S10 BTV (ORF = 610) AHSV (ORF = 620)	NS3A	

1.5. The Orbivirus Life Cycle

The BTV virus life cycle will be discussed in order to model the replication of orbiviruses. The cycle starts when binding to a host cell occurs and is mediated by VP2 (Hassan & Roy, 1999). The outer capsid protein, VP2, mediates binding by recognizing and attaching to the host cell receptor, which is yet to be identified. The receptor is hypothesized to be a glycophorin or a sialoglycoprotein (Eaton & Crameri, 1989). Viral uptake into the cell occurs by endocytosis. After entry a clathrin coated vesicle containing virus is formed, the coat is rapidly lost leaving a relatively large endocytic vesicle (Hyatt & Eaton, 1990). The endocytic vesicles localize in the vicinity of the nucleus (Huismans *et al.*, 1987b). In this vesicle the viral outer capsid is rapidly degraded, specifically VP2, and this exposes VP5 (Eaton *et al.*, 1990; Hassan & Roy, 1999). VP5 has a pH-dependent permeablilisation activity causing conformational change that is believed to destabilize the vesicle and release the core particle into the cytoplasm (Diprose *et al.*, 2001; Forzan *et al.*, 2004; Hassan *et al.*, 2001; Hyatt *et al.*, 1989). Within an hour after infection particles lacking VP2 and VP5 are detectable in the cytoplasm and are ready for transcription (Hewat *et al.*, 1992a; Huismans *et al.*, 1987b; Hyatt *et al.*, 1993).

The removal of the outer capsid allows the activation of virion transcriptase. Exposure of the core to magnesium ions in the cytoplasm causes expansion of the five fold axis (Gouet *et al.*, 1999). The expansion probably then opens the aqueous channels and provides access to the inner core, specifically for substrates to the enzyme complex (Diprose *et al.*, 2001). Through these channels free nucleotides can move in and newly synthesized mRNAs can be transported out to the cytoplasm for translation or replication (Diprose *et al.*, 2001; Mertens & Diprose, 2004). VP3 dimers are mostly responsible for the characteristic orbivirus icosahedral sub-core structure (Huismans *et al.*, 1987b). The inside of the VP3 layer presents with chemically featureless grooves that may specifically provide tracks for the dsRNA that allow the required movement during transcription (Mertens & Diprose, 2004; Verwoerd, 1969).

As the host cell does not possess the machinery required to transcribe ssRNA from dsRNA, the virus provides its own within the highly organised core structure (Jayaram *et al.*, 2004). The inner core contains the transcription complex that consists of the virally produced VP6, VP1 and VP4 enzymatic proteins. There are a maximum of 12 transcriptase complexes within the inner core structure (Mertens & Diprose, 2004). Transcription is a highly coordinated process and each of the enzymatic proteins has specific functions. Both transcription of mRNA for protein synthesis and replication for converting ssRNA to dsRNA occur within the protective environment provided by the inner core (Eaton *et al.*, 1990). The

core protects dually against degradation by cellular nucleases and against recognition by the cellular antiviral defence mechanisms that could have been triggered by dsRNA (Agrawal *et al.*, 2003; Eaton *et al.*, 1990; Jayaram *et al.*, 2004; Patton *et al.*, 2007). The core particle also has the ability to bind and sequester dsRNA from damaged viruses within the cell in order to prevent induction of the latter defence mechanisms (Diprose *et al.*, 2002). By bypassing the defence mechanisms, the virus is free to perform processes required for viral replication.

The transcription aims to produce the positive or coding strand of the dsRNA and to export it for use in subsequent processes. The VP6 protein is able to bind RNA and functions as helicase and unwinds the dsRNA in order for transcription to begin (De Waal & Huismans, 2005; Kar & Roy, 2003; Stauber *et al.*, 1997). VP1, the largest protein, serves as a RNA dependent RNA polymerase (RdRp) that synthesises the RNA transcript (Roy *et al.*, 1988; Urakawa *et al.*, 1989). The negative strand is recognised specifically and used as the template for transcription driven by VP1 (Martinez-Costas *et al.*, 1998; Ramadevi *et al.*, 1998; Ramadevi & Roy, 1998; Sutton *et al.*, 2007). In vitro VP1 can initiate and carry out transcription promiscuously (Boyce *et al.*, 2004). After transcription, the transcript unwinds from the template and the parent strands renature (Banerjee & Shatkin, 1970; Van Dijk & Huismans, 1988). A model has been proposed to explain how the *Reoviridae* RdRp functions. The enzyme has four channels (Lu *et al.*, 2008; McDonald *et al.*, 2009; Tao *et al.*, 2002). Each of the four channels serves a specific function (Fig. 3). Parental positive strand binds to the RdRp cap-binding site and remains tethered outside VP1, while the parental negative strand enters the RdRp enzyme. Inside RdRp the parental negative strand is used as template for positive strand synthesis. The parental negative strand RNA and newly synthesised positive strand separate internally and both exit RdRp. The parental negative strand re-enters the core while the positive strand exits acquiring a cap on the way.

All ten of the dsRNA segments are transcribed simultaneously (Gillies *et al.*, 1971; Lawton *et al.*, 1997; Van Dijk & Huismans, 1988). However, not all of the RNA daughter segments are produced at the same rate. As can be expected, the smaller segments are produced more often, with the exception of S10 which is produced to a lesser extent (Van Dijk & Huismans, 1988).

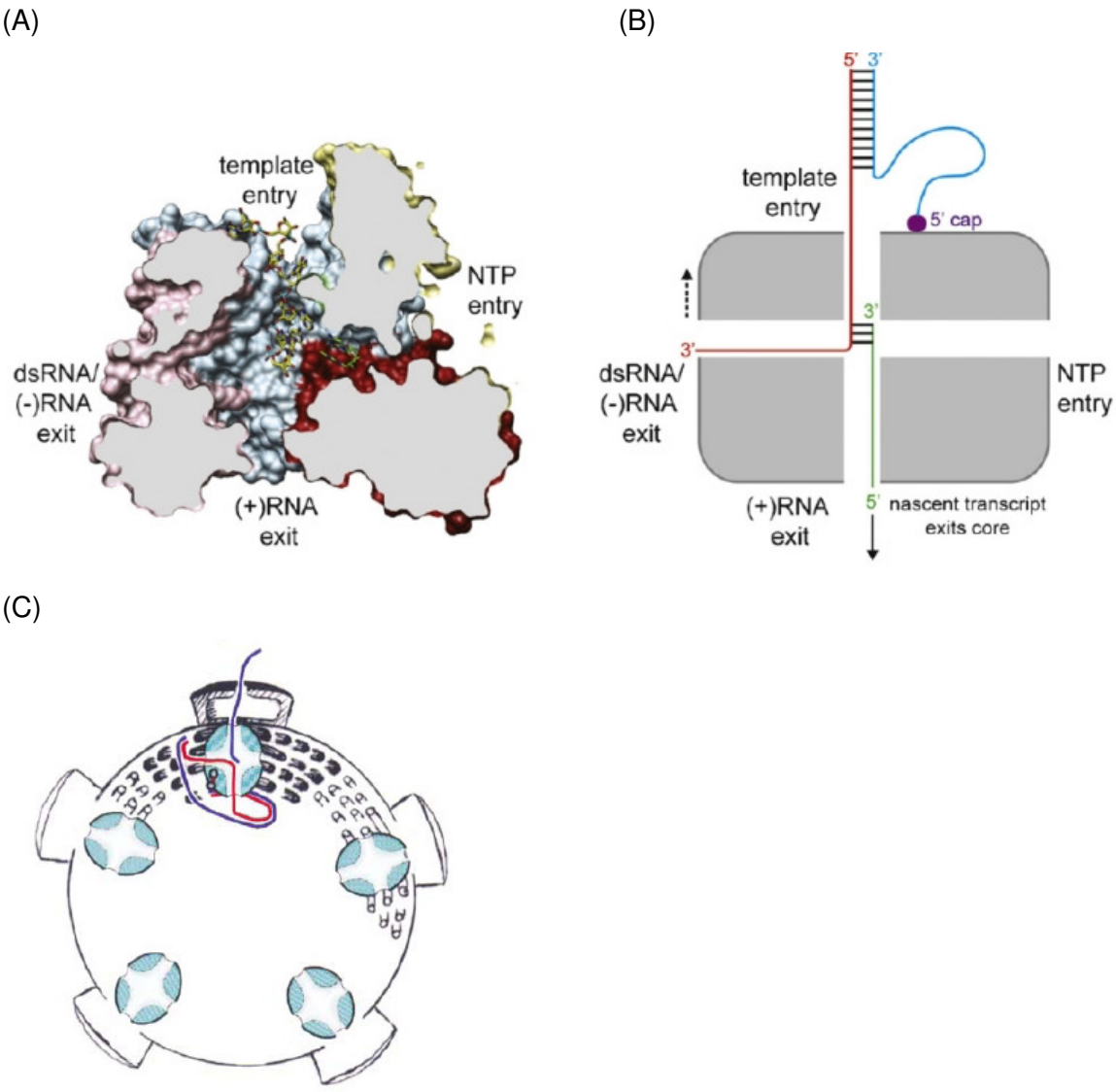

Figure 3: Structure and function of four-tunnelled *Reoviridae* RdRp; (A) VP1 (Lu *et al.*, 2008), (B) Schematic of RNA movement in VP1 during transcription (McDonald *et al.*, 2009); (C) Schematic of RdRp orientation in the core (Tao *et al.*, 2002)

The newly synthesised transcripts are targeted to specific locations in order to perform their functions. In the transcription complex the VP4 protein functions as the RNA post-transcriptional modification enzyme and enables specific export of the newly synthesized coding strand (Martinez-Costas *et al.*, 1998; Ramadevi *et al.*, 1998; Ramadevi & Roy, 1998; Sutton *et al.*, 2007). The transcript is specifically recognised and the 5' end is modified by VP4 which functions as a capping enzyme (Gouet *et al.*, 1999). The transcripts have conserved inverted terminal repeats and these allow the formation of a RNA secondary structure. The secondary structure is believed to facilitate export, increase stability during intracellular localisation and enable interaction with the translation machinery (Martinez-

Costas *et al.*, 1998; Mertens & Sangar, 1985; Ramadevi *et al.*, 1998; Rao *et al.*, 1983). After modification the transcripts are exported through the aqueous channels traversing the core structure (Gouet *et al.*, 1999). The transcripts enter the cytoplasm and are now en route to their next destinations.

The transcripts can now take one of two paths and end up producing two different classes of products. They seem to be predestined to either go to the cellular translation machinery for production of viral proteins or to be recruited to newly synthesised, assembled core particles for replication into dsRNA viral genomes (Diprose *et al.*, 2001; Urakawa *et al.*, 1989). In the cytoplasm the transcripts that associate with the ribosomes are used as templates for protein synthesis (Van Dijk & Huismans, 1988). These newly synthesised proteins then need to be assembled into virus particles. Viral assembly occurs at the periphery of granular cytoplasmic matrices known as viral inclusion bodies (VIBs) (Brookes *et al.*, 1993). The viral NS2 protein is responsible for the formation of these VIBs (Kar *et al.*, 2007). Phosphorylation of NS2 is required for VIB formation and may therefore be the activation signal (Modrof *et al.*, 2005). The VIBs are produced around the nucleus and are detectable from four hours post infection (h.p.i.) (Brookes *et al.*, 1993). The VIBs may be considered the factories that are responsible for virus production.

Within the VIBs specific processes must occur in order to produce virus progeny. These processes not only involve the interactions between specific proteins but also require the recruitment of genetic material to make viral progeny replicative. In the VIB, the VP1, VP4 and VP6 viral proteins associate with the VP3 decamers. VP7 assembles on and around the scaffold provided by VP3 (Brookes *et al.*, 1993; Kar *et al.*, 2005). NS2 N-terminus binds the coding ssRNA destined for replication (Huismans *et al.*, 1987a; Lymperopoulos *et al.*, 2006; Lymperopoulos *et al.*, 2003; Roy, 2005; Thomas *et al.*, 1990). As NS2 binds more of the ssRNA, they accumulate in the VIBs and are probably incorporated into the virus core particles (Kar *et al.*, 2007). Viral proteins VP2 and VP5, which are present at the periphery of VIBs, associate with VP7 on semi-complete cores. After association, the particles may be considered the completed product, the virus particle. VP2 and VP5 enable the particles to associate with the cell cytoskeleton filaments in the cytoplasm (Eaton *et al.*, 1987; 1988). They are no longer transcriptionally active and are ready to be released from the host cell (Hyatt & Eaton, 1988).

There may be several mechanisms involved in intracellular trafficking of the newly produced viral particles. NS1 is the most highly synthesized protein in the viral armada. NS1 proteins associate into tubules, which are found in large quantities throughout infected cells, with the highest density around the nucleus at the periphery of the VIBs (Brookes *et al.*, 1993;

Huismans & Els, 1979; Urakawa & Roy, 1988). The tubules have defined structures and interfering with NS1 function using antagonistic protein expression negates tubule formation and results in a shift from lytic to non-lytic modes of viral release (Maree & Huismans, 1997; Owens *et al.*, 2004; van Staden *et al.*, 1998). Interfering with NS1 however does not influence viral maturation or infectivity but enhances viral release. The NS1 tubules may play a role in virus intracellular trafficking and committing to the lytic pathway of viral release (Owens *et al.*, 2004). The NS1 enhances lytic release and therefore greatly contributes to cytopathology and the resulting pathogenesis. The lytic pathway however is not the only mechanism that the virus uses for exiting host cells.

Viral release can occur by one of two possible mechanisms, namely by budding or by extrusion (Hyatt *et al.*, 1989). Budding usually occurs early in infection (Hyatt *et al.*, 1989). The budding virions acquire temporary envelopes displaying no antigens. NS3 proteins are found at the sites on the plasma membrane where the virus particles bud off and are believed to be responsible for this mechanism (Hyatt *et al.*, 1991; Stoltz *et al.*, 1996). Budding particles are followed immediately by non-enveloped virus particles (Hyatt *et al.*, 1989). The extrusion mechanism allows groups or individual virions to escape through locally disrupted parts of the plasma membrane and this does not seem to have significant effect on cell viability (Hyatt *et al.*, 1989). This viral egression does not leave permanent holes in the plasma membrane. The particles that are released remain in association with the cortical layer of the cytoskeleton (Hyatt *et al.*, 1989). The non-enveloped virus particles are either partially embedded in the plasma membrane or found in association with cell-derived material. The viral progeny are detectable in the extracellular space within 6 h.p.i. and maximum release is maintained for between 12 and 20 hours (Hyatt *et al.*, 1989). Released virus progeny differ from intracellular viruses in terms of VP2. The extracellular viral progeny are more compact which may indicate that a conformational change occurred upon release. Progeny have the ability to re-enter the cell by means of endocytosis. These “super infectious progeny” increase the multiplicity of infection and enhance the kinetics of viral replication (Hyatt *et al.*, 1989).

The focus of this study is the investigation of certain aspects of AHSV NS3 that may facilitate clarification of the protein’s function in the viral life cycle. The study forms a part of a research programme into the role of each of the specific AHSV proteins in virulence and pathogenicity. To facilitate this purpose, aspects of the NS3 protein that have specific relevance to this project will be discussed.

1.6. Sequence Based Analysis of AHSV and BTV S10/NS3

Sequences for S10 representing all nine of the known AHSV serotypes have been published (de Sa *et al.*, 1994; Martin *et al.*, 1998; Sailleau *et al.*, 1997; van Niekerk *et al.*, 2001b; van Staden *et al.*, 1991). The S10 gene segment of AHSV ranges between 755 and 764 nucleotides in length and the S10 of all the BTV serotypes evaluated up to date have been 822 nucleotides in length (Hwang *et al.*, 1992; Lee & Roy, 1986; Pierce *et al.*, 1998; Quan *et al.*, 2008; Sailleau *et al.*, 1997). The dsRNA S10 segment of BTV and AHSV has two in phase initiation codons with reading frames that overlap. The first initiation codon initiates the translation of NS3 and the second that of NS3A (Gould, 1988; Lee & Roy, 1986; Wu *et al.*, 1992). In BTV NS3 is the primary product and NS3A is synthesised to a lesser extent, where as in AHSV, NS3 and NS3A are synthesized in equimolar amounts (French *et al.*, 1989; van Staden *et al.*, 1995). This phenomena may be due to mRNA secondary structure stemloops at either side of the BTV NS3A initiation codon which are not present in AHSV (Hwang *et al.*, 1992; van Staden *et al.*, 1995). The sequences of various NS3 proteins have been compared extensively and such studies and have allowed insights into the putative structural conformation and possible functional domains.

Of the proteins encoded by AHSV, the NS3 protein has a variability that is second only to that of the VP2 protein of the viral outer capsid. The amino acid sequence variation of AHSV NS3 is up to 37% between serotypes and 28% within serotypes (de Sa *et al.*, 1994; Sailleau *et al.*, 1997; van Niekerk *et al.*, 2001b). Amino acid sequence alignments have allowed the identification of five motifs, which are common in NS3 between the related orbiviruses. These include a potential N-myristylation site (van Niekerk *et al.*, 2001b); a cluster of prolines within the N-terminal region (called the L-domain); two hydrophobic domains in the C-terminal half of the protein which are believed to be responsible for the membrane association of the NS3 protein (Gould, 1988; Jensen *et al.*, 1994; Lee & Roy, 1986; Moss *et al.*, 1992; van Staden *et al.*, 1991); two conserved cystein residues within the first HD; and a conserved 50 amino acid (aa) region with high sequence conservation between residues 45 and 95 (van Niekerk *et al.*, 2003; van Niekerk *et al.*, 2001b; van Staden *et al.*, 1995). Depicted in Fig. 4 is a schematic representation of the S10 gene segment and its protein product NS3, with the main conserved and variable regions indicated. The information used in the diagram was compiled from several sources (de Sa *et al.*, 1994; Hwang *et al.*, 1992; Quan *et al.*, 2008; Sailleau *et al.*, 1997; van Niekerk *et al.*, 2003; van Niekerk *et al.*, 2001b). The motifs might have functional importance in NS3 secondary structure, inter-protein interaction, intracellular trafficking and other NS3 related events.

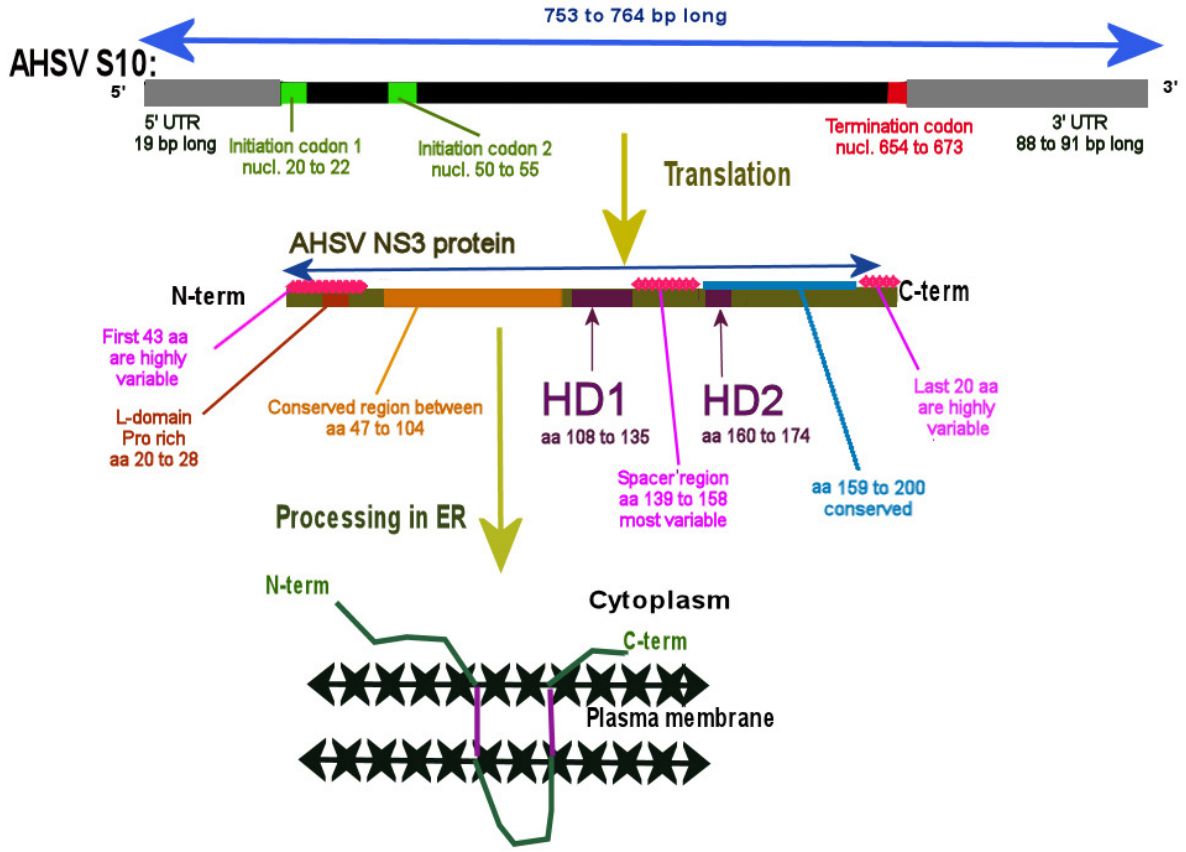

Figure 4: A schematic representation of the AHSV S10 gene segment and its product, non-structural protein NS3. Variable and conserved domains are indicated as well as the hypothesised membrane-associated conformation.

Though sequence conservation data gives highly informative and valuable indication of local purifying selection and putative functional importance, it is not the only informative data gained from sequence alignments. The large sequence variation between AHSV serotypes may be indicative of a relatively high level of diversifying selection, i.e. regions which may be exposed to the immune system with roles in immune evasion. Regions highlighted by alignments, those that were found to be the most variable in the protein amino acid sequence include the first 43 aa on the N-terminus; the region between aa 93 and 153; and the 20 aa on the C-terminus (Quan *et al.*, 2008). The intervening spacer region (ISR) between aa 139 and 158 may vary up to 82.4% across all serotypes (Quan *et al.*, 2008; van Niekerk *et al.*, 2001b). The ISR is believed to be exposed on the outside of the plasma membrane, and therefore subject to positive immuno-selective pressure (Quan *et al.*, 2008; van Staden *et al.*, 1995). Sequence data was thereby used to predict that the HDs of NS3 span the plasma membrane with the N- and C-terminal regions of NS3 exposed on the cytoplasmic face, as illustrated in Fig. 4 (Bansal *et al.*, 1998; van Staden *et al.*, 1995). It may be deduced that the NS3 gene product is subject to selective pressure and thereby the variation may be due to the evolutionary pressure on the virus.

Variation within the protein sequence may affect mechanisms such as processing, secondary structure formation and tertiary intermolecular interaction, which in turn could influence the protein's function. When different serotypes were compared in mice it was found that NS3 variation may influence virulence (O'Hara *et al.*, 1998). In *Culicoides* cell cultures infected with reassortant viruses it was shown that showed that AHSV NS3 aa sequence variations can influence the timing of virus release and virulence phenotypes (Martin *et al.*, 1998; Meiring *et al.*, 2009b). This however has not been found in BTV where aa sequence conservation ranges between 92% to 100% (Bonneau *et al.*, 2002; Hwang *et al.*, 1992; Pierce *et al.*, 1998). Sequence variation within BTV NS3 does not seem to correlate with variation in virulence (Pierce *et al.*, 1998). The S10 gene segment of orbiviruses is believed to be under strong purifying selection (Quan *et al.*, 2008). Purifying selection drives genes to fixation, therefore the BTV NS3 variability may have been removed by selection (Balasuriya *et al.*, 2008).

By using mutational approaches in a number of studies, specific domains in the NS3 protein have been shown to contribute to different aspects of the protein's characteristics and/or functions. When the actions of individual domains were disrupted by mutation or deletion, the manifestation was apparent in specific phenotypes. These domains are illustrated in Fig. 5 (data was compiled from several sources) (Bansal *et al.*, 1998; Han & Harty, 2004; van Niekerk *et al.*, 2001a; van Staden *et al.*, 1998).

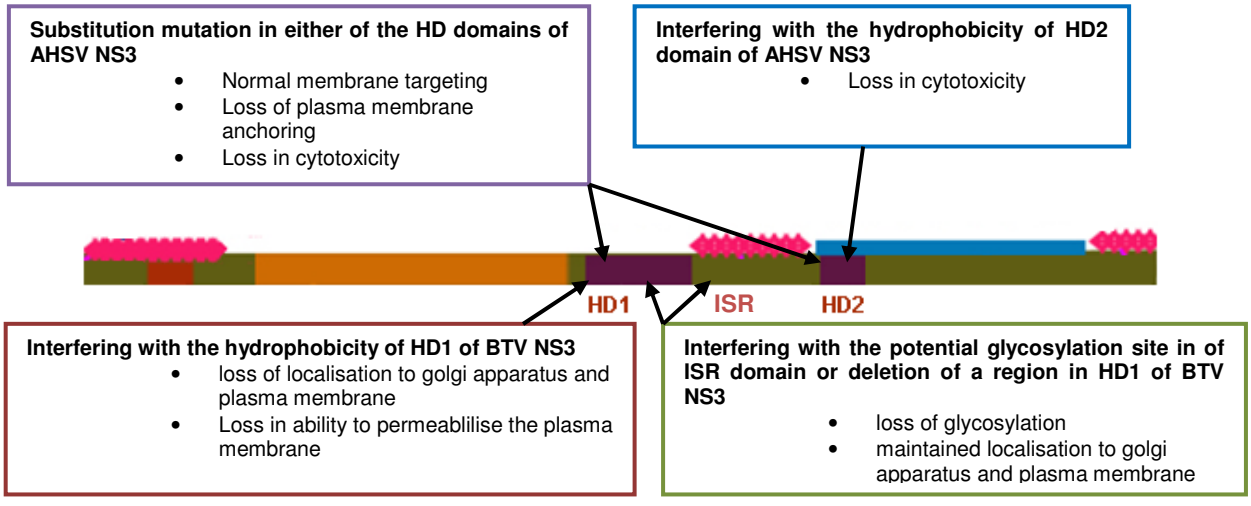

Figure 5: Disruption of specific domains in the NS3 protein has been shown to be manifest in specific phenotypes.

A detailed sequence alignment comparison was performed where the NS3 protein sequences of all serotypes of AHSV, as well as the cognate proteins of three related

orbiviruses were compared (van der Sluis, 2007). The evaluation focussed mainly on the two HDs and the ISR and revealed a number of highly conserved residues in all three of these domains (Fig. 5). These residues, postulated to play a role in protein folding, homo-oligomerisation and/or membrane interaction and topology are listed and discussed in Table 3.

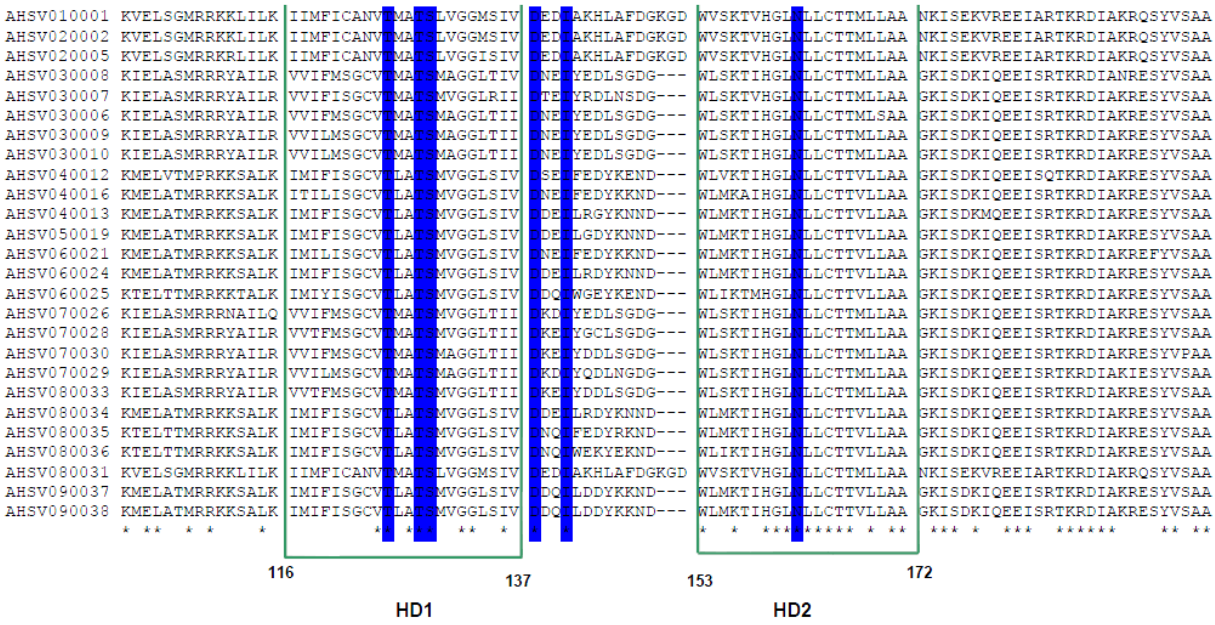

Figure 6: ClustalX 1.81 alignment of AHSV NS3 protein (HDs and flanking regions) sequence data representing all serotypes. Conserved aa with putative functional importance are highlighted (van der Sluis, 2007).

Table 3: Conserved amino acids identified in all serotypes of AHSV

Position in amino acid sequence	Amino acid	Description
HD1		
128 & 129	threonine & serine (TS)	Hydrophilic residues that form part of known motifs that are important for driving alpha helix formation (Dawson *et al.*, 2002)
Spacer region		
141	isoleucine (I)	Hydrophobic residue with only one favourable rotamer thus may be important for conformation/folding
149 to 151	lysine glycine aspartic acid (KGD)	Additional three residues present only in the highly pathogenic AHSV serotype 2
138	aspardic acid (D)	D is a hydrophilic amino acid that may form hydrogen bonds or be important for the pore function of viroporin proteins (de Jong *et al.*, 2004).
138-150 (or 153)	length of 12 aa to 15 aa	Shorter than the ISR in equine encephalosis virus, (a closely related *Orbivirus)*. The length of the ISR may affect protein topology (Goder *et al.*, 1999)
HD2		
162	asparagine (N)	Polar aa with possible structural role and/or a role in homo-oligomerisation (Curran & Engelman, 2003).

1.7. The NS3 Protein's Functional Characteristics

Generally, orbiviruses are released by means of cell lysis, but in insect cells, release is non-lytic. BTV NS3 is expressed at high levels in insect cells, but transiently expressed in low levels in mammalian cells (French *et al.*, 1989; Guirakhoo *et al.*, 1995). When BTV was adapted through serial passage in mosquito cells, and then reintroduced into mammalian cells, it was evident that the virus had a significantly reduced replication. This effect was accompanied by the relative over-expression of the NS3/NS3A proteins and release of infective particles into supernatant (Guirakhoo *et al.*, 1995). The NS3/NS3A proteins are required for budding and release of virus like particles (Hyatt *et al.*, 1993). Therefore the BTV NS3 protein is believed to be essential for the non-lytic release of virus progeny (Beaton *et al.*, 2002).

NS3 is an integral membrane protein, containing two HDs separated by a short spacer region (van Staden *et al.*, 1995). The protein localizes non-uniformly in cells. It is located on the plasma membrane where the virus progeny are being extruded or budded off. NS3 is also located in vesicular components in the cytoplasm of AHSV and BTV infected cells (Hyatt *et al.*, 1991; Stoltz *et al.*, 1996; van Staden *et al.*, 1995). NS3 is present in transiently acquired membrane fragments during viral release but absent from the extracellular surface of undamaged cells (Hyatt *et al.*, 1991; Stoltz *et al.*, 1996). The protein remains cell associated and is not released into culture medium (van Staden *et al.*, 1995). The NS3 protein therefore has a very strong membrane association and we may conclude that it functions specifically at the membrane.

In cells infected with AHSV, the NS3 protein is expressed at relatively low levels. The naturally low levels of expression make studying the protein difficult. Because the NS3 localisation is not dependent on the presence of virus particles it can be studied in an expression system. The cDNA of the AHSV S10 gene segment was cloned and expressed in a baculovirus system (van Staden *et al.*, 1995). The expression of the AHSV NS3 protein in this system had a strong cytotoxic effect in Sf9 insect cells, cells presented with completely disrupted plasma membranes, granular cytoplasms and distorted nuclei (van Niekerk *et al.*, 2001a; van Staden *et al.*, 1995). Using the baculovirus system, mutational analysis indicated that disrupting the hydrophobic nature of either HD1 or HD2 reduced the cytotoxic effect of the protein by about 45%, indicating that the specific hydrophobic nature may be required for interaction with membrane components (van Niekerk *et al.*, 2001a; van Staden *et al.*, 1998). The NS3 protein is responsible for cellular damage when expressed alone and this phenomenon is dependent on specific protein domains. In effect, the NS3

protein may be partly responsible for the AHS characteristic symptoms: oedema, effusion and haemorrhage. The observations may be explained by the following hypothesis.

1.8. NS3 acts as a viroporin and allows non-lytic viral release

The plasma membrane is responsible for maintenance and regulation of many cellular processes. Alterations in membrane permeability may therefore affect various parts of cellular metabolism and facilitate viral release by either lytic or non-lytic means (Carrasco *et al.*, 1989). Some non-enveloped viruses modify membrane permeability to allow viral release. Viroporins are a family of virus proteins that enhance membrane permeability. Viroporins are generally short proteins of between 50 and 120 aa in length. They generally have a higher leucine and isoleucine content and contain less glycine residues than the average virally encoded membrane proteins. All viroporins have at least one HD that is approximately 20 aa in length and forms an amphipathic helix. This hydrophobic domain often contains basic aa, which may aid in the destabilization of the plasma membrane. Viroporins tend to oligomerise, often as tetramers. This leaves a hydrophilic pore through which molecules including ions and low molecular weight hydrophilic molecules can pass in and out in an unregulated manner. The pores facilitate entry of calcium and hydrogen ions. Thus by removing the ion gradient of the membrane, they cause instability and lead to partially disrupted plasma membranes. The localisation of these viroporins may specifically promote release of viral progeny populations within the cell (Carrasco, 1995).

The NS3 of BTV has characteristics of viroporins. The characteristics include the two HDs and the ability to oligomerise. The NS3 protein also has the ability to permeabilise the plasma membrane allowing molecules to traverse the membrane into the cell cytoplasm (Han & Harty, 2004). As a viroporin the NS3 protein could partially disrupt the plasma membrane and allow virus progeny to extrude.

NS3 may function dually in lytic and non-lytic viral release. The intracellular localisation of NS3 may strongly influence the mode of NS3 action in driving viral release. There are two possible modes for NS3 intracellular transport: NS3 may be trafficked via conventional transport mechanisms and/or by lipid rafts. The virus is dependent on cellular machinery for protein folding, oligomeric assembly, transport and intracellular targeting (Hegde & Lingappa, 1997). Processes involved in the processing of viral membrane proteins, specifically the AHSV non-structural protein NS3 will be discussed.

1.9. The Machinery Involved in Processing NS3 into a Functional Product

Viral membrane glycoproteins are always synthesised in the endoplasmic reticulum (ER). These proteins undergo several non-spontaneous post-translational modifications catalysed by cellular folding enzymes and molecular chaperones. The ER provides these activities. Viral mRNAs are typically translated on membrane bound ribosomes and inserted into the ER in an unfolded form by the translocon machinery. Leader peptides are recognised and bound in the cytosol by signal recognition peptides (SRP). The SRPs guide the protein into the ER. The translocon recognises HDs and orientates them in the membrane (Hegde & Lingappa, 1997; Maggioni & Braakman, 2005). Within the ER specific processes occur which are responsible for producing functional proteins.

Hypothetically the folding process should be able to occur spontaneously because all the required information is present in the proteins primary structure (Anfinsen, 1973; Maggioni & Braakman, 2005). Protein aggregation may become a factor when the intracellular protein concentration is high and proteins are in close proximity to other proteins (macromolecular crowding) (Ellis, 2001; Maggioni & Braakman, 2005). Therefore the folding processes are driven and the folding process starts while translation is taking place (Doms *et al.*, 1993; Maggioni & Braakman, 2005). Folding occurs by aid of molecular chaperones, which do not direct folding but rather shield proteins from undesirable interactions with other molecules (Ellis, 2001; Fewell *et al.*, 2001; Maggioni & Braakman, 2005). The chaperones may be protein family specific and recognise specific amino acid sequences. The chaperones may also be promiscuous in that they do not differentiate between protein families but rather recognise characteristics such as hydrophobic patches, mobile loops or a lack of compactness (Maggioni & Braakman, 2005). Folding enzymes catalyse reactions required for the folding process. These processes include disulphide bond formation by protein disulphate isomerases, electron transfer by oxidoreductases, isomerisation by cis-trans isomerases etc. (Maggioni & Braakman, 2005). Protein folding is not a random, unstructured occurrence but rather a specifically and actively driven process.

The ER provides three biochemically distinct environments where protein processing takes place (Doms *et al.*, 1993; Maggioni & Braakman, 2005). In the ER lumen the ectodomains, all of the carbohydrate moieties and potential disulphide bond sites are folded. The HDs form α-helices in the ER membrane bilayer. All the domains undergo folding independently of each other (Doms *et al.*, 1993). The specificity of protein processing is therefore conferred by specific motifs. Evolutionarily conserved regions such as those identified in

AHSV NS3 (Fig. 4) may be required for proper folding of the protein into a functionally active conformation.

Active processes require energy from the cell and are often regulated. The folding process is no exception. During folding the proteins are monitored by quality control machinery (Maggioni & Braakman, 2005). Folding factors are associated with proteins which are being folded. This association remains until the protein is correctly folded. This association causes retention. Only when correctly folded do the folding factors dissociate, which allows the folded protein to exit the ER (Ellgaard *et al.*, 1999; Maggioni & Braakman, 2005). Some proteins then move to and into the Golgi apparatus for additional modification. These modifications may include proteolytic cleavage and carbohydrate processing (Doms *et al.*, 1993). If folding errors occur, be it due to mutation in conserved domains or interference from macromolecular crowding or some other reason, the folding factors keep misfolded proteins in the ER (Ellgaard *et al.*, 1999).

This phenomenon where misfolded protein export is selectively inhibited is termed “quality control” (Hurtley *et al.*, 1989). Prolonged retention leads to an accumulation of misfolded proteins and these then undergo ER-associated degradation (Brodsky & McCracken, 1999; Lippincott-Schwartz *et al.*, 1988; Maggioni & Braakman, 2005). This has direct implications on mutational analysis studies and this is of particular relevance to this project. Mutations may affect folding of the proteins. The consequences of mutations are dependent on the protein structure and post-translational modification pathways. Residues such as cystein, which are involved in secondary structure formation, may be essential for folding. Glycosylation sites may be essential for proper folding and oligomerisation (Doms *et al.*, 1993). Thorough knowledge of the events involved in protein processing may aid in the prediction of some mutational consequences as well as the interpretation of observations made when evaluating mutant proteins.

Almost all viral membrane proteins have oligomeric tendencies which could be hetero- or homo-oligomeric (Maggioni & Braakman, 2005). Assembly of oligomers usually takes place after translation and modification. This oligomerisation may occur before transport to the Golgi apparatus, because “naïve” newly processed proteins may contain unprocessed N-linked oligosaccharides. The oligomer stability may be variable, and may be influenced by the protein’s conformation. The conformation may be altered by pH to which the protein is exposed. The monomers usually need specific folded domains to be able to interact with each other (Doms *et al.*, 1993). Oligomerisation is relevant because BTV NS3 has to be able to oligomerise in order to function as a viroporin (Han & Harty, 2004). If a mutation

occurs that affects oligomerisation, then one might expect that the viroporin function would be lost and should therefore alter the permeablilisation activity of the mutant relative to the wild type NS3 protein. This once again illustrates the importance of specific domains in protein function.

As mentioned earlier the NS3 protein contains several highly conserved residues. Among these are a TS in HD1 and an N in HD2 and an I and D in the ISR (Table 3). The T,S and N residues are able to drive alpha helix formation by intra-helical bond formation (Choma *et al.*, 2000; Gray & Matthews, 1984). These polar residues form hydrogen bonds that stabilize the protein helical secondary structure (Dawson *et al.*, 2002). The D in the spacer may also form hydrogen bonds or provide a hydrophilic charge within the viroporin channel. Hypothetically the NS3 protein is folded in the ER to a conformation where the two hydrophobic domains span the plasma membrane and both the C- and N-termini are in the cytoplasm (van Staden *et al.*, 1995).

After a protein has been folded into its correct functional conformation, it has to be trafficked to the location within the cell where its function is required. Target specific transport of proteins within a cell is required to enable their function at their specific localities. Some proteins may remain in the cytoplasm to function intracellularly; others are transported to the plasma membrane to act there or to be secreted for a specific extracellular function (Hegde & Lingappa, 1997). As stated earlier, the intracellular localisation of NS3 may strongly influence the mode of NS3 action in driving viral release. I will now discuss processes that have been implicated in intracellular transport of the NS3 protein.

1.10. Vesicular Pathways involved in NS3 transport

Highly specific trafficking and localisation is essential for protein function (Hegde & Lingappa, 1997). In a cell there are several trafficking pathways, however, most membrane associated proteins are transported using the secretory pathway (Hegde & Lingappa, 1997). Viruses exploit these pathways in order to facilitate parts of their replication process (Maggioni & Braakman, 2005). After being folded the BTV NS3 protein is transported through the Golgi apparatus to the cell plasma membrane (Bansal *et al.*, 1998).

For the ESCRT machinery, the main tools are multivesicular bodies (MVBs), which function as vehicles for protein transport. They allow the sorting and degradation of proteins. In some specialized cell types, MVBs serve as secretory bodies that are fused with the cell membrane, and their contents are released into the extracellular space. MVBs are formed

through invaginating and pinching off bits of the endosomal membrane. Three conserved multi-subunit complexes are essential for this function, namely ESCRT-I,-II and –III (Raiborg *et al.*, 2003). Ubiquitination functions as a sorting signal for protein cargo and regulates traffic between the membrane compartments (Hicke & Dunn, 2003). Enzymes like ubiquitin ligases regulate the timing and specificity of the endocytic pathway. Monoubiquitin signals for proteins to enter into the endocytic pathway. The signal is recognized by endocytic proteins that contain ubiquitin-binding motifs (UIM). Proteins like epsins and Hrs link ubiquitinated cargo to the clathrin-based sorting machinery (Hicke & Dunn, 2003).

Enveloped RNA viruses can use the MVB machinery for budding by using their late domain containing P(S/T)AP or PPXY motifs. Intraluminal vesicles may provide vehicles for transmembrane proteins that are released in a regulated manner. Viruses then redirect the ESCRT complexes to the plasma membrane to facilitate sub-cellular trafficking and localisation (Raiborg *et al.*, 2003). Viruses such as the Kaposi's sarcoma associated herpes virus encode proteins that target immune proteins, such as MHC-class proteins, for degradation through these complexes, thus providing a mechanism for immune evasion (Pornillos *et al.*, 2002).

The Tsg101 protein, which is a component of the ESCRT-I complex, aids in vacuolar protein sorting and controls which proteins bud into the endosome to create MVBs (Raiborg *et al.*, 2003). It has the ability to recognise PTAP/PSAP motifs and sort proteins containing these motifs into the appropriate vesicles (Raiborg *et al.*, 2003). The human immunodeficiency virus (HIV) requires the PTAP motif on its Gag protein for budding. Tsg101 binds the PTAP and thereby facilitates HIV release (Yasuda, 2005). Viral proteins containing PPXY motifs may mimic the Hrs proteins at the plasma membrane (Raiborg *et al.*, 2003). As mentioned earlier the Hrs proteins contain UIM and these bind ubiquitin and are involved in sorting proteins into appropriate vesicles (Bishop *et al.*, 2002; Lloyd *et al.*, 2002; Polo *et al.*, 2002; Raiborg *et al.*, 2002; Shi *et al.*, 2002). Tsg101 also contains an ubiquitin E2 variant domain that binds ubiquitin with low affinity and sorts proteins with the appropriate signal into the appropriate vesicles (Raiborg *et al.*, 2003).

The NS3 protein contains highly conserved PPXY and PSAP motifs that may facilitate virion release (Han & Harty, 2004). NS3 binds strongly to Tsg101 via the PSAP motifs and also interacts with the NEDD4-like ubiquitin ligases via its PPXY motif (Wirblich *et al.*, 2006). The NS3 PPXY motif recruits host ubiquitin ligases and ubiquitination is the signal for sorting into MVBs (Raiborg *et al.*, 2003). By using a newly developed BTV reverse genetics system, it

was shown that the NS3-Tsg101 interaction was required for the virus to bud from the plasma membrane (Celma & Roy, 2009).

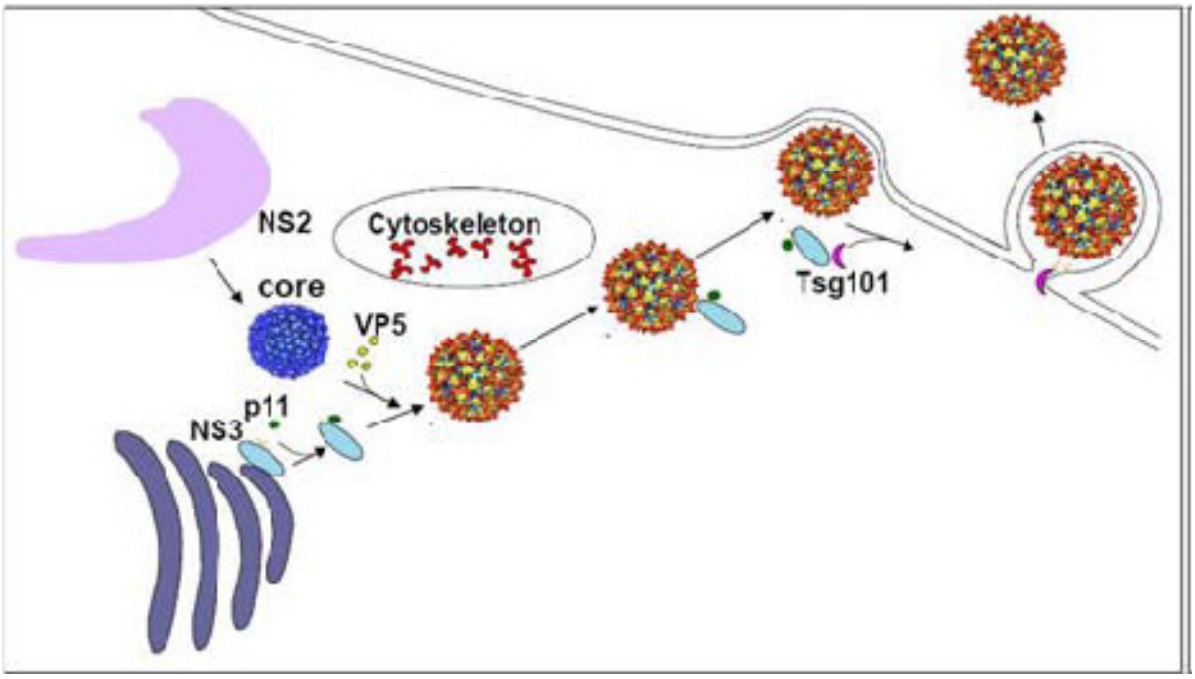

Figure 7: A schematic diagram illustrating the function of the NS3 protein in facilitating budding from infected cells. In this schematic the NS3 protein provides the link between cellular transport machinery and the viral particle (Taken from Roy 2008).

The virus proteins VP2, VP5 and NS3 are all required for the release of core-like particles from cells (Hyatt *et al.*, 1993). This can be explained by the Tsg101 dependant mechanism for viral release (Bhattacharya *et al.*, 2007). In this model, mature virions associate with vimentin via the VP2 protein, which is part of the outer capsid with the VP5 protein. Using the vimentin network, they are transported to the plasma membrane (Bhattacharya *et al.*, 2007). At the membrane the VP2 protein binds to the C-terminus of NS3 while the N-terminus of NS3 binds strongly to Tsg101 (Beaton *et al.*, 2002; Celma & Roy, 2009). Tsg101 enables the virions to enter the ESCRT budding pathway and viruses are budded off (Wirblich *et al.*, 2006). Interfering with either the VP2–NS3 or NS3-Tsg101 disrupts budding (Celma & Roy, 2009). NS3 acts as the intermediate between the virus and hosts machinery thus facilitating virus release.

The p11 protein that is the light chain component of the calpactin complex, also interacts with NS3 (Beaton *et al.*, 2002; Wirblich *et al.*, 2006). The NS3 protein contains a putative amphipathic helix in its first 13 aa that may be responsible for interaction with p11. The interaction occurs at the same site as the annexin heavy chain (p36) and therefore may mimic it (Beaton *et al.*, 2002). The calpactin complex is important for many cellular processes including Ca^{2+}-dependent exocytosis and trafficking of proteins out of the cell

(Nakata *et al*., 1990; Sarafian *et al*., 1991). By exploiting this mechanism, the virus progeny may also be able to exit the cell in a non-lytic manner.

The NS3 protein has evolved to be highly specialised in its function in viral release. It has the ability to mimic and exploit various proteins in order to conduct the virus into different pathways that will ultimately lead to viral release. The lipid raft pathway is another pathway that has been implicated in NS3 function. It has been shown that the BTV NS3 protein interacts with VP5, which in turn interacts with the lipid raft proteins. In this way, the lipid rafts may provide a scaffold for virus assembly. The NS3 protein maintains the outer capsid protein (VP2 and VP5) proximity for the final assembly of the virus cores in BTV replication (Bhattacharya & Roy, 2008). It is not yet clear whether AHSV NS3 associates with lipid rafts directly.

1.11. Lipid Rafts

The plasma membrane is compartmentalized into a assortment of microdomains with spatially specific functionalities. These microdomains may function in signalling, cell adhesion and membrane trafficking (Harder & Simons, 1997). Clusters of small cholesterol dependent sphingolipid bodies exist transiently in discrete regions within plasma membranes. These detergent resistant bodies have been termed caveolae and lipid rafts (Laude & Prior, 2004; Simons & Ikonen, 1997).

Caveolae are invaginations in the plasma membrane (Laude & Prior, 2004). They are characterized by the presence of the protein caveolin (Rothberg et al., 1992). Caveolin synthesis takes place in the ER and is then transported to the Golgi apparatus where it oligomerizes. Oligomers are then transported to the plasma membrane where several small rafts merge and form caveoli (Fra et al., 1995). The rafts are believed to function in signal transduction and sorting, as well as trafficking through secretory and endocytic pathways (Brown & London, 1998).

Lipid rafts are believed to have an important function in targeting proteins to the plasma membrane (Brown & Breton, 2000). The rafts are able to travel through the membranous fluid bilayer (Simons & Ikonen, 1997). The membrane microdomains of sphingolipids and cholesterol preferentially associate with specific proteins (Harder & Simons, 1997). The rafts are believed to function in signal transduction and sorting, as well as trafficking through secretory and endocytic pathways (Brown & London, 1998). Lipid rafts are associated with several proteins including membrane associated proteins (Laude & Prior, 2004; Simons & Ikonen, 1997). Raft assembly is believed to occur in the Golgi apparatus (Simons & Ikonen,

1997; van Meer, 1989; Wu *et al.*, 1992) where NS3 is localised. Lipid rafts may interact with soluble NSF attachment receptor proteins (SNAREs). SNARE proteins are involved in all intracellular membrane fusion events in *Eukarya*. The SNAREs on two different membranes fuse, thus integrating the membranes and any proteins that may have been associated with them. The rafts may therefore be involved in membrane fusion reactions and this may provide the means for release of transported transmembrane proteins and associated particles, for example viral particles (Salaun *et al.*, 2004).

1.12. Visualizing NS3 trafficking and localisation

Part of this study will be conducted using confocal microscopy of immunolabelled or green fluorescent protein (eGFP) fusion proteins. The eGFP is used to investigate the localisation of chimeric proteins within cells that express it. The origin of eGFP is the light-emitting organ of *Aequorea victoria,* a jellyfish, and the sea pansy *Renilla reniformis*. In an energy transfer reaction, it is able to produce green light. The proteins from these different organisms are thought to have the consensus sequence for the GFP chromophore (Chalfie, 1995). In a construct where the GFP is inserted into the reading frame of the protein that is to be studied, the fluorescence can be used as a marker for temporal and spatial gene expression in living tissues (Chalfie, 1995). The relatively large GFP protein of 27 kDa is able to absorb UV and blue light and emits green light (Lippincott-Schwartz & Smith, 1997) The main advantage of chimeras with fluorescent capability is that cells can be monitored in their biologically active unfixed form (Chalfie, 1995). Tissue preparation, fixation and immunolabelling are tedious and often time consuming. The use of GFP chimeras completely remove the need for these efforts (Ehrhardt, 2003). There is an enhanced version of the GFP protein which has improved stability; higher intensity of fluorescence and low levels of photobleaching, which means that tagged proteins may be visualized over a longer period of time (Ashby *et al.*, 2004; Zhang *et al.*, 1996).

1.13. Conclusion and Aims

This project forms part of a research programme that is concerned with studying the roles of different AHSV proteins in virulence, pathogenicity and disease. This study is focused specifically on investigating non-structural protein NS3. When expressed in tissue culture the AHSV NS3 protein has the ability to disrupt membrane integrity of cells causing cell death (Han & Harty, 2004; van Niekerk *et al.*, 2001a; van Staden *et al.*, 1995). The AHS disease itself is characterised by loss of endothelial cell barrier function through loss of membrane integrity leading to oedema and ultimately death of the infected host (Laegreid *et al.*, 1992a; Laegreid *et al.*, 1992b; Mellor & Hamblin, 2004). A bioinformatics-based analysis of all available AHSV NS3 sequences revealed the presence of a number of highly conserved domains or single amino acids (van der Sluis, 2007). Variation within the protein's primary structure, specifically in conserved regions, may affect mechanisms such as processing, secondary structure formation and tertiary intermolecular interaction, which in turn could influence the proteins function and or localisation. Using mutational approaches, specific domains in the protein have been shown to contribute to different parts of NS3's function. The current project is focused on roles of specific conserved residues in the two hydrophobic domains and the intervening spacer region of NS3. This study aims to evaluate the roles of these conserved motifs.

The main objective of this study was to investigate if some of the conserved amino acids and sequence domains of AHSV NS3 contribute to its subcellular localisation, trafficking and cytotoxicity in insect cells. To do this we targeted these domains for site directed mutagenesis, expressed the mutant proteins in a baculovirus expression system and analysed the effects of the mutations using specific assays.

CHAPTER 2:
EVALUATING THE ROLES OF HIGHLY CONSERVED DOMAINS IN THE NON-STRUCTURAL PROTEIN NS3 OF AHSV

2.1. Introduction

AHSV infection causes haemorrhage, oedema and effusion, symptoms that could be explained by the virus induced damage to the pulmonary and vascular endothelia (Laegreid *et al.*, 1992a; Laegreid *et al.*, 1992b; Mellor & Hamblin, 2004). When grown in tissue culture AHSV causes severe cytopathic effects in mammalian cells (Coetzer & Erasmus, 1994). In AHSV-infected mammalian cells, the NS3 protein is present at the disrupted areas of the plasma membrane at sites of virus exit (Stoltz *et al.*, 1996). In tissue culture, when NS3 is expressed in mammalian or insect cells, the plasma membrane integrity is disrupted and cell death occurs (Han & Harty, 2004; van Niekerk *et al.*, 2001a; van Staden *et al.*, 1995). Cytotoxicity is dependent on membrane association, and it has been proposed that the NS3 protein functions as a viroporin causing membrane permeability to allow virus release (Han & Harty, 2004; Van Niekerk *et al.*, 2001a). A bioinformatics-based analysis of all available AHSV NS3 sequences revealed the presence of a number of highly conserved motifs with putative functions (van der Sluis, 2007). The motifs and their contribution to the function of the NS3 protein have not been studied. At the onset of this study, there was no reverse genetics system available for AHSV. The baculovirus system provides the means to study NS3 using mutational approaches. In this system a baculovirus (*Autographa califonica* multiple nucleopolyhedrosis virus) has been engineered to provide a eukaryotic platform for protein expression in tissue culture, it allows with production of milligram quantities of correctly folded protein (Luckow *et al.*, 1993).

For this project, mutational approaches were used to characterise the roles of the specific motifs in the subcellular localisation and cytotoxicity of AHSV NS3. Targets for mutation were identified and mutations were designed that involved either the hydrophobic domain 1 (HD1), hydrophobic domain 2 (HD2) or the intervening spacer region (ISR). Three recombinant baculovirus constructs were already available prior to the commencement of this project, these were AHSV-2 NS3 proteins with mutations targeting the ISR. In the first one an isoleucine (I) residue in the ISR was replaced with a serine (S). I is a hydrophobic residue with only one favourable rotamer and thus may be important for folding. In the second mutant the three residues, KGD, were deleted from the ISR of AHSV-2 NS3. These were targeted because they are only found in the NS3 protein of the highly pathogenic AHSV-2 strain. The ISR can be important for the membrane topology of the protein and therefore for the third mutant the ISR length was modified by a 15 amino acid insertion into the ISR.

Additional mutants were then designed for construction during this project. In HD1, there was a threonine-serine (TS) motif with T and S placement similar to motifs involved in

protein folding. Both are polar residues that may form hydrogen bonds and drive alpha helix formation. This TS motif was changed to isoleucine-leucine (IL). In HD2, an asparagine (N) residue was targeted because N in HD domains is believed to strongly drive alpha helix formation and thus function in protein folding or oligomerisation. The N was replaced with an isoleucine (I). The change to non-polar residues L or I was predicted to negate the H-bonding ability of the motifs. In the ISR, an aspartic acid (D) residue was targeted for changing to serine (S). D is a hydrophilic amino acid that may form hydrogen bonds or may be involved in the viroporin function of the NS3 protein (de Jong *et al.*, 2004). It was changed to a S because serine has a neutral charge and is hydrophilic.

Eight mutant constructs were produced during the course of this project (Fig. 8). Three of the mutants were constructed using the AHSV-2 reference strain S10 gene (Fig. 8 A). It was later discovered by T. L. Meiring during her PhD research that the encoded NS3 protein of the reference strain contains a putative nuclear localisation signal (*[RK](3,)?x(8,16)[RK](4,)?*) which may influence the protein's function by changing its subcellular trafficking (Meiring, 2009a). Subsequently, three analogues were constructed using the AHSV-3 reference strain S10 gene (Fig. 8 B). Two additional analogues were constructed for AHSV-3 from as chimeric S10-eGFP construct to assay the usefulness of eGFP fusion constructs in studying AHSV NS3 (Fig. 8 C). Two strategies were employed in order to generate the site directed mutant open reading frames (ORF), the Megaprimer method and the Quikchange method.

All the baculovirus constructs were expressed in Sf9 insect cells and analysed with respect to membrane interaction, intracellular distribution, trafficking and cytotoxicity in an attempt to define the contribution of each of the residues or domains to NS3's function.

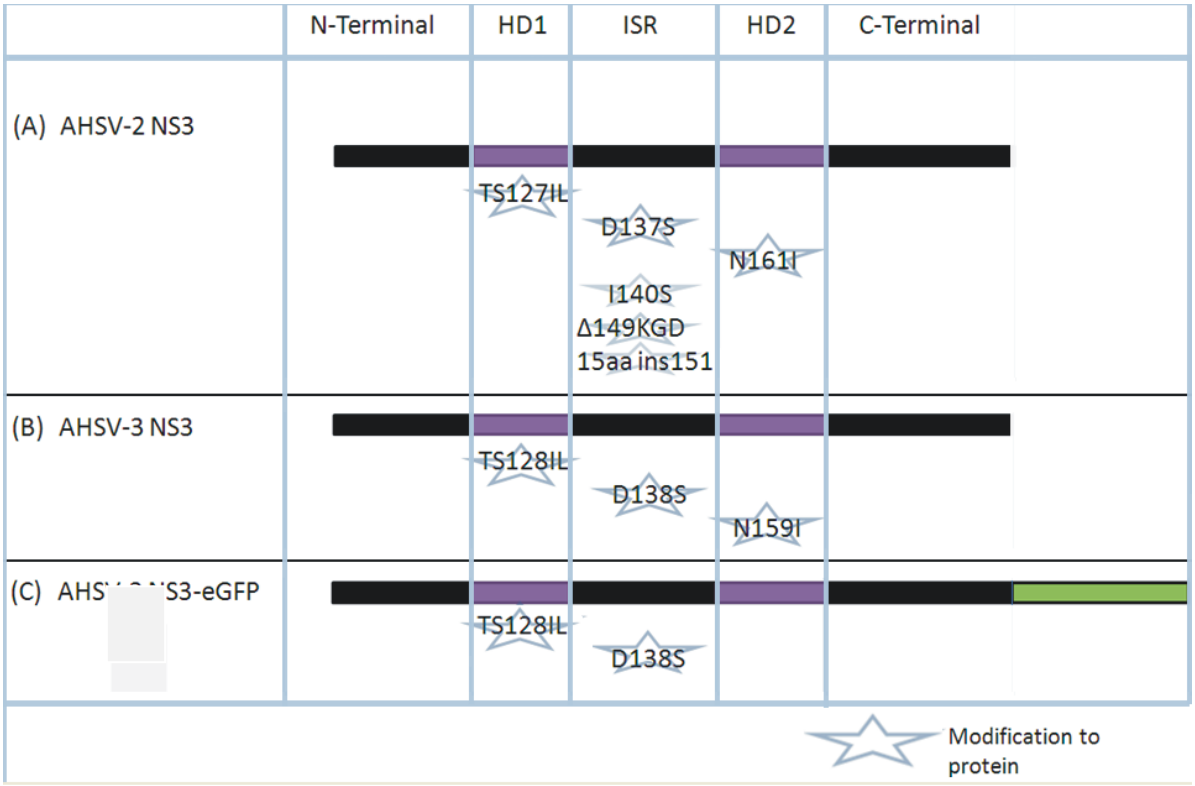

Figure 8: Schematic representation of mutational targets in the NS3 that were to be investigated; (A) AHSV-2 NS3 and mutants; (B) AHSV-3 NS3 and mutants; (C) AHSV-3 NS3-eGFP and mutants.

2.2. Materials and Methods

2.2.1. Plasmids, viruses and antibodies.

Listed below are plasmid constructs (Table 4), recombinant baculoviruses (Table 5) and antibodies (Table 6) that were available and used during the course of this project.

Table 4: Plasmids:

Plasmid	Protein encoded	Produced by (additional notes)	Antibiotic resistance
pFastbac-AHSV-2-S10 (Ref strain 82/61)	AHSV-2 NS3	Dr M van Niekerk (Department of Genetics (Dept Gen), University of Pretoria (UP))	$Gent^{R}Amp^{R}$
pFastbac-AHSV-3-S10	AHSV-3 NS3	T Hatherell (Dept Gen, UP)	$Gent^{R}Amp^{R}$
pFastbac-AHSV-3-S10-eGFP	AHSV-3 NS3-eGFP	T Hatherell (Dept Gen, UP).	$Gent^{R}Amp^{R}$
PCR8/GW/TOPO	None	Vector supplied with the PCR8/GW/TOPO TA cloning kit from Invitrogen, which is compatible with the Gateway system as an entry vector	Spc^{R}
pDest8	None	From Invitrogen and is compatible with the Gateway system as a destination vector	$Gent^{R}Amp^{R}Cm^{R}$ (Cm^{S} in recombinant)

Table 5: Recombinant baculoviruses (Bac)

Virus	Protein	Additional Notes	Produced by:
Bac-AHSV-2 NS3	AHSV-2 NS3	Full length (amino acids 1-217) wild type AHSV-2 (Ref strain 82/61) NS3 protein	Dr M van Niekerk*
Bac-AHSV-2 NS3 I140S	AHSV-2 NS3 I140S	Mutant full length (amino acids 1-217) AHSV-2 (Ref strain 82/61) NS3 with residue 140 Ile substituted with Ser.	R van der Sluis*
Bac-AHSV-2 NS3 Δ149KGD	AHSV-2 NS3 Δ149KGD	Mutant AHSV-2 (Ref strain 82/61) NS3 with residues 149 to 151 deleted	R van der Sluis*
Bac-AHSV-2 NS3 15aa_ins151	AHSV-2 NS3 15aa_ins151	Mutant AHSV-2 (Ref strain 82/61) NS3 with 15aa inserted at position 151 of the spacer region	R van der Sluis*
Bac-AHSV-3 NS3	AHSV-3 NS3	Full length (amino acids 1-218) wild type AHSV-3 (Ref strain) NS3 protein	C Smit*
Bac-AHSV-3 NS3-eGFP	AHSV-3 NS3-eGFP	Full length (amino acids 1-218) wild type AHSV-3 (Ref strain) NS3 protein with eGFP fused to the C-terminal end	T Hatherell*
Bac-eGFP	eGFP	Full length eGFP is a 29 kDa monomer with 265 amino acids. The protein has fluorescence characteristics with Ex/Em = 488/507 nm	M Victor*

*Dept Gen at UP

Table 6: Polyclonal antibodies:

Antiserum	Specificity	Dilution	Source
anti-rabbit Alexafluor 488	Fluorescently labelled antibodies, Alexa Fluor® 488 goat anti-rabbit IgG	1:250 in 1% blocking solution	Invitrogen Cat no. A-11008
anti-GFP	Antibodies raised in rabbits directed against eGFP N-terminal	1:5000 in 1% blocking solution	Sigma Cat no. G1544
anti-18aa-NS3 AHSV-3	Antibodies raised in rabbits directed against conserved 18aa region on the C-terminal of AHSV-3 NS3 (Peptide sequence: CISDKIQEEISRTKRDIA)	1:100 in 1% blocking solution	GenScript
anti-β-Gal-NS3 AHSV-2	Antibodies raised in rabbits against a β-galactosidase AHSV-2 NS3 fusion protein which was expressed in *E. coli*	1:100 in 1% blocking solution	Dr M van Niekerk (Dept Gen, UP)

2.2.2. Plasmid isolation

Plasmid DNA was extracted by the alkaline-lysis method as described by Sambrook and Russel (2001), using principles originally discovered in 1979 by Birmboim and Doly. In this method 5 ml LB-broth (1% Bacto-Tryptone, 0.5% Bacto-Yeast extract, 1% NaCl pH 7.4) culture, containing the appropriate antibiotics (2.2.4) was inoculated with a single colony and was incubated overnight at 37°C in the shaking incubator. Centrifugation of the entire inoculum into a single eppendorf tube (1.5 ml) was done using the microfuge, at 13200 rpm for 3 minutes. The cell pellet was resuspended in 100 µl of Solution I (15 mM Tris-HCl pH = 8, 10 mM EDTA) and kept at room temperature for 5 minutes and then on ice for a period of 1 minute. After this time 200 µl of alkaline SDS buffer (0.2 N NaOH, 1% SDS) was added and the mixture was kept on ice for a time period of exactly 5 minutes after which 150 µl of 3 M Sodium Acetate was added. After centrifugation at 13200 rpm for 10 minutes, the supernatant was collected. The plasmid of interest was precipitated with two volumes 96% ethanol and collected via centrifugation in the microfuge at 13200 rpm for 12 minutes. The DNA pellet was washed with 1 ml of 80% ethanol. The pellet was air-dried and resuspended in 1x TE buffer (0.01 M Tris-HCl [pH 7.6], 0.001 M EDTA).

Plasmids to be used in transformations were purified using the Roche Highpure Plasmid Purification kit according to manufacturers' protocol.

2.2.3. Polymerase chain reaction (PCR)

Optimisation of annealing temperatures for PCR reactions was done in a Thermo Hybaid Multiblock Sytem (version 2.06, MBS 0.2G), all other reactions were performed in a Thermo PxE0.2 Thermocycler PCR system. Three DNA polymerases were used during this study: *GoTaq* (Promega), *ExTaq* (Takara) and *Pfu* (Promega). *GoTaq* was used for screening. *ExTaq* was used for the megaprimer method because it adds 3' TA overhangs needed for TOPO cloning. *Pfu* was used for the Quikchange method because of its proofreading and 3' to 5' exonuclease activity. Mutagenic primers are given in Table 7. The general primers used in combination with these were: NS3pBamF (CGGGATCCGTTTAAATTATCCCTTG) forward primer, the NS3pEcoR (CGGAATTCGAATGTCGTTATCCCGG) and eGFPHindR (GCAAGCTTTTACTTGTACAGCTCGTC) reverse primers, restriction sites within primers underlined.

Screening PCR reactions contained approximately 1.25 Units (U) of *GoTaq* Flexi DNA polymerase, 50 ng template DNA (or a single colony), 10 pmol of each primer, 1.25 mmol each of dATP, dTTP, dGTP and dCTP, 2.5 mM $MgCl_2$. This was made up to the 50 µl using Ultra High Quality water (UHQ). The PCR reaction conditions were as follows: template denaturation occurred at 95℃ for 5 min, this was followed by 30 cycles of denaturation at 95℃ for 50 sec; primer annealing for 1 min at a temperature determined using the primer sequences (Tm = 81.5 + 0.41(%GC) - 675/(number of bases)); a 2 min extension step at 72℃ was included. On completion of the 30 cycles a final elongation step was at 72℃ for 5 min and finally the samples were cooled to 4℃.

For the Megaprimer method, primers were designed using the Primer designer software (SciEdCentral, 1995) to contain the desired mismatch and tested *in silico.* The first PCR reaction was set up to contain 50 ng template DNA, 100 pmol of the mutagenic primer and complementary general primer 5 µl of 10x *ExTaq* polymerase buffer (500 mM KCl, 100 mM Tris.HCl, 1% Triton X-100), 1.25 U of *ExTaq* DNA polymerase and 2 µl of a 2.5 mM dNTP mixture. Reaction conditions were: Initial template denaturation at 95℃ for 5 min, followed by 30 cycles of denaturation at 95℃ for 50 sec, a primer annealing step for (30 to 60 sec) at a temperature gradient optimised temperature and an extension step at 72℃ for 1 min/kb. After a final elongation step at 72℃ for 5 min the samples were cooled to 4℃. For the second PCR step, with exception of the increased megaprimer and the template concentrations, the same reaction conditions were used.

For the Quikchange method, primers were designed using the PrimerX web-based program (website: http://bioinformatics.org/primerx/, 23-05-2008). The primers, which are completely complementary to each other, contain a mutation flanked by regions that are complementary to the template DNA. The reaction was set up to contain 25 ng template DNA, 10 pmol of each of the two mutagenic primers, 5 µl of 10x *Pfu* polymerase buffer (100 mM KCl, 200 mM Tris.HCl, 20 mM $MgSO_4$, 100 mM $(NH_4)_2SO_4$, 1 mg/ml nuclease free BSA, 1% Triton X-100), 1.25 U of *Pfu* DNA polymerase and 2 µl of a 2.5 mM dNTP mixture. Reaction conditions were: initial template denaturation at 95℃ for 5 min, followed by 30 cycles of denaturation at 95℃ for 50 sec, a primer annealing step for (30 to 60 sec) at a temperature gradient optimised temperature and an extension step at 68℃ for 2 min/kb. After a final elongation step at 72℃ for 20 min the samples were cooled to 4℃. The PCR products were subjected to *Dpn*I restriction enzyme digestion to remove the template plasmids.

Table 7: The following primers were used during the course of this study

Target domain	Mutant primer	Sequence (5'-3')	Mutation(s) introduced in sense strand	Amino acid change(s)
HD1	AHSVNS3s2TSΔIL Forward primer	AACTATGGCTATTCTTCTAGTTGGAGG	ACT>ATT TCT>CTT	TS127IL
	AHSVS3NS3TSΔILRev Reverse primer	CGCCATCAAGATAGCCATCGTTACGC	ACC>ATC TCG>TTG	TS128IL
	Qc_AHSVS3NS3TSΔILforw Forward primer	GGTGCGTAACGATGGCTATCTTGATGGCGGGCGGGTTAACG		
	Qc_AHSVS3NS3TSΔILrev Reverse primer	CGTTAACCCGCCCGCCATCAAGATAGCCATCGTTACGCACC		

HD2	AHSVNS3s2NΔI Forward primer	CCATGGTTTAATTTTGTTATGTAC	AAT>ATT	N161I
	AHSVS3NS3NΔI Rev Reverse primer	CACAGCAAAATCAAACCGTGAATC	AAT>ATT	N159I
	Qc_AHSVS3NS3 NΔIforw Forward primer	GAAGACGATTCACGGTTTGATTTT GCTGTGTACCACTATG		
	Qc_AHSVS3NS3 NΔIrev Reverse primer	CATAGTGGTACACAGCAAAATCAA ACCGTGAATCGTCTTC		
ISR	Qc_AHSVS2NS3 DΔS2forw Forward primer	GGAGGTATGTCTATCGTTAGTGA GGATATTGCTAAGC	GAT>AGT	D137S
	Qc_AHSVS2NS3 DΔS Reverse primer	GCTTAGCAATATCCTCACTAACGA TAGACATACCTCC		
	Qc_AHSVS3S10 DΔSForw Forward primer	CGGGCGGGTTAACGATTATTAGT AATGAAATATATGAAGACC	TGA>TAG	D138S
	Qc_AHSVS3S10 DΔSrev Reverse primer	GGTCTTCATATATTTCATTACTAAT AATCGTTAACCCGCCCG		

2.2.4. Agarose gel electrophoresis

This procedure was used throughout to monitor the success of the DNA manipulations and to determine the concentration and/or state of the DNA. The Thermo Electron EC320 minicel primo Electrophoretic gel system was used and powered by a Thermo EC250/90 power pack. A 35 ml 1% agarose gel was prepared from agarose and 1 x TAE buffer (40 mM Tris-HCI, 20 mM Na-Acetate, 1 mM EDTA). A volume of 2.5 µl of 10 mg/ml Ethidium bromide was added before the gel was set. It was placed in the electrophoresis tank and filled with 1 x TAE buffer until the gel was covered. A fifth of the sample volume of loading dye was added to samples to track the progress. A total of 10 µl was loaded per well when analysing samples and 20 to 30 µl when isolating DNA from gels. The gels were run at 120 V with constant field strength and visualized using UV visualization equipment. Images were captured using IC capture software version 2.00.257 by Imagingsource. A DNA molecular weight marker was loaded to track the progress of the migration and determine the size ranges of the proteins (Fig. 9).

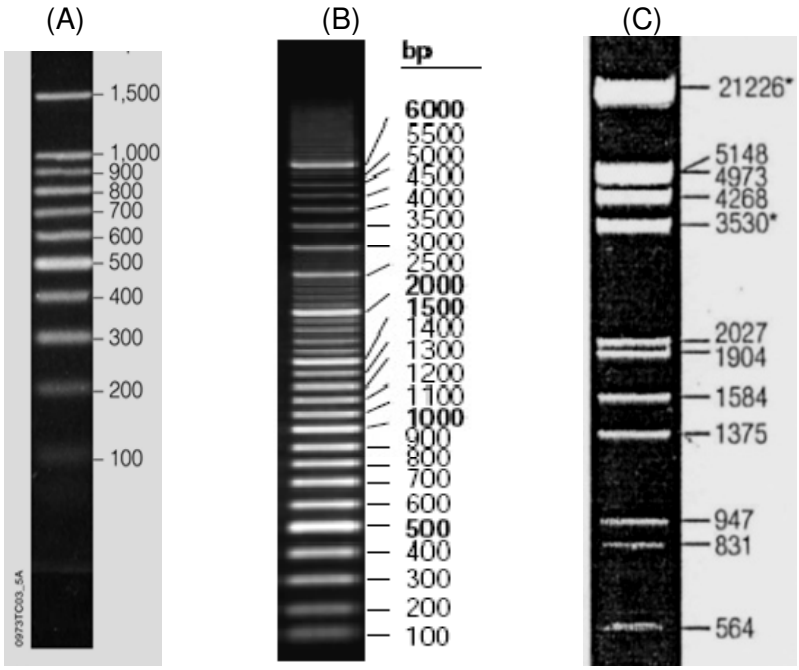

Figure 9: DNA molecular weight markers; 100 bp marker (A); 100/500 bp marker (B); Hind/Eco DNA ladder (C).

2.2.5. Gel purification

PCR amplification products were separated based on size by agarose gel electrophoresis. Amplicons of the correct size were excised from the gel under illumination of a UV light and DNA was isolated using the Roche Highpure PCR purification kit according to manufacturer's instructions.

2.2.6. DNA concentration and purity measurement

Measurement to determine concentrations were done using the Inqaba Biotec nanodrop ND-1000 spectrophotometer and software by Coleman technologies NanoDrop ND-1000 version 3.3. DNA concentration was obtained from absorbance at 260 nm. The presence of RNA contamination was deduced from the 260/280 nm refraction ratio and protein contamination from the 260/230 nm ratio.

2.2.7. Restriction enzyme digestion of DNA

Between 0.5 and 1 µg of DNA was added to 5 U of enzyme and 1 µl of the appropriate buffer and mixed on ice. UHQ water was added to give a final volume of 10 µl. The time and temperature of incubation varied according to the enzymes used. Reactions were incubated under controlled conditions in a Thermo PxE0.2 Thermocycler PCR system. The digested products were evaluated by agarose gel electrophoresis together with the relevant controls. Digestion with multiple enzymes were done in sequence with the enzyme with lowest salt buffer following the latter method. For the second digest 5 U of the second enzyme was added as well as 2 µl of the appropriate buffer, this was then topped up to 20 µl with UHQ water. If both enzymes used the same buffer then both were added simultaneously to the same reaction.

2.2.8. Preparation and electroporation of electrocompetent bacterial cells

A single colony of the cell type of interest (DH5α or DH10Bac) was inoculated into 7 ml of LB medium and incubated overnight at 37°C with shaking. Subsequently 2.5 ml of this overnight culture was inoculated into 250 ml of LB medium (containing the appropriate antibiotics). This was grown under the same conditions, monitoring growth continuously using GeneQuant pro RNA/DNA calculator. When an OD_{600} of 0.5 to 0.6 was reached, the culture was divided into two pre-chilled 250 ml centrifuge bottles and stored on ice for 20 min. Subsequently, the cells were collected by means of centrifugation at 5000 rpm for 10 min at 4°C using a Sorvall RC 5B *plus* centrifuge. The supernatant was discarded and 120 ml prechilled distilled water was added. The pellet was resuspended by swirling and then centrifuged again as above and the process repeated. The pellets were resuspended in 5 ml of a 10% glycerol solution and the suspension was transferred into 50 ml centrifuge tubes and incubated on ice for 60 min. After incubation the cells were centrifuged at 5000 rpm for 10 min. After discarding the supernatant the cells were resuspended in 0.5 ml of 10% glycerol, this was then aliquoted in 60 µl volumes into 1.5 ml eppendorf tubes and frozen away at -70°C for later use in electroporation.

A mixture containing ice thawed electrocompetent cells (60 µl) and the DNA sample to be transformed (10-50 ng) was set up and pipetted into prechilled (-20°C) cuvettes. The cuvettes were inserted into the electroporator and pulsed at 2000 V. Acceptable values after the event being above 1500 V and the time constant between 3 and 5 seconds. 100 µl S.O.C. medium was added into the cuvette directly after pulsing, cells were then transferred into 900 µl of prewarmed LB medium. This mixture was then incubated at 37°C with shaking for 1 h after which 25 µl, 50 µl and 100 µl volumes were plated onto selective media and incubated overnight. Efficiency was evaluated on the following day.

2.2.9. TOPO cloning

Cloning was done according to manufacturers' protocol (Invitrogen). This entailed creating TA overhangs by using high fidelity *ExTaq* polymerase in a PCR reaction. A saline solution containing the PCR product and the PCR8/GW/TOPO vector (Spc^R) was incubated at room temperature for 5 min. A volume of 2 µl of this solution was added to Oneshot Top10 chemically competent ($Spec^S$) cells (Invitrogen) and mixed gently by stirring. After incubation on ice for 30 min the mixture was subjected to 42°C for 30 sec in a Julabo P Protea waterbath and placed directly back on ice. A volume of 250 µl of S.O.C. medium (Invitrogen) was added and the tube incubated at 37°C with shaking (200 rpm) for 1 h. After this time, between 10 µl to 50 µl of the mixture was spread on LB plates containing 100 µg/ml spectinomycin.

2.2.10. Sequencing and sequence analysis

Cycle sequencing reactions were performed in the Thermo PxE0.2 Thermocycler PCR system using the Prism Big Dye Terminator Cycle Sequencing Ready Reaction Kit™, V. 3.0. (Perkin Elmer Applied Biosystems). Half sequencing reactions were set up using 250 ng of template DNA, 4 µl of BigDye ready reaction mix, 10 pmol of primer and distilled water to make up a total volume of 10 µl. Reactions were performed using the following thermo-cycle parameters: 96°C for 10 seconds; 50°C for 5 seconds and 60°C for 4 min repeated for 25 cycles. DNA was precipitated using 2 µl of 3 M sodium acetate (pH 4.6) and 50 µl of ice cold 96% ethanol. The DNA was collected by centrifugation at 13200 rpm for 30 min. The pellet was washed three times with 70% ethanol by centrifugation (13200 rpm for 5 min). Pellets were air dried and resuspended in loading buffer (5 parts Formamide to 1 part 25 mM EDTA pH8 containing 50 mg/ml blue dextran). Samples were analysed using an ABI PRISM 377 automated sequencer. Sequences were analysed using Vector NTI v9.1.0 and annotated in

CLC Main Workbench. 5.1 (SciEdCentral, 1995). Primers used for sequencing were NS3pBamF, NS3pEcoR and the primers given in Table 8.

Table 8: Additional primers used for sequencing

Primer	Sequence (5'-3')
NS3StopEcoR	GCGAATTCGCTGTCGCCATATTTTAC
eGFPHindR	GCAAGCTTTTACTTGTACAGCTCGTC
M13F	TGTAAAACGACGGCCAGT
M13R	CAGGAAACAGCTATGACC'
eGFPintR	GGGCATGGCGGACTTGAAGAAG

2.2.11. LR recombination reaction

A mixture was set up containing 150 ng of destination vector (pDest8), 100 ng of the entry clone (TOPO) and 10 U of clonase II enzyme and incubated overnight at 25°C. After incubation 5 U of proteinase K was added and the sample was incubated at 37°C for 10 min. The reaction was then placed on ice and directly transformed into DH5α cells by means of electroporation. Cells were plated on LB plates containing 100 µg/ml ampicillin.

2.2.12. Generation of recombinant bacmids

Using the Gateway™ method originally described by Luckow in 1993, recombinant baculoviruses were generated. Recombinant pDest8 ($Gent^R Amp^R$) plasmids containing the insert were transformed into DH10bac *E. coli* using electroporation. DH10Bac ($Kan^R Tet^R$) *E. coli* contain the Autographa californica multiple nucleopolyhedrosis virus genome (bMON14272), called the bacmid. The cells were then plated on LB plates containing 10 µg/ml tetracycline, 7 µg/ml gentamycin, 50 µg/ml kanamycin, 40 µg/ml of IPTG and 100 µg/ml of X-gal and incubated at 37°C for 48 h. A bacmid contains a LacZα to enable α-complementation of the β-galactosidase gene for blue/white screening. Cells containing recombinant bacmids were identified by their white colour. Replica plating was done to verify that white colonies where true recombinants.

2.2.13. Storage

Bacterial cultures to be stored at -70°C were made up to contain a final concentration 15% sterile glycerol. These were mixed and frozen.

DNA samples were stored at -20°C in either 96% ethanol or UHQ water.

2.2.14. *Spodoptera frugiperda* (Sf9) tissue culture

Sf9 cells were obtained from American Type Cell Collection. Tissue culture methods were done according to the BAC-to-BAC™ Baculovirus expression system manual (Invitrogen). The Sf9 cell cultures were maintained in 50-100 ml cultures in Pyrex flasks at 27°C. Cells were grown in complete medium (TC-100 Insect Medium (Highveld Biological) supplemented with antibiotics (1.2% penicillin, streptomycin and Fungizone (Highveld Biological)), 10% vol/vol foetal calf serum (Highveld Biological), and 0.8% pleuronic fluid (Highveld Biological)). Cultures were monitored daily to ensure optimal growth and cell viability. Prior to transfection or infection Sf9 cells were seeded either in confluent monolayer cultures or as suspension cultures, depending on the experiment (Table 9). Cells

were counted using a Bright-Line haemocytometer (Hausser scientific) under a Nikon TMS E100.25 light microscope (10 x Nikon objective (160/-) Ph1DL).

Table 9: Sf9 cell densities used for different applications

Culture	Cell concentration
96-well plate	3.0 x 10^4 cells/well
35mm 6-well plate	1.0 x 10^6 cells/well
25cm^3 flask	3.5 x 10^6 cells/flask
75 cm^3 flask	1.0 x 10^7 cells/flask
spinner (30-200 ml)	1.0 x 10^6 cells/ml

2.2.15. Transfection to produce recombinant baculoviruses

A volume of 2 ml of LB broth containing 7 µg/ml gentamycin, 50 µg/ml kanamycin, and 10 µg/ml tetracyclin was inoculated with the colony containing the recombinant bacmid and incubated for 24 h at 37°C. Cells were pelleted into a 1.5 ml eppendorf tube by centrifugation at 13200 rpm for 10 min. The pellet was resuspended in 300 µl of Solution I (15 mM Tris-HCl pH8, 10 mM EDTA) and 300 µl of Solution II (0.2 N NaCl, 1% SDS) was added and incubated at room temperature for 5 min. A volume of 300 µl of 3 M potassium acetate pH5.5 was added, incubated on ice for 10 min and centrifuged for 10 min at 13200 rpm. The supernatant was transferred to a new eppendorf containing 800 µl of absolute isopropanol, gently mixed and placed on ice for 10 min. Centrifugation was done for 15 min at 13200 rpm and the pellet was washed thrice with 70% ethanol. After air drying in sterile conditions the sample was resuspended into 40 µl of sterile UHQ water. The sample was used to prepare Solution A (5 µl Bacmid DNA in 100 µl SF-900 II Serum free medium (SFM)). This was mixed with solution B (6 µl Cellfectin (invitrogen) in 100 µl SF-900 II SFM) and incubated for 45 min at room temperature, after which 800 µl SF-900 II SFM was added. This preparation was added to Sf9 cells preseeded in a 35mm well of a 6-well plate. This was incubated overnight at 27°C and the following morning the medium was removed and 3 ml of complete medium was added. A mock-infected negative control was done with each transfection. Cells were monitored for cytopathic effect using a Nikon TMS E100.25 light microscope (10 x Nikon objective (160/-) Ph1DL). After four days, if 80% cell death was observable in transfection as opposed to high cell viability in negative control, cells were harvested. Supernatants were used to infect a 25cm^2 flask in order to amplify virus. After seven days or when 80% cell death was visible, the cells and virus were harvested.

2.2.16. Virus/Cell Harvest

Cells were removed from the growth surface using a 1 ml pipette and then transferred into a sterile tube. Cells were collected by centrifugation at 3000 rpm for 10 min at 4°C in a Beckman/Coulter Avanti J-E using a JS5.3 Rotor. The supernatant containing the virus was transferred into a new tube, labeled and stored away for future use. The cell pellet was resuspended in 1 ml of sterile 1x PBS and recentrifuged using the above variables in order to remove protein contaminants such as serum albumin, which may interfere with clarity of SDS-PAGE gels.

2.2.17. Titration and plaque purification of baculoviruses

Viral plaque assays were performed as described in the BAC-to-BAC™ Baculovirus expression system manual (Invitrogen) were used to determine viral titres. Sf9 cells were seeded at 8.5 x 10^5 Sf9 cells/35mm well (approximately 55% confluency) and allowed to

attach for 1 h. A ten-fold dilution series of a baculovirus stock was prepared using incomplete medium. The medium on Sf9 cells was replaced with 500 µl of the appropriate dilution. A solution of 2% w/v Agarose, Type VII (Sigma) was prepared in UHQ water, boiled and cooled to about 50°C, and diluted to 1% agarose by addition of an equal volume prewarmed double strength Grace's medium (Highveld Biological). Dilutions were aspirated and replaced with 2 ml/well 1% agarose. Cells were incubated for 7 to 10 days at 27°C until plaques were visible. These were then stained with 500 µl of 0.1% w/v Thiazolyl Blue Tetrazodium Bromide (3-[4,5-dimethyltiazol-2-yl]-2,5-diphenyltetrazolium bromide) (Sigma) in 1x PBS and left for 24 h at 27°C. The number of plaques in each dilution were counted and used to calculate the viral titre. The titre (pfu/ml) was calculated as 2 x number of plaques x dilution factor.

Plaque purifications of viral stocks were carried out as described above, but cells were not stained after the 7 to 10 day incubation. At this stage, single plaques were collected and resuspended in 1 ml complete medium. These purifications were used to infect Sf9 cells seeded on a 6-well plate for viral amplification.

2.2.18. Infection of Sf9 cells cultures with baculovirus for recombinant protein expression

As described in the BAC-to-BAC™ Baculovirus expression system manual (Invitrogen) the volume of inoculum used was calculated by means of the following equation:

$$\text{Volume of inoculum required (ml)} = \frac{\text{Desired M.O.I. x Total nr cells}}{\text{Titer of viral inoculum}}$$

The culture medium was removed from Sf9 cell monolayers and replaced with the calculated volume of virus, supplemented with medium to cover all the cells. This was incubated for 3 h at 27°C to allow infection. After this time complete medium was added to allow a constant final volume for each infection. For Sf9 spinner cultures with 10^6 cells/ml (volume varying between experiments) cells were pelleted at 1000 rpm for 10 min. Cells were resuspended in the calculated inoculum incubated for 3 h at 27°C. Following this cells were collected by centrifugation at 1000 rpm for 10 min. The virus containing supernatant was discarded and the cellular pellet was resuspended in the desired volume complete medium.

2.2.19. Sodium dodecyl sulphate polyacrylamide gel electrophoresis (SDS-PAGE)

Protein gels were made using the discontinuous stacking system devised by Ornstein in 1964. The omniPAGE mini or mini wide PAGE systems from Cleaver Scientific were used for PAGE analysis. A separating gel (12% or 15% polyacrylamide, 0.375 M Tris-HCl, pH8.8, 0.1% SDS, 0.008% TEMED and 0.08% ammonium persulphate) was overlayed with a 5% stacking gel (5% polyacrylamide, 0.125 M Tris-HCl, pH 6.8, 0.1% SDS, 0.008% TEMED and 0.08% ammonium persulphate) in a ratio of 2:1. Cell extracts containing the protein were prepared in a lysis buffer (specific to the experiment of interest). One third volume of 3 x PSB was added to the solution given a final concentration of 1x PSB (4% SDS, 20% glycerol, 10% 2-mercaptoethanol, 0.005% Bromophenol Blue, 0.125 M Tris-HCl pH 6.8). The solution was boiled for 3 min at 95°C and was then loaded into the wells of the stacking gel and the gel was run at 130 V (Thermo EC250/90 power pack). The Pageruler™ Rainbow protein molecular weight marker was loaded to track the progress of the migration and determine the size ranges of the proteins (Fig. 10).

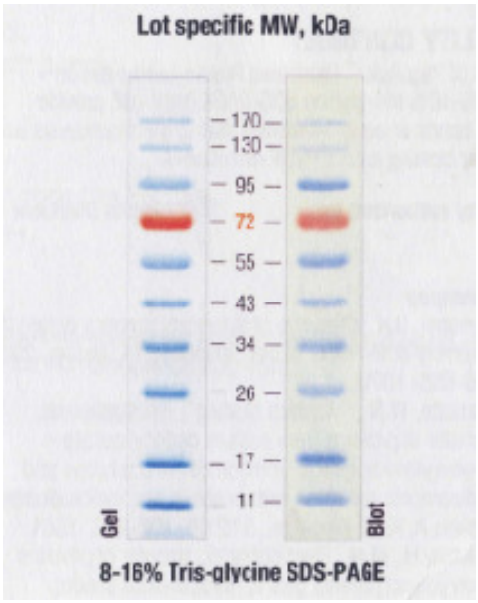

Figure 10: Pageruler Rainbow marker (Fermentas).

2.2.20. Western blot

Using concepts described by Towbin *et al*. (1979) Western blots were performed. Proteins were transferred from SDS-PAGE gels to nitrocellulose filters (Hybond TM-C; Amersham Biosciences) using an omniPAGE mini or mini wide (Cleaver Scientific) system. The gels and nitrocellulose membranes were soaked in transfer buffer (0.025 M Tris, 0.15 M glycine, 20% methanol pH8.3) for 20 min before blotting. Transfer was done at 0.13 A for 1 h. Following transfer, the nitrocellulose membrane was washed three times in 1x PBS and incubated in 1% milkpowder in 1x PBS for 30 min at room temperature. After this time, the primary antibody was added and this was incubated for 24 h at 4°C with agitation. The membrane was washed three times in washing buffer (0.05% Tween in 1x PBS) for 5 min. The membrane was then incubated in a 1:1000 dilution (in 1% blocking solution) of protein A peroxidase conjugate (Calbiochem) at room temperature for 1 h with agitation. The membrane was washed three times in washing buffer for 5 min each and once in 1x PBS. Membrane was placed in substrate (60 mg 4-chloro-1-naphtol in 20 ml ice cold methanol, 60 µl Peroxide in 100 ml 1x PBS) and was then incubated in the dark. When bands were visible, the membrane was rinsed with distilled water to stop the reaction.

2.2.21. Membrane flotation assay

Membrane flotation analysis was optimised in our laboratory from a protocol that was used by Brignati *et al*. (2003) (Beyleveld, 2007; Brignati *et al*., 2003; Hatherell, 2007; Meiring, 2009a). Sf9 cells seeded a 10^6 cells per 35mm well of a 6-well plate, were infected with recombinant baculoviruses at M.O.I. of 10 pfu/cell and incubated at 27℃. The cells were harvested after a 24 h incubation period at 27℃ and collected by centrifugation at 3000 rpm for 10 min. Cells were washed twice with 1x PBS and were resuspended in 300 µl hypotonic buffer (10 mM Tris, 0.2 mM $MgCl_2$, pH7.4, containing protease inhibitors Pepstatin and Pefabloc, maximum amounts recommended by manufacturer (Roche)). Cells were incubated on ice for 30 min followed by five passages through a 22G needle to facilitate cell rupture. Nuclei were not removed prior to flotation due to the loss of significant amounts of protein (Hatherell, 2007). A volume of 250 µl of the lysed cells was combined with 1340 µl 85% sucrose in 1 x NTE (100 mM NaCl, 10 mM Tris, 1 mM EDTA [pH 7.4]) to give a final sucrose concentration of 72%. This was loaded into a 5 ml polyallomer tube (Beckman). This fraction was overlaid with 2320 µl 65% sucrose in 1 x NTE and 1090 ml 10% sucrose in 1 x NTE. Gradients were centrifuged at 38000 rpm for 18 h at 4℃ in a Beckman SW55Ti rotor

using the Beckman Coulter OptimaTM L-100 XP Ultracentrifuge. No brake was employed after centrifugation was completed. Fractions of 500 µl were collected from the bottom of the tube through a needle. The pellet was resuspended in 500 µl of 1x NTE. Fractions were assayed by SDS-PAGE and Western blot. These were quantified by EZQuant software and the values were plotted as a line graph in Microsoft Office Excel 2007. eGFP and fusion constructs fluorescence was measured using the BioRad Versafluor^{TM} fluorometer with filters (485–495$_{Ex}$/515–525$_{Em}$) these values were also plotted as a line graph.

2.2.22. Subcellular fractionation

Sf9 cells were seeded at 1 x 10^6 cells/35mm well of a 6-well tissue culture plates. Cells were infected at a M.O.I. of 10. At 24 h.p.i. cells were harvested and the cell pellet was collected by means of centrifugation at 3000 rpm for 10 min at 4^{o}C. The cell pellet was washed twice in 1 ml 1x PBS. The cell pellet was resuspended in 300 µl of hypotonic buffer (10 mM Tris, 0.2 mM $MgCl_2$, pH7.4, containing protease inhibitors 1mg/ml Pefabloc (Roche)) and then incubated on ice for 30 min. The cells were lysed by means of six serial passages through a 22G needle. The unbroken cells and nuclei were collected by means of centrifugation at 1500 rpm for 2 min (nuclear fraction). The supernatant was then transferred into a new 1.5 ml Eppendorf tube. In order to ensure that nuclei were separated completely from other fractions the pellet was washed in 50 µl of the hypotonic buffer. The supernatant was transferred into the Eppenderf tube containing the previous supernatant. This supernatant was subjected to centrifugation at 13000 rpm, 4^{o}C for 1 h in order to pellet the insoluble material (particulate fraction). The supernatant from this step was transferred into a new eppendorf tube (soluble fraction). The pellets from all fractions were resuspended in 1x PBS. All fractions were made up to a final volume of 500 µl and stored at -20^{o}C for subsequent SDS-PAGE and Western blot analysis.

2.2.23. Immunofluorescence microscopy

Immunolabelling was performed using optimised conditions (van der Sluis, 2007). Approximately 10^6 Sf9 cells were seeded on top of sterile Esco coverslips (22 mm x 22 mm) which had been placed in the 35mm wells of a 6-well tissue culture plate. Cells were infected at a M.O.I. of 10 and incubated for 24 h at 27^{o}C. Medium was removed and cells were washed twice in 2 ml 1x PBS by means of gentle agitation for 5 min at a time. Proteins were then fixed by incubation in ice-cold 50% (v/v) methanol:acetone for 2 min. Cells were again washed once in 1x PBS as described above. The cells were then incubated in 5% blocking solution (milkpowder in 1x PBS) for 30 min. Following this the coverslips were transferred to a humidified container and 200 µl of primary antibody was added and incubated in the dark overnight. Coverslips were then placed in a new 6-well plates and washed thrice with 2 ml 0.5% (v/v) Tween20 in 1x PBS via gentle agitation for 5 min at a time. Coverslips were incubated with 200 µl of secondary antibody in the dark for 45 min. Cells were washed thrice with ml 0.5% (v/v) Tween20 in 1x PBS and then once in 1x PBS. Cells were stained with 200 µl 10 µg/ml 4'6'-diamidino-2-phenylindole (DAPI) for 15 min. Coverslips were then mounted onto slides in VECTASHIELD mounting medium (Vector Laboratories) in order to prevent/decrease photobleaching. Slides were stored at 4^{o}C in the dark.

Slides were analysed using the Zeiss LSM510 META Laser Scanning Microscope and images were captured using Zeiss LSM Image Browser Version 4.0.0.157. eGFP and Alexa488 were detected at 489nm and DAPI at 405nm.

2.2.24. Trypan blue cell viability assay

A 50 ml Sf9 cell spinner culture with 10^6 cells/ml was pelleted at 1000 rpm for 20-30 min. Cells were resuspended in an inoculum of recombinant baculoviruses at a M.O.I. of 10 pfu/cell. TC-100 medium was added a final volume of 50 ml. Cells were incubated with shaking at 27°C. Aliquots were harvested at 18, 24, 30, 36, 42 and 48 h.p.i., stained in an equal volume 0.4% Trypan blue (Sigma) and counted using a haemacytometer.

2.2.25. CellTiter-Blue™

The CellTiter-Blue™ cell viability assay was used to monitor cytotoxicity and was done according to the manufacturer's instructions (Promega). Sf9 cells were seeded on 96-well plates were infected with virus strains at a M.O.I. of 10 pfu/cell as described above. A volume of 50 µl CellTiter-Blue™ reagent was added per well at 24 and 48 h.p.i. and cells incubated at 27°C for a further 3 h. Fluorescence at 530-570$_{Ex}$/580-620$_{Em}$ was recorded (Fluoroskan Ascent FL Type 374 (ThermoLabsystems) using Ascent Software Version 2.4.2.). Background fluorescence was estimated by including wells with serum supplemented MEM in the absence of cells. Additional controls included nonviable cells and mock infected cells. The percentage viable cells was calculated by fluorescence of infected as a percentage of the fluorescence in wells containing mock infected cells.

2.2.26. Statistical analysis

Mean and standard deviations (SD) were calculated using Excel and the differences cytotoxic phenotypes were tested for significance by Student's *t* test using online statistics software (http://www.graphpad.com/quickcalcs/ttest1.cfm?Format=SD).

2.3. Results

The aim of this study was to determine the roles of specific motifs in the subcellular localisation and cytotoxicity of AHSV NS3 protein. These motifs were a threonine-serine (TS) in hydrophobic domain one (HD1), an aspartic acid (D) residue in the intervening spacer region (ISR) and an asparagine (N) residue in the second hydrophobic domain (HD2). In order to do this we planned to produce nine different plasmid clones containing mutant versions of the AHSV S10 gene segment (summarised in Table 10), these would subsequently be used to generate recombinant baculoviruses expressing mutant versions of the NS3 protein. Two strategies were employed in order to generate the site directed mutant S10 gene sequences of AHSV-2 and AHSV-3, the Megaprimer method and the Quikchange method. Eight of the nine mutant NS3 proteins were successfully cloned and expressed as recombinant baculoviruses.

Table 10: Mutant AHSV NS3 constructs generated during the course of this project

Construct	Mutation	Motivation	Method successfully used to generate
AHSV-2-S10 TS127IL	HD1 TS at position 127/128 changed to IL	TS placement similar to motifs involved in protein folding. Both are polar residues that may form hydrogen bonds and drive alpha helix formation. Change to I and L which are both non-polar	Megaprimer method
AHSV-3-S10 TS128IL			Quikchange Method
AHSV-3-S10 eGFP TS128IL			Quikchange method
AHSV-2-S10 N161I	HD2 N at position 161/159 changed to I	N residues are able to drive alpha helix formation by intra-helical bond formation. Change to I which is non-polar	Megaprimer method
AHSV-3-S10 N159I			Megaprimer method
AHSV-3-S10–eGFP N159I			Could not be produced
AHSV-2-S10 D137S	ISR D at position 137/138 changed to S	D is a hydrophilic amino acid that may form hydrogen bonds. Changed to a S because serine has a neutral charge and is hydrophilic	Megaprimer method
AHSV-3-S10 D138S			Quikchange method
AHSV-3-S10-eGFP D138S			Quikchange method

In order to generate recombinant baculovirus expressing the desired proteins, a specific strategy was employed (Fig. 11). In this strategy, a PCR8/GW/TOPO (TOPO) entry clone containing the mutant AHSV S10 insert was produced. The insert was transferred to the destination vector pDest8 containing the polyhedrin promoter via an enzyme catalyzed reaction. The mutant AHSV S10, together with the polyhedrin promotor was transferred

from the pDest8 to baculovirus genome (Bacmid) by spontaneous recombination. Bacmids were used to produce recombinant baculovirus expressing the desired protein.

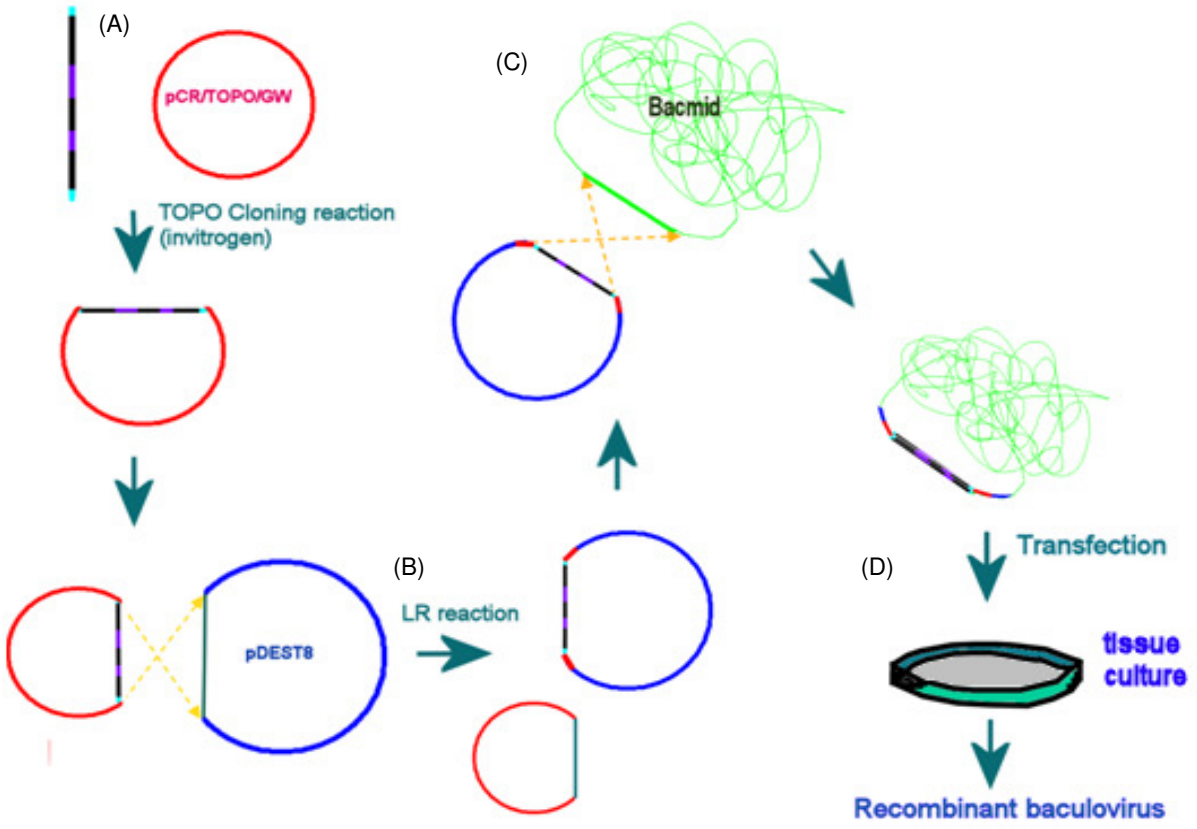

Figure 11: Strategy for producing recombinant baculoviruses; TOPO cloning (A); LR into pDest8 (B); Spontaneous recombination into bacmid (C); Transfection into Sf9 cells for generation of recombinant baculoviruses (D).

2.3.1. Generation of TOPO plasmid clones containing various mutant S10 gene sequences

2.3.1.1. The Megaprimer method

The first step was to produce modified versions of the S10 gene segment and to clone the segments into a TOPO plasmid vector. The first approach employed was the PCR based Megaprimer site-directed mutagenesis method (the basic principles are illustrated in Fig. 12). Kammann et al. (1989) originally developed this method. In brief, the mutation- containing megaprimer method entails two PCR reactions where specific primer combinations are used to produce site-directed mutations. In the first PCR, a mutant internal primer (containing designed mismatches) is used in combination with a general primer to produce the

megaprimer. The megaprimer is then used together with a corresponding general primer in a second round of amplification to produce a PCR product that contains a modified version of the gene of interest, in this case the NS3 coding region. This PCR product is purified and cloned into a suitable vector. The TOPO plasmid vector was used because it is compatible with the Gateway system for generating recombinant baculoviruses. Cloning was performed using the TOPO TA cloning kit from Invitrogen™.

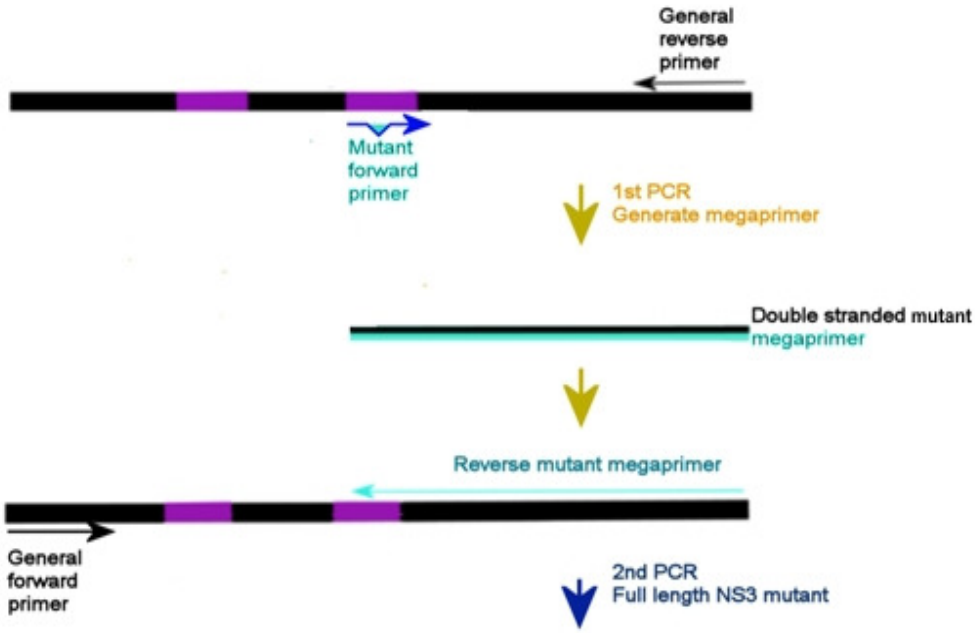

Figure 12: Principles of the Megaprimer method for site-directed mutagenesis.

Using this approach, we initially planned to make nine different constructs; however, the success rate using this method was not exceptional (Table 11). As a result, generation of only seven of these constructs was attempted using this method, i.e. AHSV-2-S10 (TS127IL, N161I and D137S), AHSV-3-S10 (TS128IL and N159I) and AHSV-3-S10 (TS128IL and N159I). Several primers were designed and tested, but most could not be used successfully to generate TOPO clones containing the desired mutation (Table 12). Some of the primers were designed for use in the Quikchange method (primer labels start with "Qc_") but could not be used successfully in that protocol (see later), these were then employed in the Megaprimer method. What worked for one construct would not necessarily work for another. Most often problems were encountered during the second round of amplification, where the megaprimer was to be used as a primer. Attempts at optimization, as substantiated by the

literature, included temperature gradient PCR (40-70°C); varying primer and template concentrations and adjusting annealing times (Barettino *et al.*, 1994; Barik, 1995; 1996; 1997a; b; 2002; Barik & Galinski, 1991; Brons-Poulsen *et al.*, 1998; Burke & Barik, 2003). Although it was attempted to generate seven constructs using this method, only four constructs were successfully produced. In order to illustrate the execution of this method specific results pertaining only to the generation of the TOPO-AHSV-3-S10 N159I mutant will be discussed in detail, while giving selected results for the other three.

Table 11: Summary of primer combinations and amplification results using the megaprimer approach to generate S10 mutants

Construct	Mutation	Template	Round 1 Megaprimer PCR Primer combinations	Successful amplification round 1 (Yes/No)	Round 2 primer combination	Successful amplification round 2 (Yes/No)	Mutation present (Yes/No)
AHSV-2-S10 TS127IL	TS127IL	pFastbac-AHSV-2-S10	AHSVNS3s2TSΔIL and NS3pEcoR	Yes	NS3pBamF and megareverse	Yes	Yes
AHSV-3-S10 TS128IL	TS128IL	pFastbac-AHSV-3-S10	AHSVS3NS3TSΔILRev and NS3pBamF	Yes	NS3pEcoR and megaforward	Yes	No (wild type cloned)
AHSV-3-S10-eGFP TS128IL		pFastbac-AHSV-3-S10-eGFP	AHSVS3NS3TSΔILRev and NS3pBamF	Yes	eGFPHindR and megaforward	No	No
AHSV-2-S10 N161I	N161I	pFastbac-AHSV-2-S10	AHSVS2NS3NΔI and NS3pEcoR	Yes	NS3pBamF and megareverse	Yes	Yes
AHSV-3-S10 N159I	N159I	pFastbac-AHSV-3-S10	AHSVS3NS3NΔIRev and NS3pBamF	Yes	NS3pEcoR and megaforward	Yes	No (wild type cloned)
			Qc_AHSVS3NS3NΔIForw and NS3pEcoR	Yes	NS3pBamF and megareverse	Yes	Yes
AHSV-3-S10-eGFP N159I		pFastbac-AHSV-3-S10-eGFP	AHSVS3NS3NΔIRev and NS3pBamF	Yes	eGFPHindR and megaforward	No	No
			Qc_AHSVS3NS3NΔIrev and NS3pBamF	Yes	eGFPHindR and megaforward	No	No
AHSV-2-S10 D137S	D137S	pFastbac-AHSV-2-S10	Qc_AHSVS2NS3DΔSForw and NS3pEcoR	Yes	NS3pBamF and megareverse	No	No
			Qc_AHSVS2S10DSRev and NS3pBamF	Yes	NS3pEcoR and megaforward	Yes	Yes

For generating the AHSV-3-S10 N159I, the first round of amplification was performed using the NS3pEcoR and Qc_AHSVS3S10NΔIForw primers and the pFastbac-AHSV-3-S10 plasmid as a template (prepared by plasmid isolation). The PCR reaction was optimised by temperature gradient PCR (not shown). Using the optimised conditions, a megaprimer of around 313 bp was produced (as expected) without any non-specific amplification (Fig. 13 lane 2). The PCR product (megaprimer) was gel purified. After isolation, the PCR product

was visualized via gel electrophoresis in order to determine extraction efficiency (not shown). The desired product was in adequate amounts as judged by intensity of fluorescence.

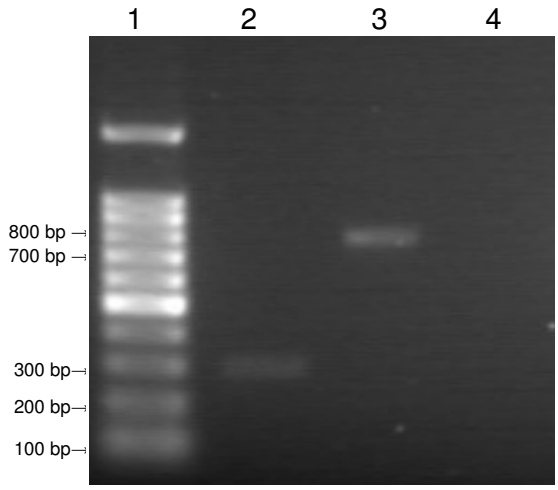

Figure 13: Agarose (1%) gel of the PCR reactions used to produce the AHSV-3-S10 N159I megaprimer; 100bp DNA marker (1); AHSV-3-S10 N159I megaprimer PCR (2); positive control (3); negative control (4).

A second PCR was performed using the purified megaprimer as a reverse primer and the NS3pBamF general forward primer on the pFastbac-AHSV-3-S10 plasmid template. The annealing temperature was optimised using a temperature gradient PCR in order to produce the full-length AHSV-3-S10 N159I (about 766 bp) with the least non-specific amplification (Fig. 14 A). The optimal annealing conditions were found to be 63.4^{o}C (Fig. 14 A lane 9). Using the optimized conditions, the reaction was performed (Fig. 14 B lane 16). The PCR product was gel purified and evaluated via agarose gel electrophoresis in order to determine extraction efficiency (Fig. 14 B lane 17). The purified product was cloned into the TOPO vector and transformed into Oneshot Top10 chemically competent *E. coli*.

(A) 1 2 3 4 5 6 7 8 9 10 11 12 13 (B) 14 15 16 17

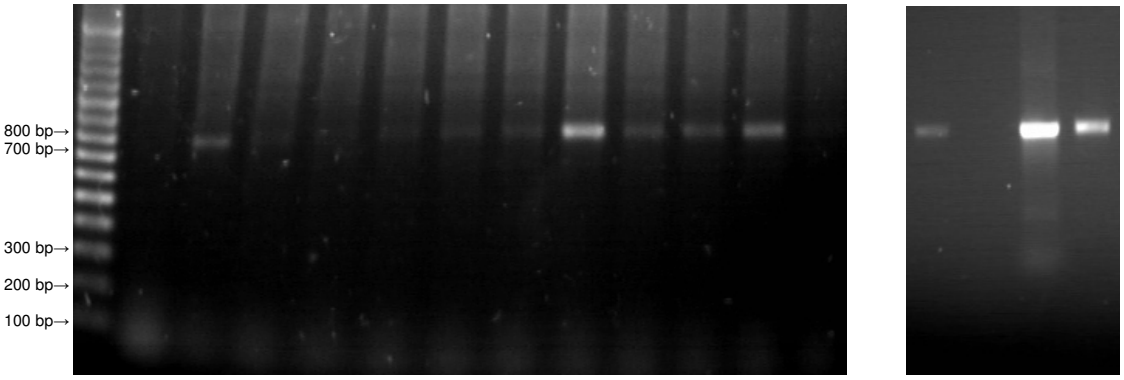

Figure 14: Agarose (1%) gels of the temperature gradient PCR (A) and optimized PCR (B) producing the full length AHSV-3-S10 N159I; 100/500bp DNA marker (1); negative control (2, 15); PCR with annealing temp of 55.5°C (3), 56.5°C (4), 57.5°C (5), 58.5°C (6), 59.5°C (7), 61.4°C (8), 63.4°C (9), 65.4°C (10) 67.6°C (11), 69°C (12), 69.8°C (13); positive control (14); AHSV-3-S10 N159I amplification at 63.4°C before (16) and after (17) gel purification.

The transformed cells were streaked out on agar plates containing Spectinomycin and single colonies were picked for screening. Plasmids were isolated by miniprep plasmid isolation and evaluated via agarose gel electrophoresis. The differences in migration profile between the non-recombinant (smaller) and the recombinant (larger) TOPO plasmids was used as an indication of the presence of the desired inserts (Fig. 15). The same procedure was used to clone the other five constructs indicated by "Yes" in column 7 of Table 11 (results not shown). These clones were then all analyzed by restriction enzyme digestion and sequencing.

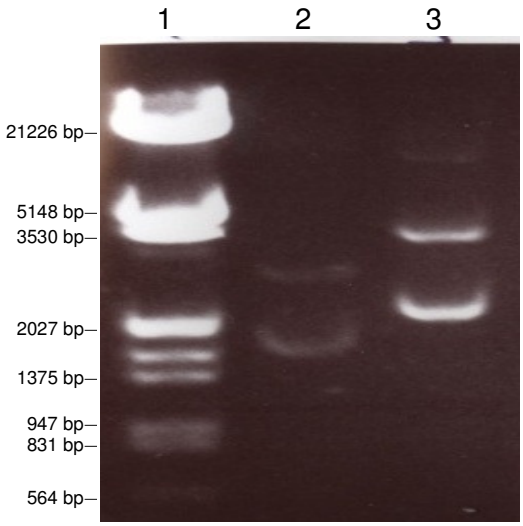

Figure 15: Agarose (1%) gel of the TOPO-AHSV-3-S10 N159I recombinant plasmid; Hind/Eco DNA marker (1); non-recombinant TOPO (2); TOPO-AHSV-3-S10 N159I (3).

The non-recombinant TOPO is 2817 bp in size with one *Eco*RV site at a distance of 100 bp downstream of the multiple cloning site. According to the available template sequence data,

the AHSV-2-S10 and AHSV-3-S10 both had a unique *Bam*HI site at the 5' end of the gene (from the original cloning strategy). Subsequently by digesting with *Eco*RV and *Bam*HI one could confirm the presence and the orientation of the insert. If the cloned insert is present in the correct orientation, two products should be present (866 bp and 2717 bp). This was true for TOPO-AHSV-2-S10 TS127IL, N161I and D137S (Fig. 15 lanes 5 to 7). However, in the case of TOPO-AHSV-3-S10 N159I, digestion yielded three products of respectively a 100 bp (indicated by arrow), 766 bp and 2717 bp (Fig. 15 lane 4). To clarify this discrepancy, samples were sequenced using M13Forw and M13Rev primers. The original template (pFastbac-AHSV-3-S10) was also sequenced. The sequences were analyzed using Vector NTI v9.1.0 in which forward and reverse sequences were aligned and used to construct a contig. It was found that in the pFastbac-AHSV-3-S10 template, the AHSV-3 NS3 gene was flanked by two *Bam*HI restriction sites. This was not the case for the pFastbac-AHSV-2-S10 template. This provided an explanation for the presence of the additional 100 bp fragment obtained in the digestions. Further evaluation of the sequences allowed the confirmation of the presence of the full length open reading frames (ORFs) of the NS3 protein in the clones TOPO-AHSV-3-S10 N159I, TOPO-AHSV-2-S10 TS127IL, N161I and D137S. With the exception of the desired mutations there were no additional mutations (APPENDIX A) and these four constructs could thus be used for expression.

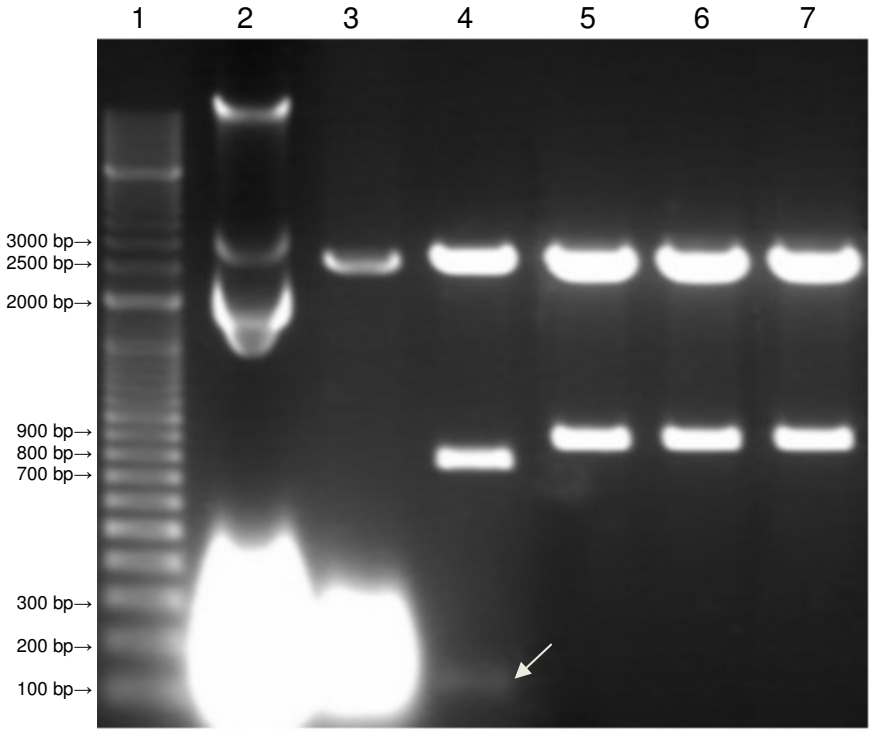

Figure 16: Agarose (1%) gel of the *Eco*RV/*Bam*HI double digests of TOPO constructs; 100/500 bp DNA marker (1); undigested TOPO negative control (2); digested TOPO positive control (3);

digested TOPO-AHSV-3-S10 N159I (4); TOPO-AHSV-2-S10 TS127IL (5); TOPO-AHSV-2-S10 N161I (6) and TOPO-AHSV-2-S10 D137S (7); (Arrow indicates 100 bp fragment).

The following constructs could not be successfully produced using this method: TOPO-AHSV-3-S10 TS128IL, TOPO-AHSV-3-S10-eGFP TS128IL, AHSV-3-S10 D138S, TOPO-AHSV-3-S10-eGFP D138S and TOPO-AHSV-3-S10-eGFP N159I. For example, upon sequencing TOPO-AHSV-3 S10 TS128IL constructed using this method, it was found to be identical to the unmutated AHSV-3 S10. The general reverse primer (NS3pEcoR) had out competed the megaprimer for a priming site on the 5' end of the gene, thus could function as both the forward and the reverse primer. This had resulted in subsequent cloning of the wild type AHSV-3-S10 into the TOPO vector. This construct was named TOPO-AHSV-3-S10 and was used as a template for the Quikchange method discussed in the following section. An alternative method had to be explored that could be used to produce these constructs.

2.3.1.2. Quikchange method

The Quikchange method provides an attractive method for site-directed mutagenesis (Fig. 17). It works on the basis that the amplification reaction produces a linear DNA fragment containing the entire vector including any inserted sequences. This amplification is reminiscent of plasmid replication in that amplification occurs from one central position like an origin of replication. Amplification occurs in both directions from a central point, creating copies of each of the template strands. After amplification the template can be removed by a methylation specific restriction enzyme (*Dpn*I), *in vitro* synthesized strands are unmethylated and will therefore persist whilst the methlylated template will be digested.

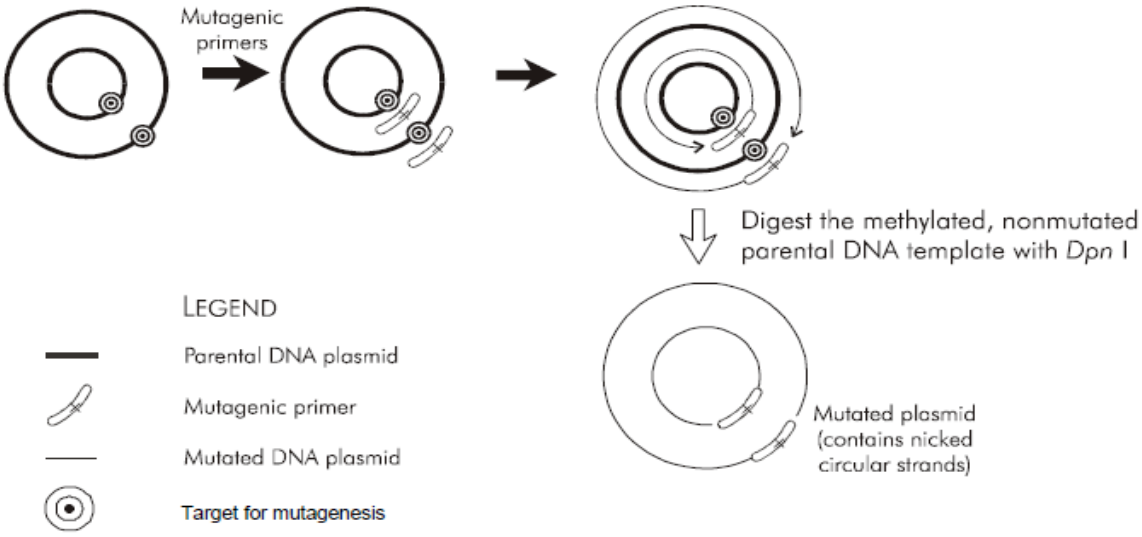

Figure 17: Illustration of the Quikchange method (adapted from QuikChange® XL Site-Directed Mutagenesis Kit instruction manual).

We set out to produce seven constructs using the Quikchange method (Table 12). The following four TOPO constructs were successfully generated using this approach: AHSV-3-S10 TS128IL, AHSV-3-S10-eGFP TS128IL, AHSV-3-S10 D138S and AHSV-3-S10-eGFP D138S. You may note that TOPO-AHSV-3-S10 N159I and TOPO-AHSV-2-S10-D137S had already been generated in the previous section. These were produced using the Quikchange primers for the Megaprimer method after failing to use them with the Quikchange method. The TOPO-AHSV-3-S10 and TOPO-AHSV-3-S10-eGFP clones were used as the templates for the Quikchange method. Using the specific mutant Qc_primer pair combinations, individual PCR reactions were optimised for each of the four mutants. In order to illustrate the execution of the method, only specific results pertaining to the generation of the TOPO-AHSV-3-S10 TS128IL and the TOPO-AHSV-3-S10-eGFP TS128IL will be discussed in detail.

Table 12: Summary of primer combinations and amplification results using the Quikchange approach to generate S10 mutants

Construct	Mutation	Template	Quikchange PCR primers	Success (Yes/No)	Mutation present (Yes/No)
AHSV-3-S10 TS128IL	TS128IL	TOPO-AHSV-3-S10	Qc_AHSVS3NS3TSΔILforw and Qc_AHSVS3NS3TSΔILrev	Yes	Yes
AHSV-3-S10-eGFP TS128IL		TOPO-AHSV-3-S10-eGFP		Yes	Yes
AHSV-3-S10 N159I	N159I	TOPO-AHSV-3-S10	Qc_AHSVS3NS3NΔIforw and Qc_AHSVS3NS3NΔIrev	No	No
AHSV-3-S10-eGFP		TOPO-AHSV-3-S10-eGFP		No	No

N159I					
AHSV-2-S10 D137S	D137S	TOPO-AHSV-2-S10	Qc_AHSVS2NS3DΔSforw and Qc_AHSVS2NS3DΔSrev	No	No
AHSV-3-S10 D138S	D138S	TOPO-AHSV-3-S10	Qc_AHSVS3S10DΔSForw and Qc_AHSVS3S10DΔSrev	Yes	Yes
AHSV-3-S10-eGFP D138S		TOPO-AHSV-3-S10-eGFP		Yes	Yes

The first step required for application of this method was to prepare the template TOPO plasmids (AHSV-3-S10 and AHSV-3-S10-eGFP). The TOPO-AHSV-3-S10 plasmid was produced during the megaprimer method, the NS3 ORF was verified by sequencing. This means that only the TOPO-AHSV-3-S10-eGFP plasmid still had to be prepared. For the generation of TOPO-AHSV-3-S10-eGFP clone, the insert was amplified by PCR using NS3pBamF and eGFPHindR from pFastbac-AHSV-3-S10-eGFP through optimised conditions (not shown). This was then gel purified, cloned into TOPO and transformed into Top10 cells. Cells were streaked onto agar plates containing Spectinomycin. Single colonies were picked, plasmids were isolated and screened via restriction digestion using *Bam*HI and *Eco*RV, which as discussed earlier assays for the insert and orientation. The products obtained were consistent with what was expected (TOPO-AHSV-3-S10-eGFP = 1521 bp + 2717 bp) (Fig. 18 lane 3). The construct was then further analysed by sequencing using vector specific M13F and M13R primers, and insert specific NS3pBamF, eGFPHindR, eGFPintR and NS3StopEcoR primers. The sequences were assembled into a contig using Vector NTI v9.1.0. Sequence analysis confirmed that both AHSV-3-S10 and AHSV-3-S10-eGFP were successfully recloned into TOPO without introducing any mutations (Appendix A).

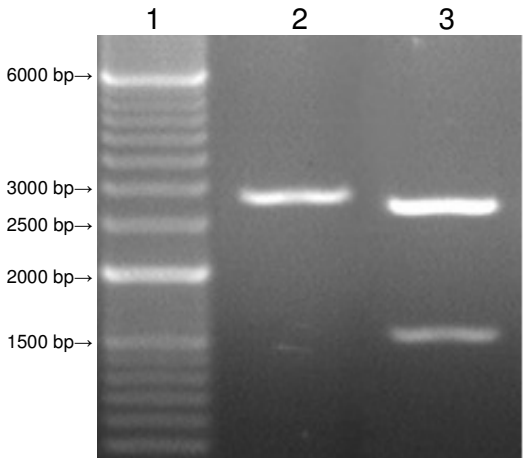

Figure 18: Agarose (1%) gel of the *Eco*RV/*Bam*HI double digests of TOPO-AHSV-3-S10-eGFP; 100/500 bp DNA marker (1); digested TOPO (2); digested TOPO-AHSV-3-S10-eGFP (3).

The same Quickchange primer pair was used to introduce the TS128IL mutation into both TOPO-AHSV-3-S10 and TOPO-AHSV-3-S10-eGFP. Reactions were optimised by temperature gradient PCR. For example, the temperature gradient for TOPO-AHSV-3-S10 TS128IL, where an amplicon of 3583 bp was expected, indicated that the optimal annealing temperature was at 52.9ºC (Fig. 19). Using the optimised conditions, the reactions were performed to generate mutant amplicons for transformation. The reactions were treated with *Dpn*I and evaluated via agarose gel (Fig. 20). A 3583 bp product was expected for TOPO-AHSV-3-S10 TS128IL and 4238 bp for the TOPO-AHSV-3-S10-eGFP TS128IL. The amplification products that were obtained were of the correct size (Fig. 20 lanes 7 and 8) and were not digested upon treatment with by *Dpn*I. The template TOPO-AHSV-3-S10 was degraded by *Dpn*I, indicating its methylated status (Fig. 20 lane 5 versus 6). The *Dpn*I treated mutant reaction products were used to transform Top10 cells and single colonies were selected.

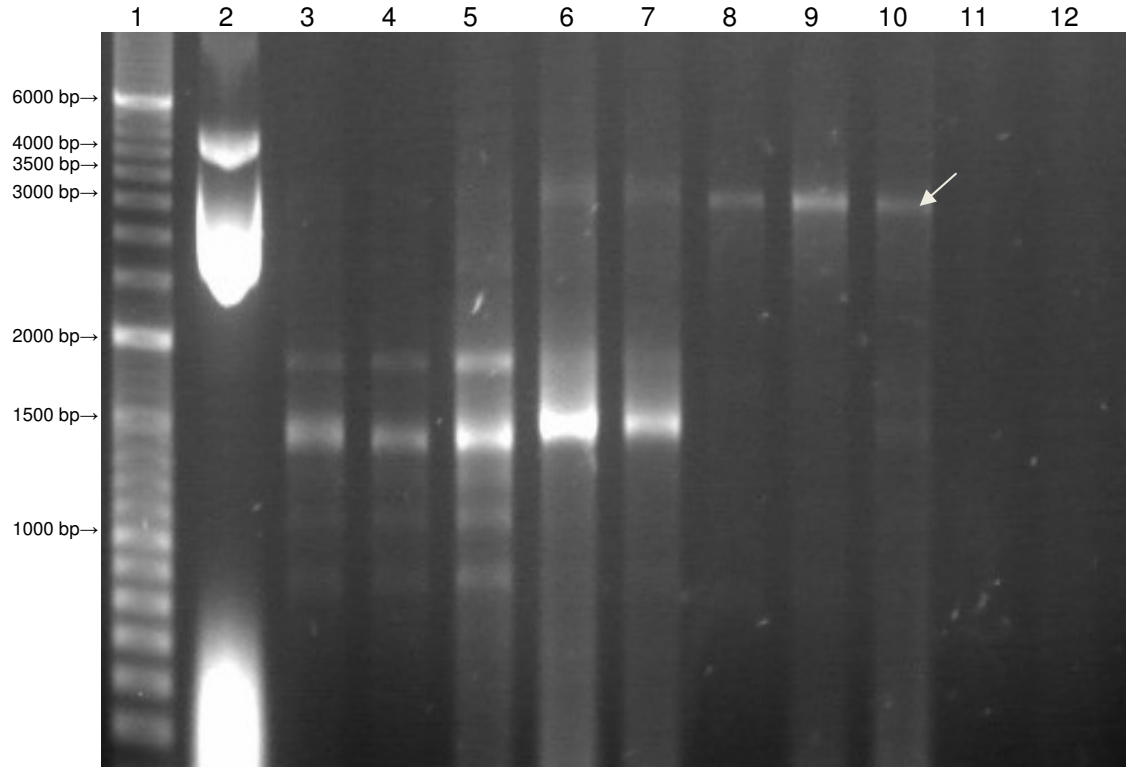

Figure 19: Agarose (1%) gel of the PCR temperature gradient producing TOPO-AHSV-3-S10 TS128IL; 100/500bp DNA marker (1); TOPO-AHSV-3-S10 template(2), PCR at 45°C (3), 45.3°C (4), 46°C (5), 47.3°C (6), 49°C (7), 50.9°C (8), 52.9°C (9), 54.9°C (10) 57.1°C (11) and 58.5°C (12); (Arrow indicates products of the desired size).

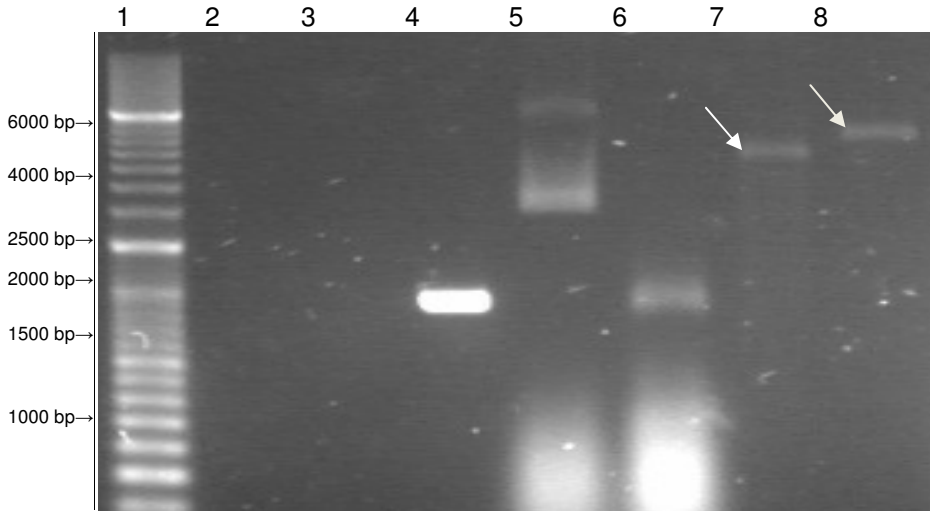

Figure 20: Agarose (1%) gel of the Quikchange method PCR reactions and *Dpn*I digestions for generating the TS128IL mutants; 100/500 bp DNA ladder marker (1); PCR negative controls (2 and 3); PCR positive control (4); TOPO- undigested (5) or *DpnI* treated (6); *DpnI* treated PCR products of TOPO-AHSV-3-S10 TS128IL (7) and TOPO-AHSV-3-S10-eGFP TS128IL (8); (Arrows indicate products of the desired size).

The TOPO-AHSV-3-S10 TS128IL and TOPO-AHSV-3-S10-eGFP TS128IL single colonies were initially screened via colony PCR using the M13F and M13R primers and PCR reactions visualized by agarose gel electrophoresis (Fig. 21). For the TOPO-AHSV-3-S10 TS128IL a 1081 bp product was expected (Fig. 21 A lane 4). A 1736 bp product was expected for the TOPO-AHSV-3-S10-eGFP TS128IL (Fig. 21 B lane 8). In both cases, an additional product of around +/-900bp was present in the colony PCR reactions. This product was not present when amplifying from the plasmid positive controls (Fig. 21 lane 3 and 7). It may therefore represent a product amplified from the Top10 cells.

(A) 1 2 3 4 (B) 5 6 7 8

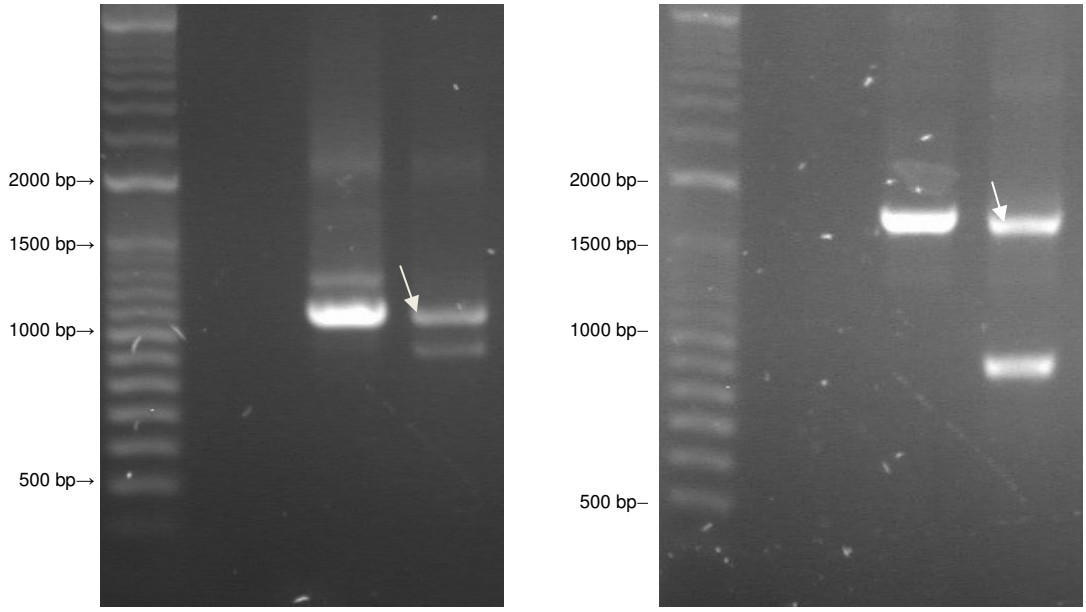

Figure 21: Agarose (1%) gel of the Colony PCR screening of TS128IL mutant TOPO-AHSV-3-S10 (A) and TOPO-AHSV-3-S10-eGFP (B); 100/500 bp DNA marker (1 and 5); PCR negative control (2 and 6); TOPO-AHSV-3-S10 PCR positive control (3); TOPO-AHSV-3-S10 TS128IL (4); TOPO-AHSV-3-S10-eGFP PCR positive control (7); TOPO-AHSV-3-S10-eGFP TS128IL (8); (Arrows indicate products of the desired size).

Plasmids from these colonies were isolated using the Roche high pure plasmid isolation kit and further analysed by sequencing with M13F, M13R, NS3pBamF, eGFPHindR, eGFPintR and NS3StopEcoR primers. The constructs both sequences were identical to the wild type AHSV-3-S10 or AHSV-3-S10-eGFP, except that they contained the desired TS128IL mutation (Appendix A). The same principles were applied to generate the two additional mutants: TOPO-AHSV-3-S10 D138S and TOPO-AHSV-3-S10-eGFP D138S (results not shown).

To summarise, eight different mutant constructs targeting the NS3 gene were generated as inserts cloned into the TOPO vector. These are AHSV-2-S10 (TS127IL, N161I and D137S), AHSV-3-S10 (TS128IL, N159I and D138S) and AHSV-3-S10-eGFP (TS128IL and D138S). The one mutant still outstanding, TOPO-AHSV-3-S10-eGFP N159I, could not be produced using either of the two techniques employed. For purposes of this study, we decided to continue without this construct.

2.3.2. Generation of recombinant baculoviruses expressing the various mutant AHSV NS3 proteins

To express proteins from recombinant baculoviruses, the next step was the transfer of the insert from TOPO into the destination vector, pDest8. This was achieved via an enzyme-catalyzed lambda recombination (LR) reaction. In this reaction, site-specific recombination occurs between the compatible lambda phage sequence elements present on the recombinant TOPO plasmid and the pDest8 plasmid vectors. A recombinant pDest8 containing the insert downstream from a polyhedron promoter is generated. After confirming that a pDest8 plasmid contains the insert, the recombinant pDest8 is transformed into *E. coli* (DH10bac cells) containing the bacmid genome. In these cells a spontaneous homologous recombination reaction occurs and the promoter and insert are both recombined into the bacmid genomic DNA. The recombinant bacmid DNA can then be isolated and used to generate recombinant baculoviruses, this approach is known as Gateway (Luckow *et al.*, 1993). To illustrate the process followed, construction of the Bac-AHSV-3 NS3 N159I from TOPO-AHSV-3-S10 N159I will be discussed in detail, while key results will be given for the other seven constructs.

The LR reaction was set up for the nonrecombinant pDest8 and the recombinant TOPO-AHSV-3-S10 N159I plasmids. This reaction was used to transform electrocompetent DH5α cells by electroporation. Colonies were plated on ampicillin containing agar plates. Single colonies were transferred to two replica plates one containing ampicillin and the other containing ampicillin and chloroamphenenicol (Cm). This was done because during the LR reaction the pDest8 *cm*^{r} resistance gene is lost, meaning that recombinants would have a Cm^{S} phenotype. Plasmids were isolated from Amp^{R}Cm^{S} colonies. Gene orientation was not under question because of the directional nature of recombination. Isolated plasmids were *Eco*RI digested in order to confirm the insert size (Fig. 22). For a non-recombinant pDest8 vector the expected size is 6526 bp, as was obtained (Fig. 22 lane 3). The products obtained for the pDest8-AHSV-3-S10 N159I digestion were consistent with the expected 4739 bp and 788 bp products (Fig. 22 lane 4). The total size difference between bands representing the recombinant pDest8 vector (5527 bp) and the non-recombinant pDest8 vector (6526 bp) is due to the loss of *cm*^{r} resistance gene. pDest8 clones were all further analyzed by sequencing using relevant primers (NS3pBamF, eGFPHindR, eGFPintR and NS3EcoStopRev). Sequence analysis confirmed that ORFs were intact, in the correct orientation and contained only

the desired mutations.

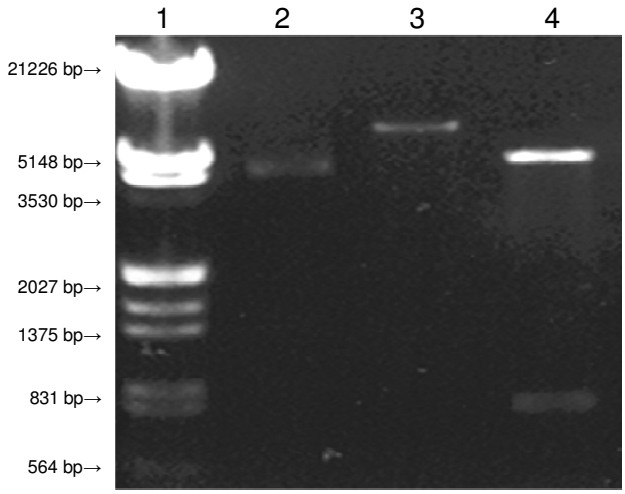

Figure 22: Agarose (1%) gel of the *Eco*RI restriction digestions of the pDest8-AHSV-3-S10 N159I construct; Hind/Eco DNA ladder marker (1); pDest8 native plasmid as untreated (2) and digested (3); digested pDest8-AHSV-3-S10 N159I (4).

Confirmed pDest8-AHSV-3-S10 N159I plasmids were transformed into DH10Bac cells using electroporation. The cells were plated onto plates containing gentamycin/ ampicillin/ kanamycin, IPTG and X-gal. Blue white screening was performed in order to identify colonies where recombination had occurred. The white colonies were replica plated onto the same type of media for identification of the true white colonies.

True white colonies were tested via colony PCR using the M13F and M13R primers. The products were evaluated via gel electrophoresis (Fig. 23). The size product expected for the blue colony containing the non-recombinant bacmid is 300 bp (Fig. 23 lane 3). As was expected the PCR on the recombinant AHSV-3-S10 N159I bacmid colony gave a product of around 2500 bp (Fig. 23 lane 4). An additional nonspecific amplification product of about 1000 bp was present in all the samples except the negative control (Fig. 23 lane 2). This indicates that the primers were able to amplify another segment. The non-specific amplicon must have been generated from the DH10bac cells as they were present in all the colonies tested (not shown).

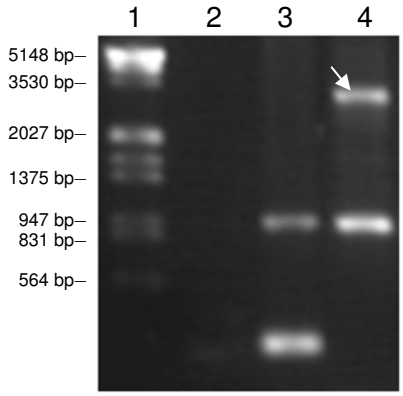

Figure 23: Agarose (1%) gel of the colony PCR of Bacmid-AHSV-3-S10 N159I; Hind/Eco DNA marker (1); PCR negative control (2); blue colony PCR positive control (3); Bacmid-AHSV-3-S10 N159I (4); (Arrow indicates product of the desired size).

This process was used to produce Bacmid-AHSV-2-S10 TS127IL, N161I and D137S; Bacmid-AHSV-3-S10 TS128IL, N159I and D138S; and Bacmid-AHSV-3-S10-eGFP TS128IL and D138S (Fig. 24). The colony PCR reactions for Bacmid-AHSV-3-S10-eGFP constructs were expected to give a product of around 3300 bp (Fig. 24 lanes 5 and 7).

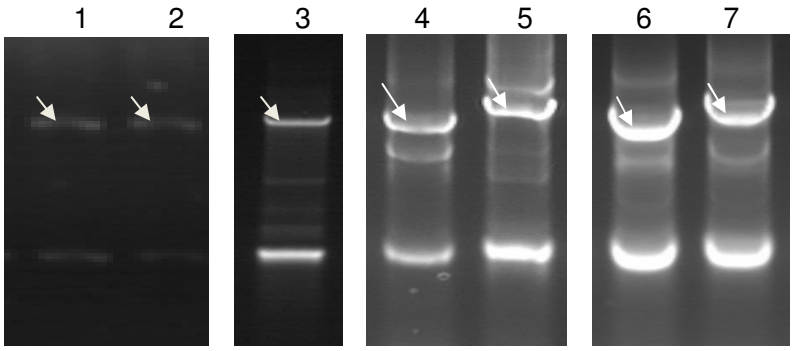

Figure 24: Agarose (1%) gels of the various colony PCR of Bacmids; Bacmid-AHSV-2-S10 TS127IL (1), N161I (2) and D137S (3); Bacmid-AHSV-3-S10 TS128IL (4); Bacmid-AHSV-3-S10-eGFP TS128IL (5), Bacmid-AHSV-3-S10 D138S (6) and Bacmid-AHSV-3-S10-eGFP D138S (7); (Arrows indicate products of the desired size).

In order to generate a recombinant baculovirus, bacmid DNA was isolated for each of the eight constructs and transfected into Sf9 insect cells using Cellfectin (Invitrogen). Cellfectin is a cationic lipid formulation that enables the uptake of exogenous DNA. Bacmid gene expression results in the generation of recombinant baculoviruses.

Expression of the exogenous gene (NS3) occurs at later stages of infection because the polyhedrin promotor only becomes active later and expression is detectable from 18 h.p.i. Expression of the NS3 proteins was tested by analysis of the cell lysates on a SDS-PAGE gel, subjected to Western blot. For the Western blots, a unique signal was expected at 25 kDa for AHSV-2 NS3 and AHSV-3 NS3 proteins and 51 kDa for the AHSV-3 NS3-eGFP protein. Western blotting was optimised (blocking time and incubation time) for the different antibodies and the different constructs against wild type NS3 proteins. For example, the anti-β-Gal-NS3 AHSV-2 serum (see Table 6) often gave large amounts of background signal (Fig. 25). There was non-specific banding around the 72 kDa range, this did however not interfere with the unique AHSV-2 NS3 signal at 24kDa which was clearly identifiable (Fig. 25 lane 4 as shown by arrow). The nitrocellulose membrane was also labelled at nonspecific places causing spots on the membrane. By using a 5% blocking solution and an overnight blocking step, most of this background could be removed.

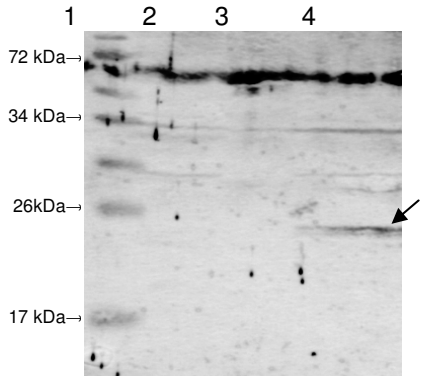

Figure 25: Western blot (anti-β-Gal-NS3 AHSV-2 serum) from 15% SDS-PAGE of Bac-AHSV-2 NS3; Pageruler rainbow marker (1); Mock infected (2); Wildtype baculovirus (3); Bac-AHSV-2 NS3 (4); (Arrow indicates product of the desired size).

Three replicates of the Bacmid-AHSV-3 NS3 N159I transfection were performed and expression was assessed by Western blot (Fig. 26). Two of the transfections gave no signal on the Western blot indicating that they were not successful (Fig. 26 lane 4 and 5). The transfection corresponding to Fig. 26 lane 6 yielded a signal matching the Bac-AHSV-3 NS3 positive control (Fig. 26 lane 3). The recombinant baculovirus (Bac-AHSV-3 NS3 N159I) expressing the AHSV-3 NS3 N159I protein had been successfully generated (Fig. 26). Expression was specific in that the wild type baculovirus did not react with the serum (Fig. 26 lane 2).

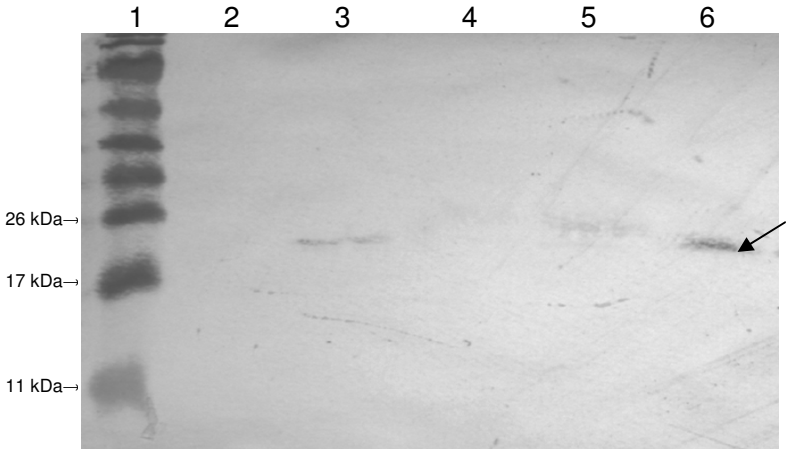

Figure 26: Western blot (anti-18aa-NS3 AHSV-3 serum) from 15% SDS-PAGE of Bac-AHSV-3 NS3 N159I transfection; Pageruler rainbow marker (1); Wildtype baculovirus infected control (2); Bac-AHSV-3 NS3 infected control (3); Bac-AHSV-3 NS3 N159I transfections 1 to 3 (4 to 6); (Arrow indicates product of the desired size).

The Bac-AHSV-3 NS3 N159I virus-containing medium was subjected to plaque purification. This was done to ensure a homogeneous virus population, originating from a single plaque. All six of the plaques tested for the AHSV-3 NS3 N159I protein showed the desired signal with slightly varying intensities. Shown in Fig. 27 lanes 3 to 7 are five of the tested plaques all showing signal of approximately 25 kDa in size. No non-specific banding was present for the anti-18aa-NS3 AHSV-3 antibodies. A virus stock was subsequently amplified from a single plaque, titrated and used for all subsequent assays.

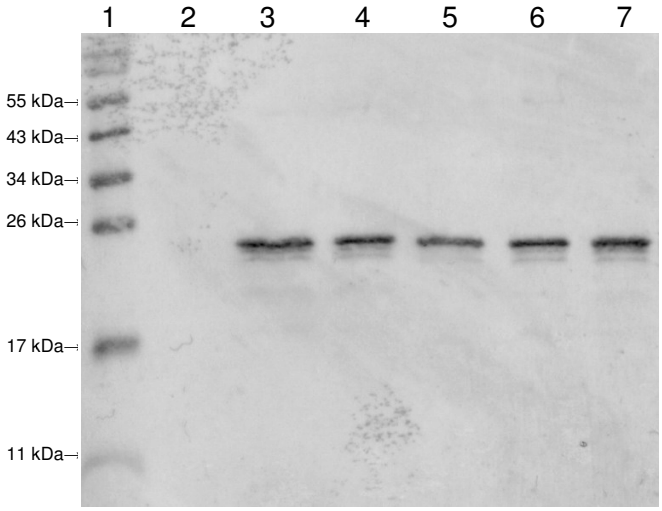

Figure 27: Western blot (anti-18aa-NS3 AHSV-3 serum) from 15% SDS-PAGE of Bac-AHSV-3 NS3 N159I plaques; Pageruler rainbow marker (1); Wildtype baculovirus (2); Bac-AHSV-3 NS3 N159I plaques 1 to 5 (3 to 7).

Using the same approach the other seven TOPO constructs were used to produce recombinant baculoviruses. The protein expression of all the Bac-AHSV-2 NS3 (Fig. 28), the Bac-AHSV-3 NS3 (Fig. 29) and Bac-AHSV-3 NS3-eGFP (Fig. 30) constructs were verified by SDS-PAGE and Western blot. Virus stocks were prepared for subsequent experiments. R. van der Sluis had previously constructed three recombinant baculovirus constructs expressing AHSV-2 NS3 with mutations targeting the intervening spacer region (ISR) during her MSc, these however have not yet been fully characterized. The mutants entailed an isoleucine to serine substitution, deletions of residues KGD and doubling the length of the spacer region (Fig. 7 F to H) (van der Sluis, 2007). These three additional baculoviruses expressing mutant AHSV-2 NS3 proteins, i.e. Bac-AHSV-2-NS3 I140S, Bac-AHSV-2-NS3 Δ149KGD and Bac-AHSV-2-NS3 15aa ins151 (Fig. 28 lane 7 to 9). were also included in the assays during this study.

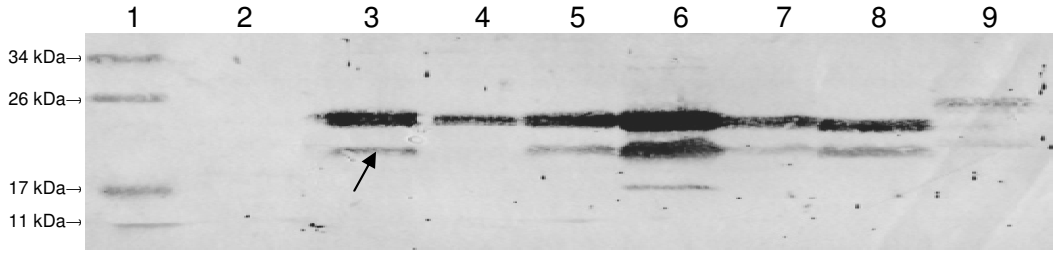

Figure 28: Western blot (anti-β-Gal-NS3 AHSV-2 serum) from 15% SDS-PAGE of Bac-AHSV-2 NS3; Pageruler rainbow marker (1); Wildtype baculovirus (2); Bac-AHSV-2 NS3 (3) and corresponding mutants TS127IL (4), N161I (5), D137S (6), I140S (7), Δ149KGD (8) and 15aa ins151 (9). (Arrow indicates position of additional band)

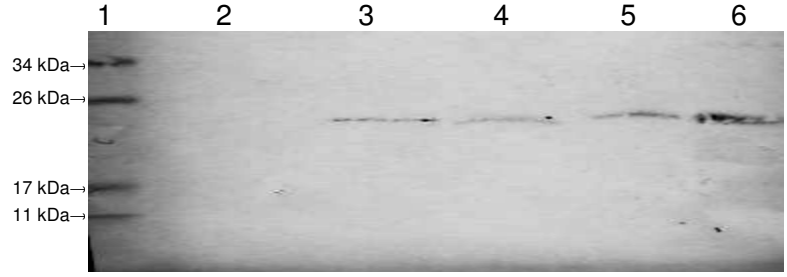

Figure 29: Western blot (anti-18aa-NS3 AHSV-3 serum) from 15% SDS-PAGE of Bac-AHSV-3 NS3; Pageruler rainbow marker (1); Wildtype baculovirus (2); Bac-AHSV-3 NS3 (3) and corresponding mutants TS128IL (4), N159I (5) and D138S (6).

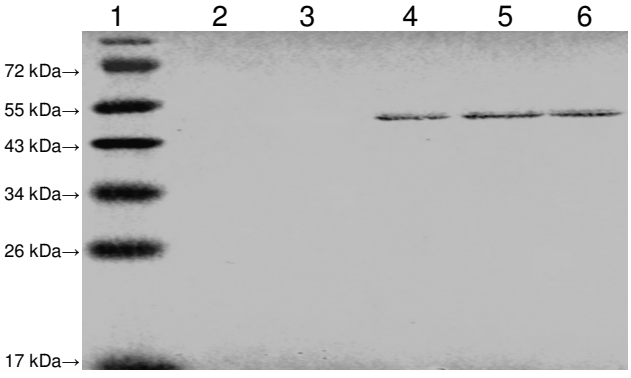

Figure 30: Western blot (anti-18aa-NS3 AHSV-3 serum) from 12% SDS-PAGE of Bac-AHSV-3 NS3-eGFP; Pageruler rainbow marker (1); Mock (2); Wildtype baculovirus (3); Bac-AHSV-3 NS3-eGFP (4) and corresponding mutants TS128IL (5), and D138S (6).

The samples shown on Fig. 28 and Fig. 29 were prepared using the same procedure (same size cell population, same MOI and same incubation time of 48 hours). Cells

were harvested and lysed using the same procedure. Equal volumes of each sample were evaluated by Western blot. The expression levels of the various AHSV-2 NS3 constructs Fig. 28 were not equal. Expression levels of Bac-AHSV-2 NS3 were similar to the levels obtained for the baculoviruses expressing the N161I, I140S, and Δ149KGD versions of the AHSV-2 NS3 protein (Fig. 28 lanes 3, 5, 7 and 8). The baculoviruses yielding reduced levels of extragenous protein expression include the TS127IL and 15aa ins151 versions of the Bac-AHSV-2 NS3 constructs (Fig. 28 lanes 4 and 9). The AHSV-2 NS3 15aa ins151 expression levels were extremely low and therefore proved difficult to detect. The only construct showing increased levels of expression relative to Bac-AHSV-2 NS3 was the D137S mutant (Fig. 28 lane 6). The Bac-AHSV-3 NS3 mutant constructs, when compared to the wild type, did not show major differences in expression levels, there was a slightly increased amount of signal strength for the Bac-AHSV-3 NS3 D138S mutant construct (Fig. 29 lane 6). A much smaller fraction of the volume of cellular lysate was evaluated for samples infected with recombinant baculoviruses expressing the eGFP tagged AHSV-3 NS3 constructs. These constructs had very high expression levels relative to the untagged AHSV-3 NS3. There were no major differences in levels of expression between the wild type and the mutant Bac-AHSV-3 NS3-eGFP constructs (Fig. 30). These variations in expression levels were evident in all experimental repetitions.

There was an additional band present below the AHSV-2 NS3 protein band indicated by the arrow on Fig. 28. This band may represent protein NS3A or possibly different conformations of the AHSV-2 NS3 due to varying degrees of denaturation or perhaps degradation. This protein band was absent from the Bac-AHSV-2 NS3 TS127IL containing sample. This may be due the relatively lower protein expression levels.

An additional problem with the Bac-AHSV-3 NS3-eGFP constructs was identified. In some of the Western blots a second band would develop in addition to the full length NS3-eGFP fusion. This band was the size of AHSV-3 NS3 when labelled with anti-18aa-NS3 AHSV-3 (Fig. 31 lane 5) and the size of eGFP (27kDa) (Fig. 31 lane 7) when labelled with anti-eGFP. Therefore two additional products were present, one corresponding to AHSV-3 NS3 and the other to the eGFP protein. At first, it was thought that the viral stock had been contaminated but when testing new stocks the same was observed. When the protein was loaded without severe agitation then the

AHSV-3 NS3-eGFP protein gave only a single product (Fig. 32 lane 3). The additional may be identified using peptide sequencing techniques, however this was not done.

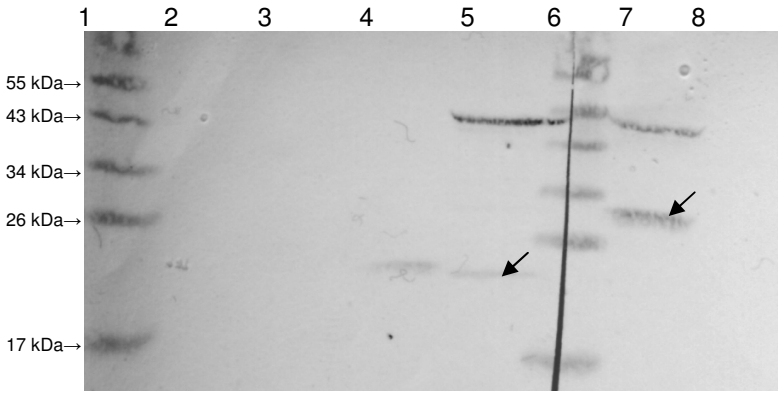

Figure 31: Western blot from 12% SDS-PAGE of Bac-AHSV-3 NS3-eGFP where the membrane was cut in half and each reacted with a different antibody; Pageruler rainbow marker (1, 6); anti-18aa-NS3 AHSV-3 serum treated samples: Mock (2), Wildtype baculovirus (3), AHSV-3 NS3 (4), and Bac-AHSV-3 NS3-eGFP (5); anti-eGFP serum treated samples: Bac-AHSV-3 NS3-eGFP (7) and Wildtype baculovirus (8); (Arrows indicate additional products).

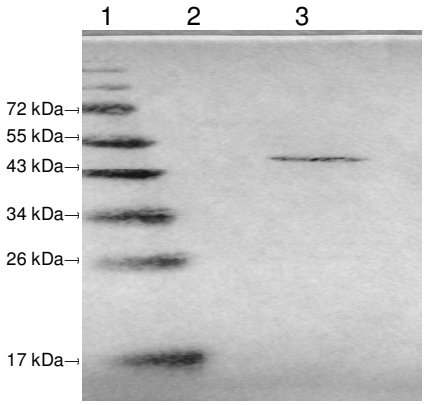

Figure 32: Western blot (anti-18aa-NS3 AHSV-3 serum) from 12% SDS-PAGE of Bac-AHSV-3 NS3-eGFP; Pageruler rainbow marker (1); Wildtype baculovirus (2) and Bac-AHSV-3 NS3-eGFP (3);

To summarise, a full set of mutants targeting the TS in HD1, D in the ISR and N in HD2 were generated for both Bac-AHSV-2 NS3 and Bac-AHSV-3 NS3. In addition, two mutants targeting TS and D respectively as a part of a eGFP fusion protein were produced as Bac-AHSV-3 NS3-eGFP. In the following sections, these will be compared to the control baculoviruses (Bac-AHSV-2 NS3 and Bac-AHSV-3 NS3, Bac-AHSV-3

NS3-eGFP and Bac-eGFP) in terms of subcellular localisation, trafficking and cytotoxicity assays. Three additional AHSV-2 NS3 constructs (I140S, Δ149KGD and 15aa ins151) which had not yet been fully characterised were included in the various assays.

2.3.3. Subcellular fractionation

When the folding of a protein is disrupted, then its intracellular targeting and localisation may be altered. Quality control mechanisms monitor the export of proteins from the ER and misfolded proteins may be prevented from leaving the ER. In order to determine if the mutations had affected protein intracellular trafficking, Sf9 cells were infected with different recombinant baculoviruses at MOI of 10, harvested at 24 h.p.i cells, and lysed. Lysates were fractionated by differential centrifugation. Nuclei were collected by low-speed centrifugation and stored as the nuclear (N) fraction. The post-nuclear supernatant was separated into particulate (P) and soluble (S) fractions by high-speed centrifugation. Insoluble and plasma membrane associated proteins separate into the particulate fraction and soluble cytoplasmic proteins separate into the soluble fraction. After differential centrifugation, fractions were analysed by Western blot with appropriate antibodies. Western blot contrast and brightness was standardised and quantified by EZQuant software. The values were represented as a percentage of total signal and plotted on a bar graph. For the eGFP and eGFP-fusion constructs, the proportion of fluorescence in each fraction was also measured using a fluorometer and similarly plotted. The assays were performed at 24 h.p.i because cell death starts to occur from 24 h.p.i. and therefore cellular trafficking may be affected. The fractionations were performed using Bac-eGFP as an internal control; eGFP was expected to be associated with the soluble fraction as eGFP is a highly soluble protein.

Results are presented in Fig. 33 – 34, for easy interpretation, they are presented as three sets, corresponding to the three domains that were mutated. The same control images were used in all the figures (eGFP, AHSV-2 NS3, AHSV-3 NS3 and AHSV-3 NS3-eGFP. The eGFP proteins were limited to the S fraction (Fig. 33 A). The AHSV-2 NS3 proteins were found in N, P and S fractions. The bulk was in the P fraction, with almost equivalent proportions in both the N and S fractions (Fig. 33 B and H). Previously it was reported that the AHSV-2 NS3 had no S associated signal, however in that study the proteins were precipitated with acetone (van der Sluis, 2007). The AHSV-3 NS3 was

limited to the N and P fractions with no protein in the S fraction, 45% was in the N where 55% was in the P fraction (Fig. 33 F). Comparably, the AHSV-3 NS3-eGFP protein was also limited to the N and P fractions at 47% and 52% respectively.

Mutation targeting the NS3 HD1 TS motif differed in the effect it had on AHSV-2 NS3 compared to AHSV-3 NS3 in terms of the distribution of the protein in the three fractions (Fig. 33). The AHSV-2 NS3 TS127IL mutant protein had no P association and was limited to the N and S fractions, compared to the AHSV-2 NS3 protein where the majority was P associated. This may reflect a shift from P to S thus yielding the major increase in S fraction associated protein (Fig. 33 B). In the case of AHSV-3 NS3, the mutant TS128IL protein had a similar distribution to that of the wild type AHSV-3 NS3 (Fig. 33 E). The AHSV-3 NS3-eGFP TS128IL protein also had equivalent proportions, about 50%, in the N and P fractions similar to the AHSV-3 NS3-eGFP.

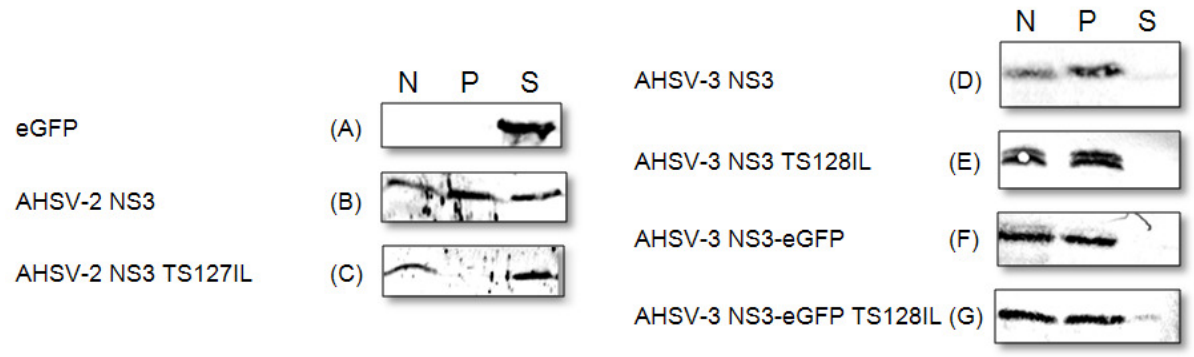

(H)

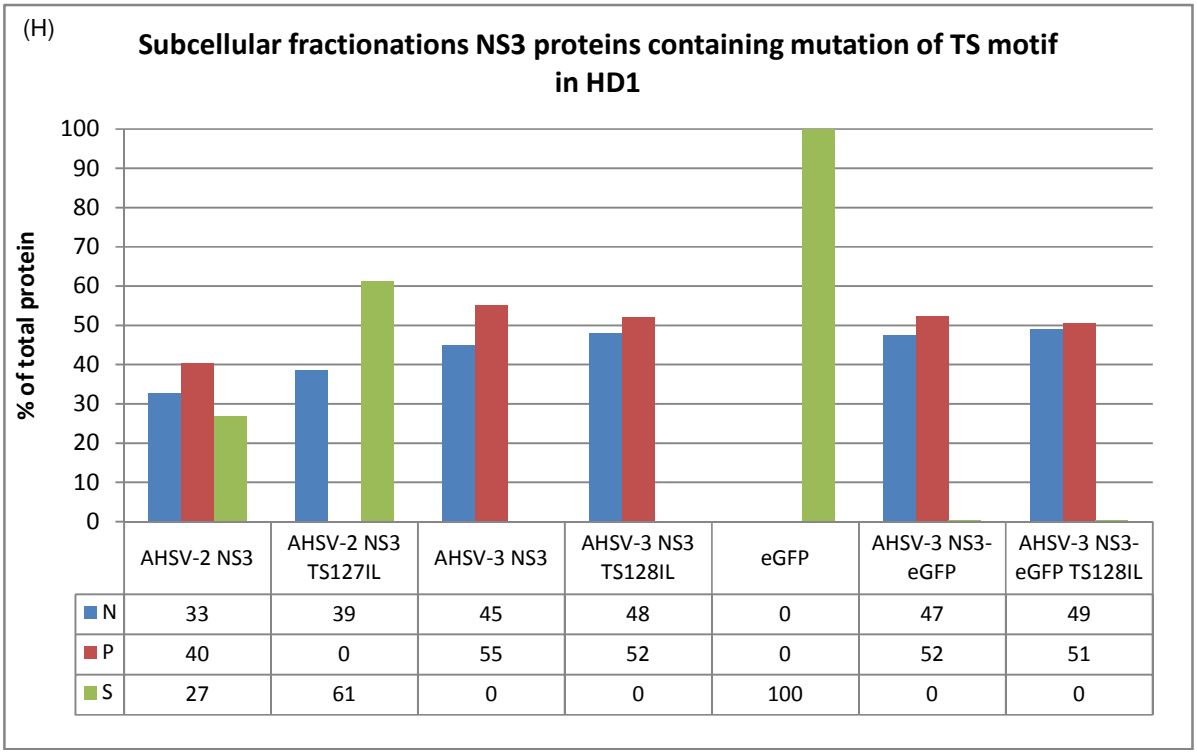

	AHSV-2 NS3	AHSV-2 NS3 TS127IL	AHSV-3 NS3	AHSV-3 NS3 TS128IL	eGFP	AHSV-3 NS3-eGFP	AHSV-3 NS3-eGFP TS128IL
N	33	39	45	48	0	47	49
P	40	0	55	52	0	52	51
S	27	61	0	0	100	0	0

Figure 33: Western blot analysis of fractions from subcellular fractionation of NS3 proteins with modifications to HD1 TS motif (24 h.p.i); Bac-eGFP (A); Bac-AHSV-2 NS3 (B); Bac-AHSV-2 NS3 TS127IL (C), Bac-AHSV-3 NS3 (D); Bac-AHSV-3 NS3 TS128IL (E); Bac-AHSV-3 NS3-eGFP (F); Bac-AHSV-3 NS3-eGFP TS128IL (G); EZQuant values plotted in Excel (H); (N = nuclear fraction, P = particulate fraction and S = soluble fraction);

Modification of the HD2 domain N motif of NS3 resulted in AHSV-2 NS3 N161I protein with no distribution to the P fraction and an increase in both the N (46%) and S (54%) fractions compared to the wild type AHSV-2 NS3 (Fig. 34 C and F). The AHSV-3 NS3 N159I had a 1% association with the S fraction not found in AHSV-3 NS3, while the N associated increased to 50% compared to 45% in wild type AHSV-3 NS3 (Fig. 34 E and F).

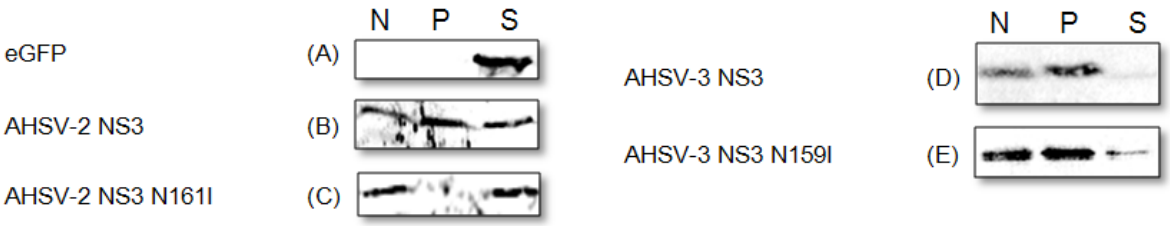

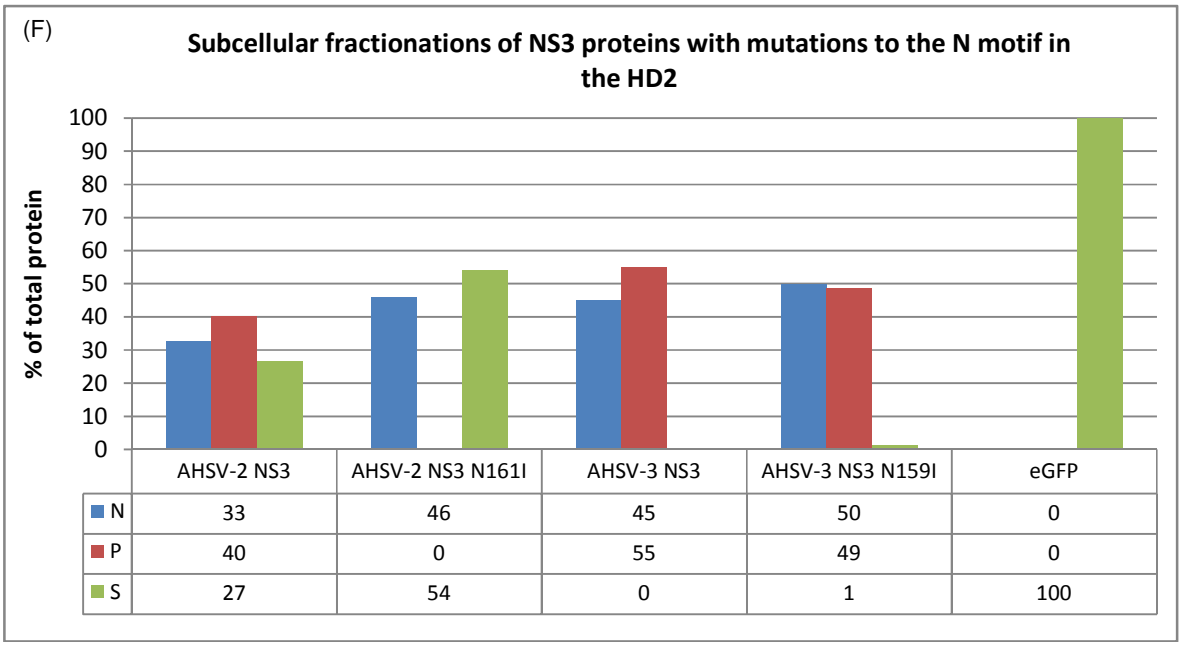

Figure 34: Western blot analysis of fractions from subcellular fractionation of NS3 proteins with modifications to HD2 N motif (24 h.p.i); Bac-eGFP (A); Bac-AHSV-2 NS3 (B); Bac-AHSV-2 NS3 N161I (C), Bac-AHSV-3 NS3 (D); Bac-AHSV-3 NS3 N159I (E); EZQuant values plotted in Excel (F); (N = nuclear fraction, P = particulate fraction and S = soluble fraction);

Mutations targeting the ISR had different effects on the distribution of the NS3 proteins into the fractions (Fig. 35). The AHSV-2 NS3 I140S, Δ149KGD and 15aa ins151 proteins were difficult to detect by Western blot after fractionation and there was a lot of variation in the N-P-S ratios between different repeats of the experiments. The majority of the AHSV-2 NS3 I140S protein was in the N fraction with about with equivalent amounts in the P and S, which was about 30% (Fig. 35 D and K). The Δ149KGD had 40% of the total protein in the S fraction, 35% in the N and 25% in P (Fig. 35 E and K). In one biological repeat of the experiment the 15aa ins151 was completely limited to the S fraction as reported previously (van der Sluis, 2007). In other repeats, the 15aa ins151 protein had N, P and S association, with about equal proportions in each (Fig. 35 F and K). The variation in the subcellular fractionations results obtained for AHSV-2

NS3 I140S, Δ149KGD and 15aa ins151 mutant constructs was noteworthy. The experiments could not be optimised to give easily repeatable results, thus lowering the confidence in the reliability of these results and partially negating the ability to draw conclusions from them.

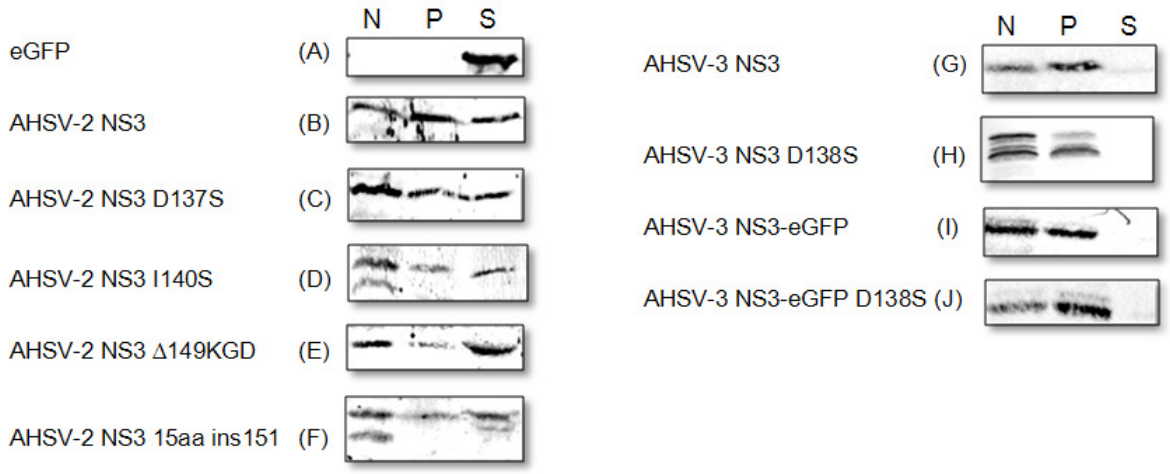

(K)

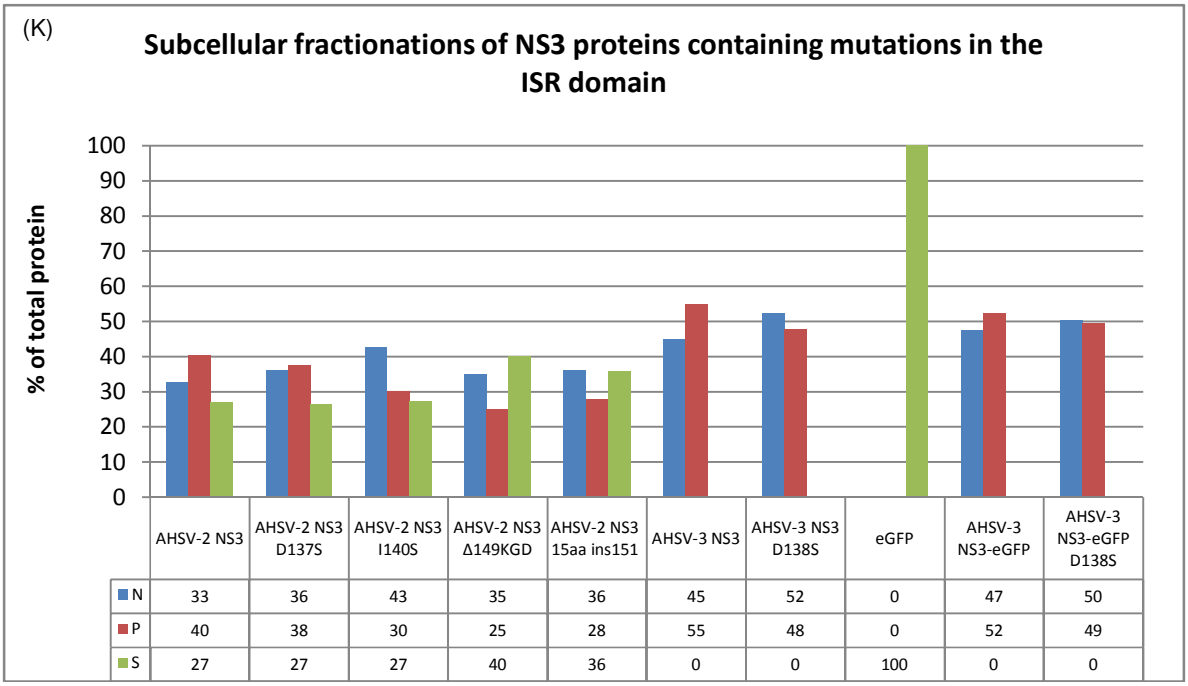

	AHSV-2 NS3	AHSV-2 NS3 D137S	AHSV-2 NS3 I140S	AHSV-2 NS3 Δ149KGD	AHSV-2 NS3 15aa ins151	AHSV-3 NS3	AHSV-3 NS3 D138S	eGFP	AHSV-3 NS3-eGFP	AHSV-3 NS3-eGFP D138S
N	33	36	43	35	36	45	52	0	47	50
P	40	38	30	25	28	55	48	0	52	49
S	27	27	27	40	36	0	0	100	0	0

Figure 35: Western blot analysis of fractions from subcellular fractionation of NS3 proteins with modifications to ISR domain (24 h.p.i); Bac-eGFP (A); Bac-AHSV-2 NS3 (B) and related ISR mutants: I140S (C), Δ149KGD (D), 15aa ins151 (E), and D137S (F); Bac-AHSV-3 NS3 (G); Bac-AHSV-3 NS3 D138S (H); Bac-AHSV-3 NS3-eGFP (I); Bac-AHSV-3 NS3-eGFP D138S (J); EZQuant values plotted in Excel (K); (N = nuclear fraction, P = particulate fraction and S = soluble fraction);

The AHSV-2 NS3 D137S signal was present in the N, P and S fractions with a 36%, 38% and 27% respectively (Fig. 35 F and K). Like AHSV-3 NS3, the D138S mutant proteins were limited to the N and P fractions with nothing in the S fractions. The AHSV-3 NS3 D138 had 52% in the N fraction and 48% in the P fraction (Fig. 35 H and K). Similarly the AHSV-3 NS3-eGFP D138S was limited to N and P with 50% and 49% respectively.

In order to verify the data from the Western blots, fluorescence values were measured and compared. The eGFP tagged proteins in the subcellular fractionations were quantified either from Western blots using EZQuant or by measuring fluorescence emission per fraction as measured by Ascent Fluoroscan (Fig. 36). According to the EZQuant data, 100% of the total eGFP protein was located in the S fraction whereas according to the fluorescence data 97% was (Fig. 33). EZQuant data placed AHSV-3 NS3-eGFP in about equal proportions in the N and P with no protein in the S fractions (Fig. 33). Similar distributions were obtained for both AHSV-3 NS3-eGFP TS128IL (Fig. 33) and D138S (Fig. 35).

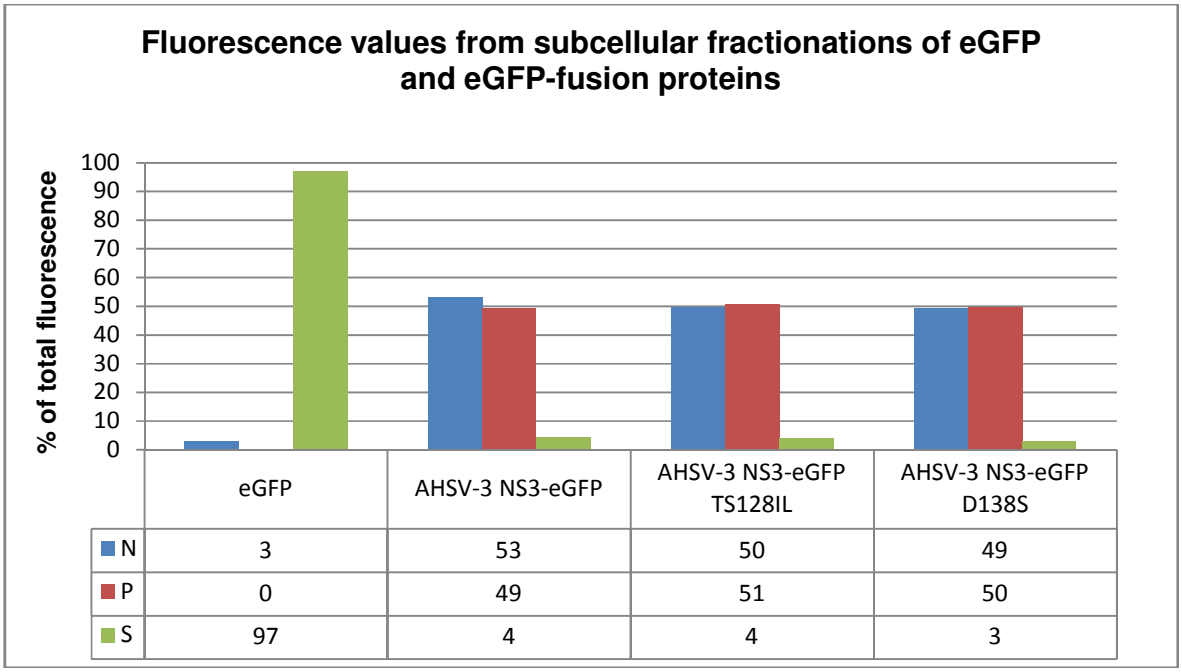

	eGFP	AHSV-3 NS3-eGFP	AHSV-3 NS3-eGFP TS128IL	AHSV-3 NS3-eGFP D138S
N	3	53	50	49
P	0	49	51	50
S	97	4	4	3

Figure 36: Graphs showing the relative proportion of eGFP and fusion proteins (24 h.p.i) in each fraction collected from fractionation; Fluorescence per fraction as measured by Ascent Fluoroscan; Constructs evaluated were Bac-eGFP, Bac-AHSV-3 NS3-eGFP with corresponding mutants TS128IL and D138S as compared to the AHSV-3 NS3 with corresponding mutants TS128IL and D138S; (N = nuclear fraction, P = particulate fraction and S = soluble fraction);

In summary, the HD1 TS127IL and HD2 N161I modifications to the AHSV-2 NS3 protein resulted in the absence of the mutant protein from the P fraction, and shift to the S fraction. None of the mutations introduced into AHSV-3 NS3 caused major changes in the N-P-S ratios relative to the AHSV-3 NS3. The AHSV-3 NS3 protein had a similar distribution to that of the AHSV-3 NS3-eGFP fusion protein. The TS128IL and N159I had similar profiles in eGFP tagged and untagged forms. The AHSV-3 NS3 and NS3-eGFP EZQuant and fluorescent profiles were comparatively similar. P fraction represents the plasma membrane and cellular membranous components. Subsequently at this stage however it was not clear if membrane association had been completely lost in those constructs where P fraction association had been negated, as the association with the nuclear membrane and closely associated endoplasmic reticulum may be reflected in the N fraction. N may also represent the soluble intranuclear component. In order to assess the membrane association membrane flotation analysis was performed.

2.3.4. Membrane flotation analysis

It is postulated that the highly conserved domains or specific residues in the AHSV NS3 protein are involved in protein folding and membrane interaction, therefore mutating them may detrimentally affect these processes (van der Sluis, 2007). In a membrane flotation assay, protein separation is based on density in a sucrose gradient. Three different sucrose densities are layered into a 5 ml ultracentrifuge tube, with the cell lysate in the highest density fraction at the bottom of the tube, and centrifuged. All soluble cytoplasmic components remain in the bottom fraction. Conversely, all membrane lipid associated proteins float to the top fractions (Beyleveld, 2007; Brignati *et al.*, 2003; Meiring, 2009a). After centrifugation, the sucrose gradient was fractionated from the bottom into 10 fractions of approximately 500 µl each. Fractions were analyzed by Western blot with appropriate antibodies. Western blot contrast and brightness was standardised to a control (the size marker) and quantified by EZQuant software. The values were represented as a percentage of total signal and plotted on a line graph. For the eGFP fusion constructs the proportion of fluorescence in each fraction was measured using a fluorometer and similarly plotted.

Using this technique it has previously been shown that AHSV-2 NS3, AHSV-3 NS3 and AHSV-3 NS3-eGFP were all associated with the membrane associated, low density fractions (LDF) 6 to 10 in the top of the tube (Beyleveld, 2007; Meiring, 2009a). This

method was applied here to determine if the mutations affected the membrane association of the proteins. The assays were all performed at 24 h.p.i because changes in cell morphology and cell death ensue from 24 h.p.i. and therefore cellular trafficking may be affected. The results are shown in Figs 36 to 38.

The flotations were performed using Bac-eGFP as an internal control; eGFP was expected to be associated with the bottom higher density fractions (HDF) 1 to 5 as eGFP is a highly soluble protein. It was found that 81% of the eGFP proteins were in the HDF. The AHSV-2 and AHSV-3 NS3 proteins were present exclusively in the upper LDF fractions, indicating lipid membrane association. For the AHSV-3 NS3-eGFP proteins, there was 7% associated with the HDF, with the bulk present in the LDF similar to the AHSV-3 NS3 protein. For uniformity in comparison, the same set of representative images of the four controls were used in all of the membrane flotation figures (Fig. 37 to 38), i.e. those of eGFP, AHSV-2 NS3, AHSV-3 NS3 and AHSV-3 NS3-eGFP.

Modification of the HD1 domain TS motif of NS3 resulted in different profiles for the two serotypes (Fig. 37). The AHSV-2 NS3 TS127IL mutant had a more general distribution though the gradient (Fig. 37 C), and about 57% of the TS127IL proteins had shifted to the HDF of the gradient. The AHSV-3 NS3 TS128IL protein was exclusively in the LDF, similar to the wild type AHSV-3 NS3. The AHSV-3 NS3-eGFP TS128IL had similar distribution to that of AHSV-3 NS3-eGFP with 94% in the LDF and small soluble component.

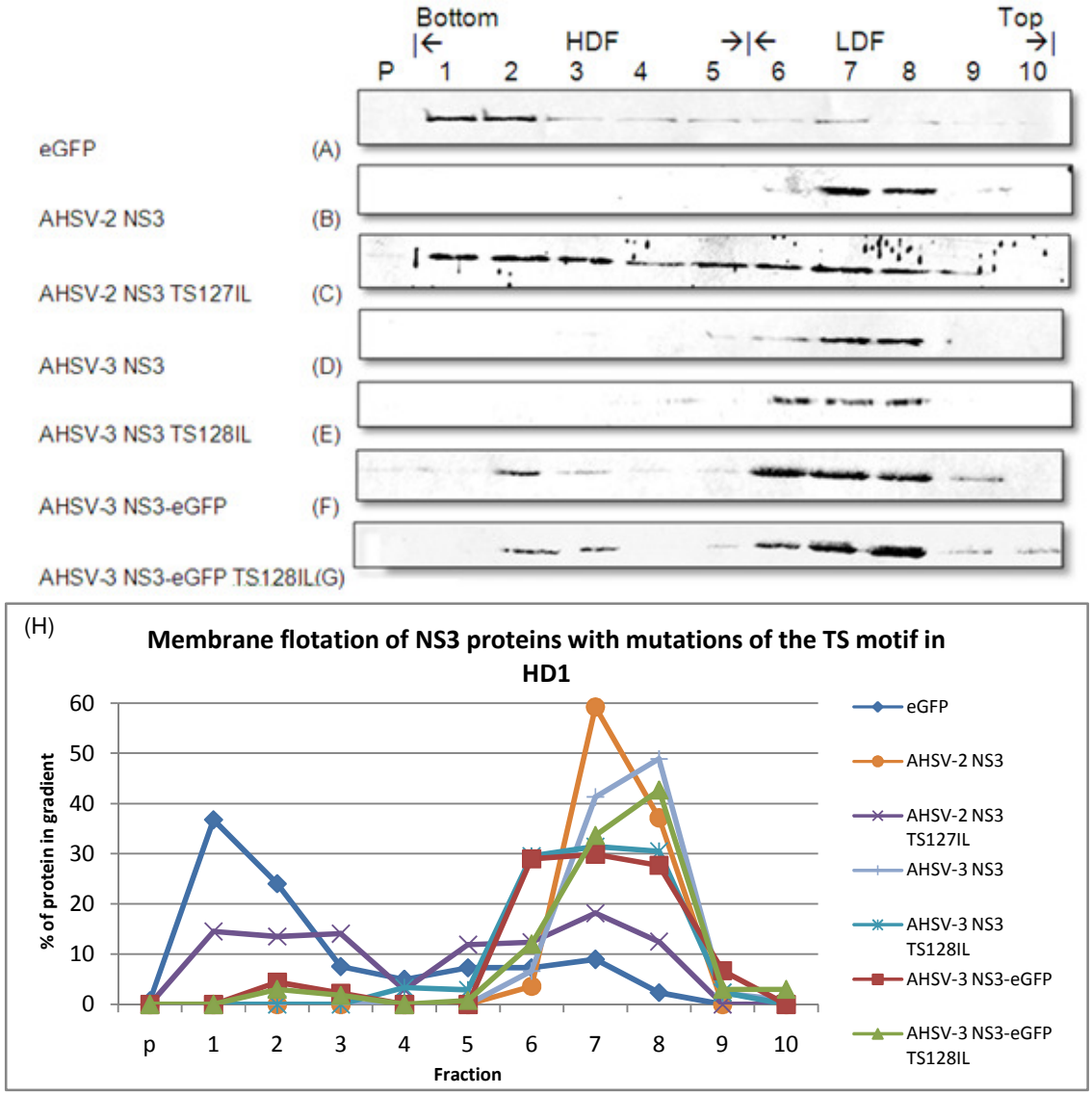

Figure 37: Western blot analysis of fractions from membrane flotation gradients of NS3 proteins with modifications to HD1 TS motif (24 h.p.i); Bac-eGFP (A); Bac-AHSV-2 NS3 (B); Bac-AHSV-2 NS3 TS127IL (C), Bac-AHSV-3 NS3 (D); Bac-AHSV-3 NS3 TS128IL (E); Bac-AHSV-3 NS3-eGFP (F); Bac-AHSV-3 NS3-eGFP TS128IL (G); EZQuant values plotted in Excel (H);

Modifications targeting the in N motif in NS3 HD2 did not result in total NS3 dissociation from the LDF for any of the mutant proteins (Fig. 38). However, the modification shifted 23% of the AHSV-2 NS3 N161I protein to the HDF of the gradient. The AHSV-3 NS3 N159I protein, like AHSV-3 NS3, was limited to the LDF.

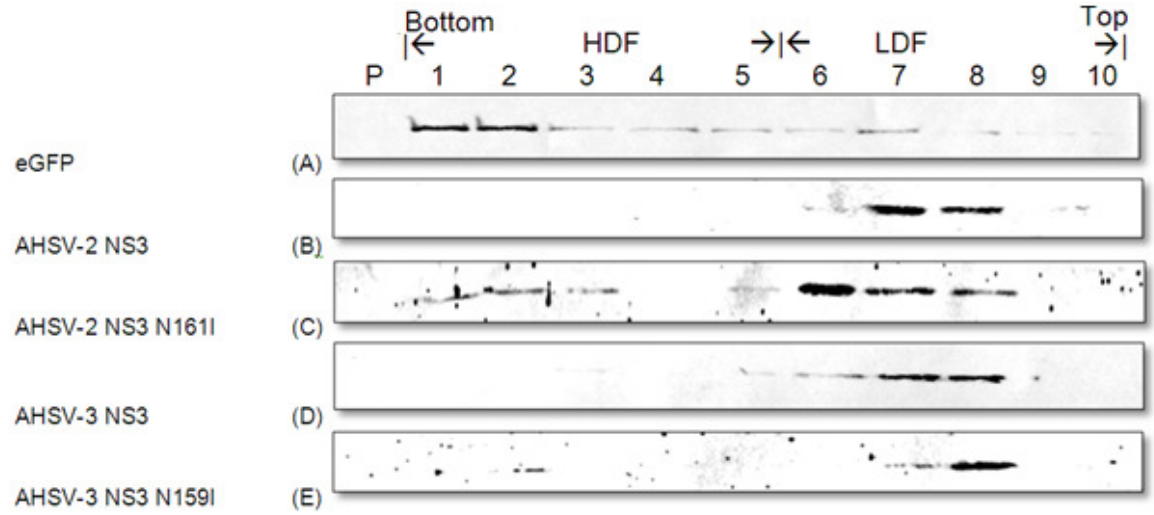

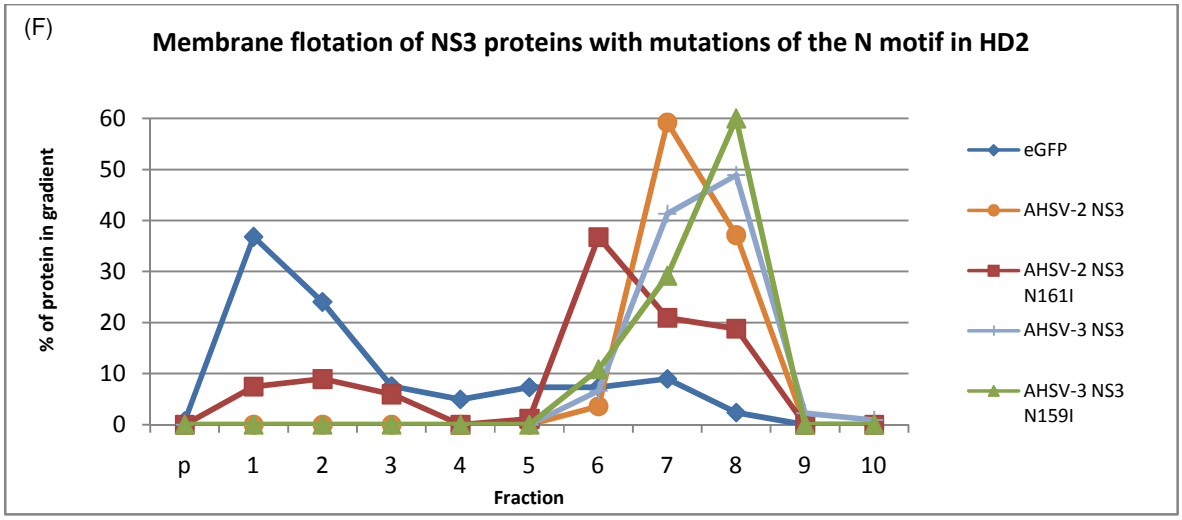

Figure 38: Western blot analysis of fractions from membrane flotation gradients of NS3 proteins with modifications to HD2 N motif (24 h.p.i); Bac-eGFP (A); Bac-AHSV-2 NS3 (B); Bac-AHSV-2 NS3 N161I (C), Bac-AHSV-3 NS3 (D); Bac-AHSV-3 NS3 N159I (E); EZQuant values plotted in Excel (F);

Modification of the intervening spacer region (ISR) between HD1 and HD2 had different effects on the distribution of the NS3 proteins in the membrane flotation profile for the different serotypes (Fig. 39). The ISR length mutant, AHSV-2 NS3 15aa ins151, showed a 60% shift to the HDF. The AHSV-2 NS3 I140S and Δ149KGD had 38% and 43% in HDF respectively. The AHSV-2 NS3 ISR D137S mutant showed a 31% shift to HDF. The AHSV-3 NS3 D138S showed no change in distribution when compared to AHSV-3 NS3. The AHSV-3 NS3-eGFP D138S had 91% associated with the LDF whereas the AHSV-3 NS3-eGFP had 93% associated with LDF. All of the AHSV-2 NS3 changes

resulted in some loss of membrane association where the AHSV-3 NS3 showed no change.

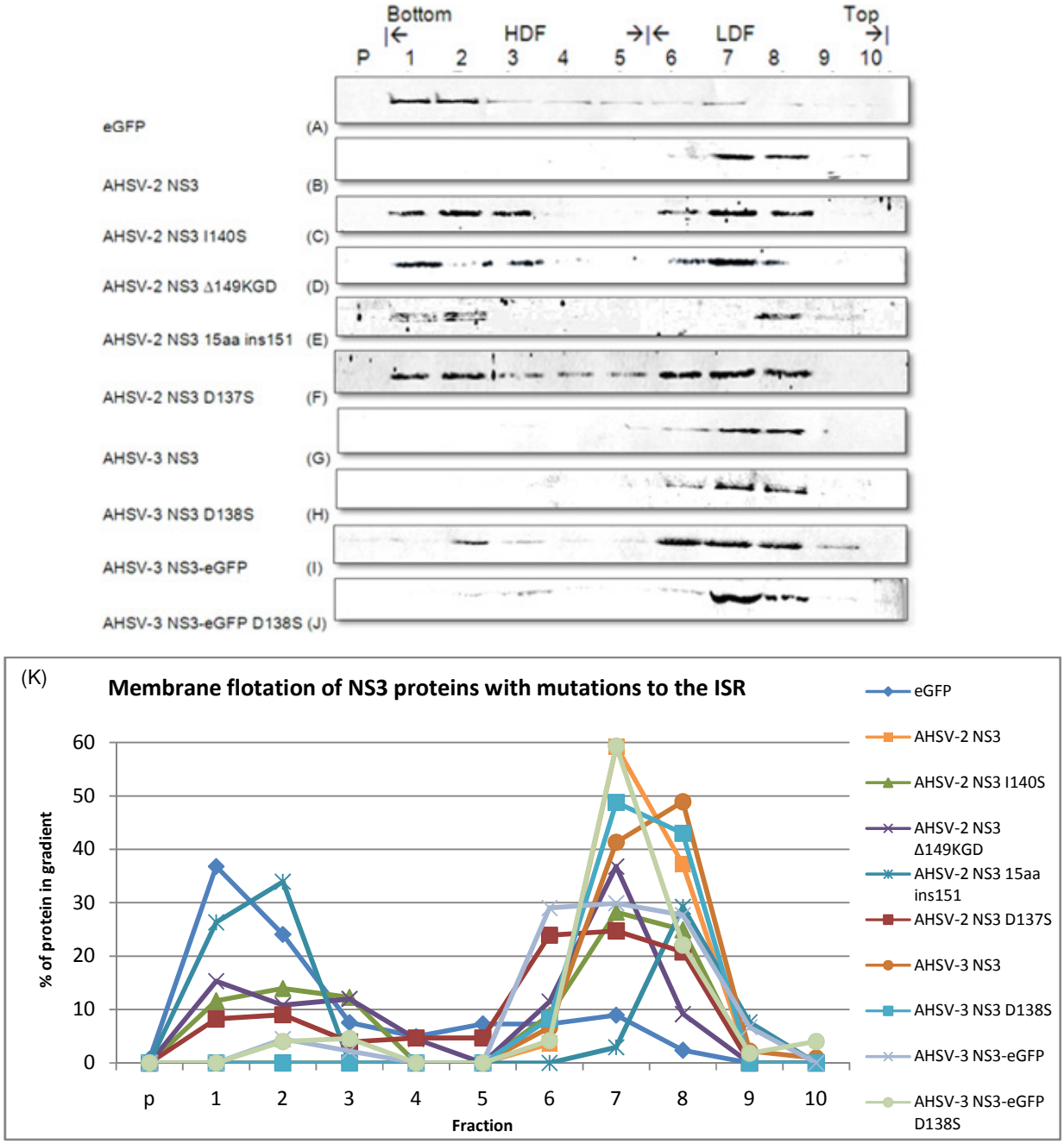

Figure 39: Western blot analysis of fractions from membrane flotation gradients of NS3 proteins with modifications to ISR (24 h.p.i); Bac-eGFP (A); Bac-AHSV-2 NS3 (B) and related ISR mutants: I140S (C), Δ149KGD (D), 15aa ins151 (E), and D137S (F); Bac-AHSV-3 NS3 (G); Bac-AHSV-3 NS3 D138S (H); Bac-AHSV-3 NS3-eGFP (I); Bac-AHSV-3 NS3-eGFP D138S (J); EZQuant values plotted in Excel (K);

To compare data obtained from scans of Western blots to fluorescence values of eGFP tagged proteins, flotations were quantified either from Western blots using EZQuant or from fluorescence emissions per fraction as measured by Ascent Fluoroscan. According to the EZQuant data, 81% of the total eGFP protein was located in the HDF whereas according to the fluorescence data 72% was (Fig. 40). The fluorescence data placed approximately 20% of AHSV-3 NS3-eGFP, NS3-eGFP TS128IL and NS3-eGFP D138S protein in the HDF where EZQuant data placed less than 10% for each of them.

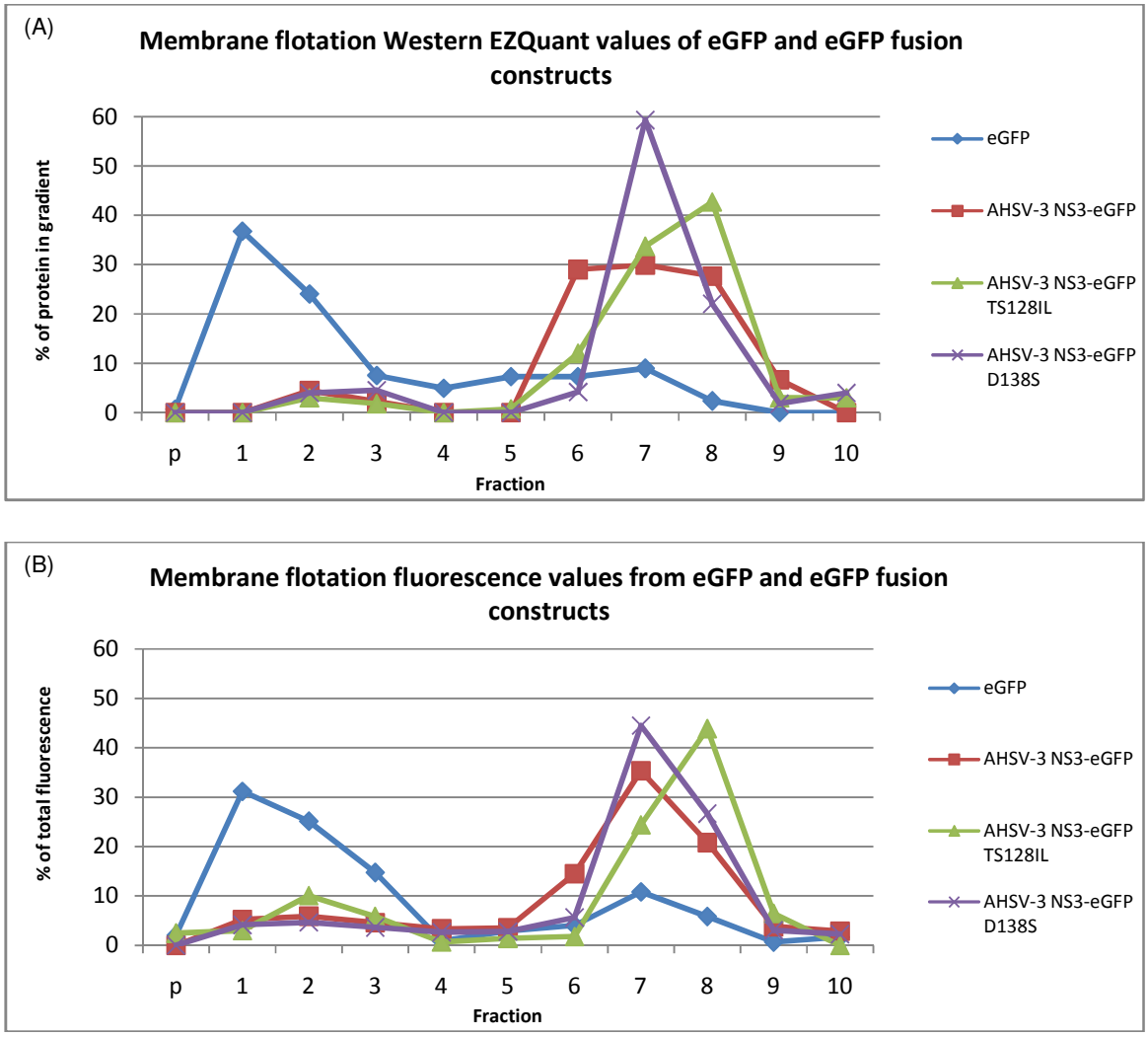

Figure 40: Comparison of EZQuant and Fluorescence distributions of eGFP and fusion proteins (24 h.p.i) in a membrane flotation gradient; EZQuant quantified from Western blot (A) and fluorescence per fraction as measured by Ascent Fluoroscan (B);

In summary, none of the modifications made to the NS3 protein completely negated association with the membrane associated LDF, but the some of the modifications resulted in a change in protein distribution in membrane flotation profile. The HD1 TS127IL mutation to AHSV-2 NS3 proteins resulted in a more general distribution through the gradient. The HD2 N161I showed a similar change in distribution but this shift was less pronounced. Modifications to the ISR of the AHSV-2 NS3 had the greatest disruptive effect on the LDF association as is apparent for all four (I140S, Δ149KGD, 15aa ins151, and D137S) of the AHSV-2 NS3 ISR mutants. The mutations that affected AHSV-2 NS3 LDF association seemed to have little to no effect on the LDF association of AHSV-3 NS3 and NS3-eGFP proteins.

2.3.5. Confocal microscopy

In order to visualize protein trafficking and subcellular localisation within a cell, fluorescent immunolabelling techniques are often employed. Sf9 cells were grown on coverslips and infected with recombinant baculoviruses expressing the mutant proteins. At 24 h.p.i. cells were fixed using acetone/methanol. The eGFP-fusion proteins were visualised after fixation without further processing. Immunofluorescence was used to visualize the untagged NS3 proteins (primary antibody directed against NS3, secondary antibody Alexa-fluor 488 conjugated). Cells were visualised by confocal scanning laser microscopy and images were captured using Zeiss LSM Image software. The displayed images were chosen to represent the dominant phenotype in the population of cells.

A number of controls were included for comparison. The mock infected cells had a minute amount of autofluorescence (Fig. 41 A). The wildtype baculovirus had some perinuclear signal (Fig. 41 B). The Bac-eGFP infected cells had a general fluorescent signal that was distributed through the nucleus and cytoplasm but no specific membrane association (Fig. 41 C).

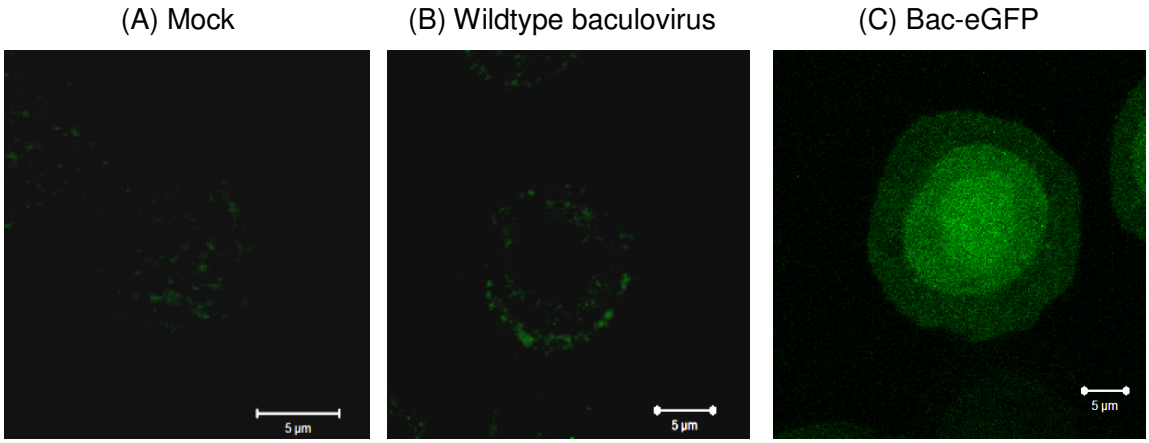

Figure 41: Confocal images captured from Sf9 cell controls; Mock infected (A); wildtype baculovirus infected (B) and Bac-eGFP infected cells (C) (Magnification = 100x, Scale bar = 5 µm).

Images of cells expressing the AHSV-2 NS3 protein had a very distinctive pattern (Fig. 42 A). The AHSV-2 NS3 protein had a distinct outer plasma membrane localisation. Cellular nuclei were stained using a 4'6'-diamidino-2-phenylindole (DAPI) and the AHSV-2 NS3 protein appeared as though it was localised around the nucleus and to a small extent in nucleoplasm (Fig. 42). The protein had a punctate perinucleur cytoplasmic localisation with relatively large discrete foci in the nuclear field (intranuclear bodies (INB)) (Fig. 42 C). It is important to note the large size of the Sf9 nucleus relative to the cell, the consequence being difficulty in resolving the cytoplasm and its associated structures. This complicated differentiation between perinuclear and cytoplasmic distribution of proteins, hence the somewhat generalised description "punctate perinucleur cytoplasmic localisation" (PNS). The nucleoplasmic (NP) signal intensity varied greatly with different exposures, in some instances was not even present. NP may not be a reliable marker for NS3 specific signal as it could not be standardised and was not considered further.

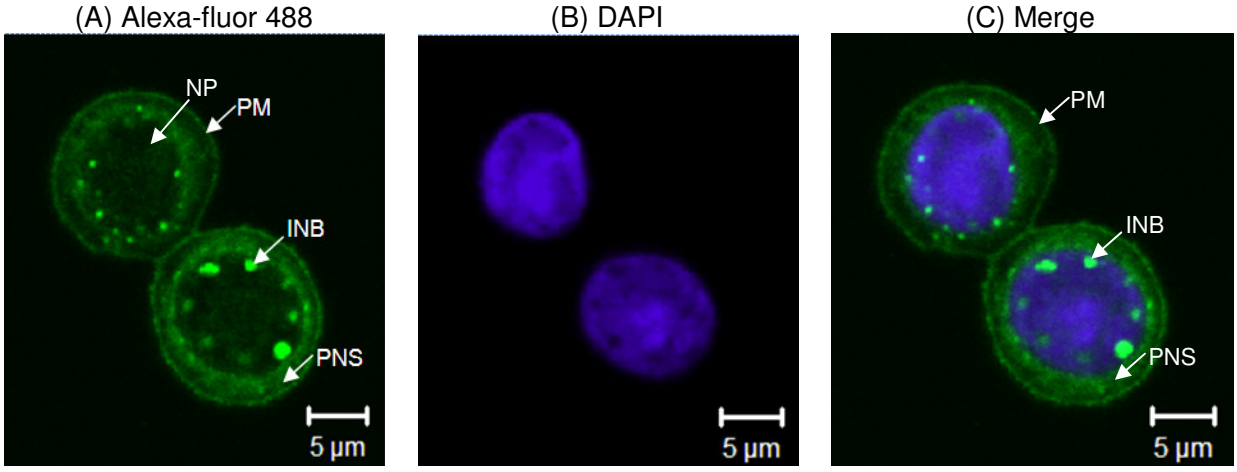

Figure 42: Confocal images of Sf9 cells infected with recombinant baculoviruses expressing AHSV-2 NS3 protein; Bac-AHSV-2 NS3 expressing cells with protein NS3 labelled with Alexa-fluor 488 (A), nuclei labelled with DAPI (B) and superimposed images (C). On the captured images, the nucleoplasm (NP), plasma membrane (PM) intranuclear bodies (INB) and punctate perinuclear and cytoplasmic signal (PNS) were noted. (DAPI = Blue, Alexa-fluor 488 = Green, Magnification = 100x, Scale bar = 5 µm).

From these images, it was not clear if the INB foci were large aggregates free inside the nuclear space, at the periphery of the nucleus or associated with the nuclear membrane. To further resolve the position of the aggregates, bioinformatic techniques were employed. Several horizontal slices/images were captured of one cell (called a Z-stack) these could be stacked to represent the entire volume of the cell. Of these, half of the slices were discarded leaving a series of images representing one hemisphere of the cell. These images were used to generate a three-dimensional model of the bottom half of the cell using the freeware version of Huygens essential suite version 3.3.2p3 by Scientific Volume Imaging B.V. (Fig. 43). It was observed that the discrete intranuclear foci (labelled INB) were connected to the nuclear membrane or associated structures like the ER and protruded into the nuclear space.

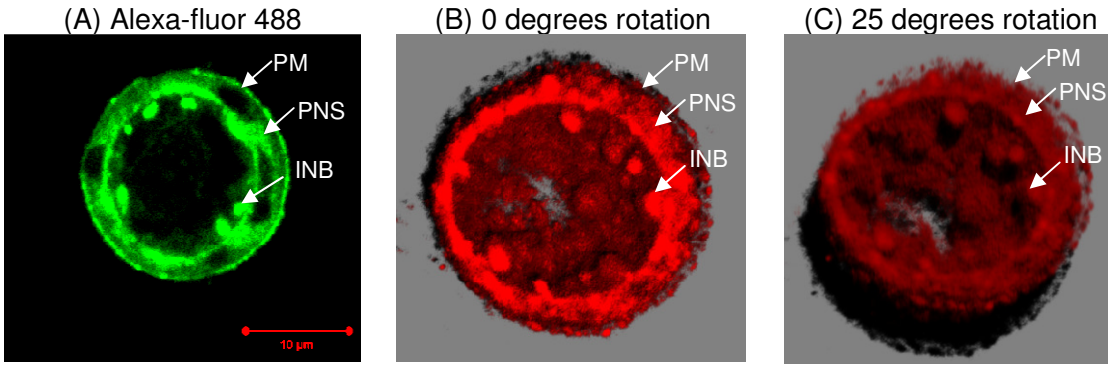

Figure 43: Three dimensional simulation of Sf9 cells infected with recombinant baculoviruses expressing AHSV-2 NS3 protein; Bac-AHSV-2 NS3 expressing cells with protein NS3 labelled with Alexa-fluor 488 (A). Three dimensional computer simulated model of half a cell expressing AHSV-2 NS3 as seen from the top (B) and from 25 degrees (C). On the captured images, the plasma membrane (PM) intranuclear bodies (INB) and punctate perinuclear and cytoplasmic signal (PNS) were noted. (Alexa-fluor 488 = Green, Magnification = 100x, Scale bar = 5 µm).

There was a lower intensity of fluorescent signal immunolabelled AHSV-3 NS3 as compared to AHSV-2 NS3 expressing cells. However, cells expressing the AHSV-3 NS3 protein had pattern similar to that of AHSV-2 NS3 expressing cells (Fig. 44). The AHSV-3 NS3 protein had a PNS localisation with discrete foci protruding inward from the nuclear envelope and a distinct plasma membrane localisation. The AHSV-3 NS3 INB were far less pronounced than for AHSV-2 NS3, and were not present in all cells. The AHSV-3 NS3-eGFP proteins displayed a PNS and specific plasma membrane localisation but no INB (Fig. 44 E). For uniformity in comparison, the same set of representative images of the three controls were used in all of the confocal figures (Fig. 44 to 45), i.e. those of AHSV-2 NS3, AHSV-3 NS3 and AHSV-3 NS3-eGFP.

Modification to the HD1 TS motif resulted in altered localisation patterns. The AHSV-2 NS3 TS127IL proteins showed a more homogeneous cytoplasmic distribution with small aggregates, there was no PM associated signal (Fig. 44 B). The AHSV-3 NS3 TS128IL and NS3-eGFP TS128IL had similar patterns, both the proteins presented in close

proximity around the nucleus with neither the INB and nor PM localisation specific signal found in the wildtype AHSV-3 NS3 (Fig. 44 C and F).

(A) AHSV-2 NS3

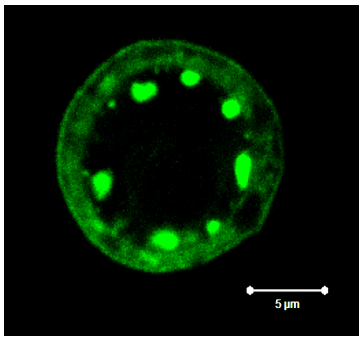

(B) AHSV-2 NS3 TS127IL

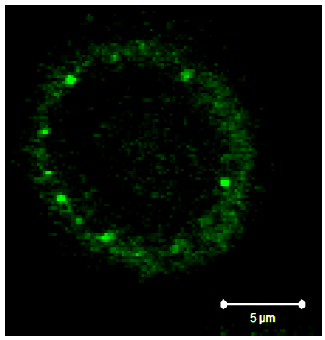

(C) AHSV-3 NS3

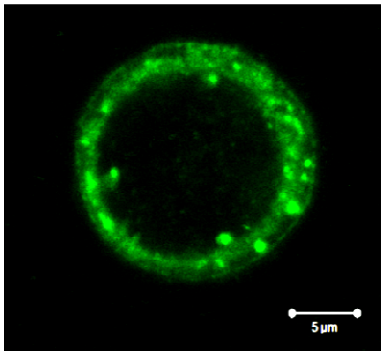

(D) AHSV-3 NS3 TS128IL

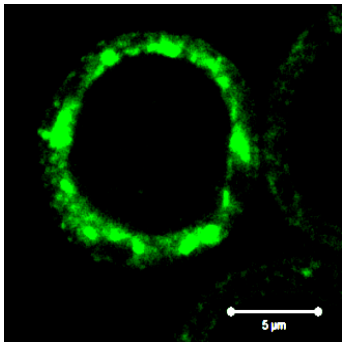

(E) AHSV-3 NS3-eGFP

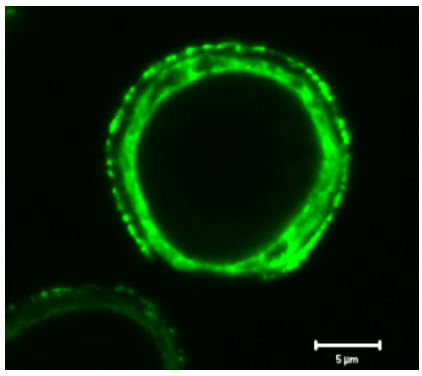

(F) AHSV-3 NS3-eGFP TS128IL

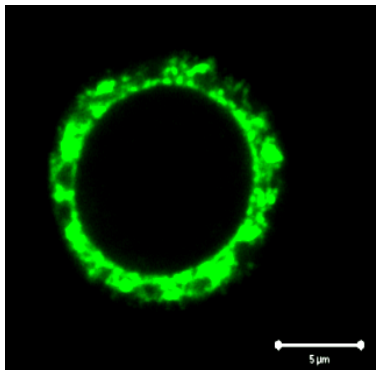

Figure 44: Confocal images of Sf9 cells infected with recombinant baculoviruses expressing versions of the NS3 protein with HD1 TS motif mutation; Bac-AHSV-2 NS3 (A) and corresponding TS127IL (B); Bac-AHSV-3 NS3 (C) and TS128IL (D); Bac-AHSV-3 NS3-eGFP (E) and corresponding TS128IL (F); (Alexa-fluor 488 = Green, Magnification = 100x, Scale bar = 5 µm).

Modification to the HD2 N residue had a similar effect on protein localisation as modification to the HD1 TS. The AHSV-2 NS3 N161I was localised in small PNS bodies with no plasma membrane association (Fig. 45 B). The AHSV-3 NS3 N159I, like AHSV-3 NS3 TS128IL, had only general PNS distribution, and showed a lack of plasma membrane localisation (Fig. 45 D).

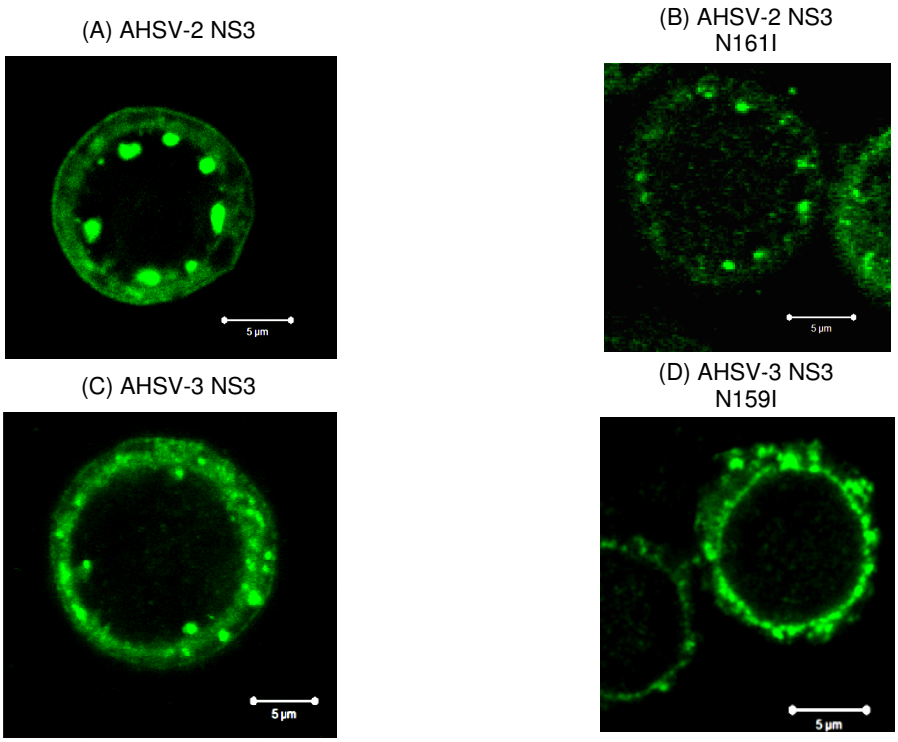

Figure 45: Confocal images of Sf9 cells infected with recombinant baculoviruses expressing versions of the NS3 protein with HD2 N motif mutation; Bac-AHSV-2 NS3 (A) and corresponding N161I (B); Bac-AHSV-3 NS3 (C) and related N159I (D); (Alexa-fluor 488 = Green, Magnification = 100x, Scale bar = 5 µm).

Modification to the ISR resulted in different phenotypes for the different modifications (Fig. 46). The AHSV-2 NS3 I140S and 15aa ins151 proteins both had a more general distribution throughout the cell with no definite perinuclear, intranuclear or plasma membrane localisations, as was found previously by R. Van der Sluis (Fig. 46 C and E). It is important to note that the confocal images captured of cells expressing these proteins were captured under high exposure due to very low fluorescent signal and may not be reliable representations of the proteins localisation through cells due to high background intensity due to overexposure. The AHSV-2 NS3 D137S and Δ149KGD proteins had similar distribution to unmodified AHSV-2 NS3 protein with some subtle differences (Fig. 46 B and D). The AHSV-2 NS3 Δ149KGD proteins had much smaller

and less pronounced intranuclear bodies (Fig. 46 D). The AHSV-2 NS3 D137S had the same plasma membrane, perinuclear localisation as well as the discrete intranuclear foci (Fig. 46 B). In addition to this, AHSV-2 NS3 D137S had a more general homogenous intranuclear component that could explain the HDF fraction association found in the membrane flotation assay (Fig. 39 F). The AHSV-3 NS3 D138S had plasma membrane specific signal and perinuclear but no intranuclear foci (Fig. 46 G). The AHSV-3 NS3-eGFP D138S protein did not show any changes in localisation (Fig 45 I).

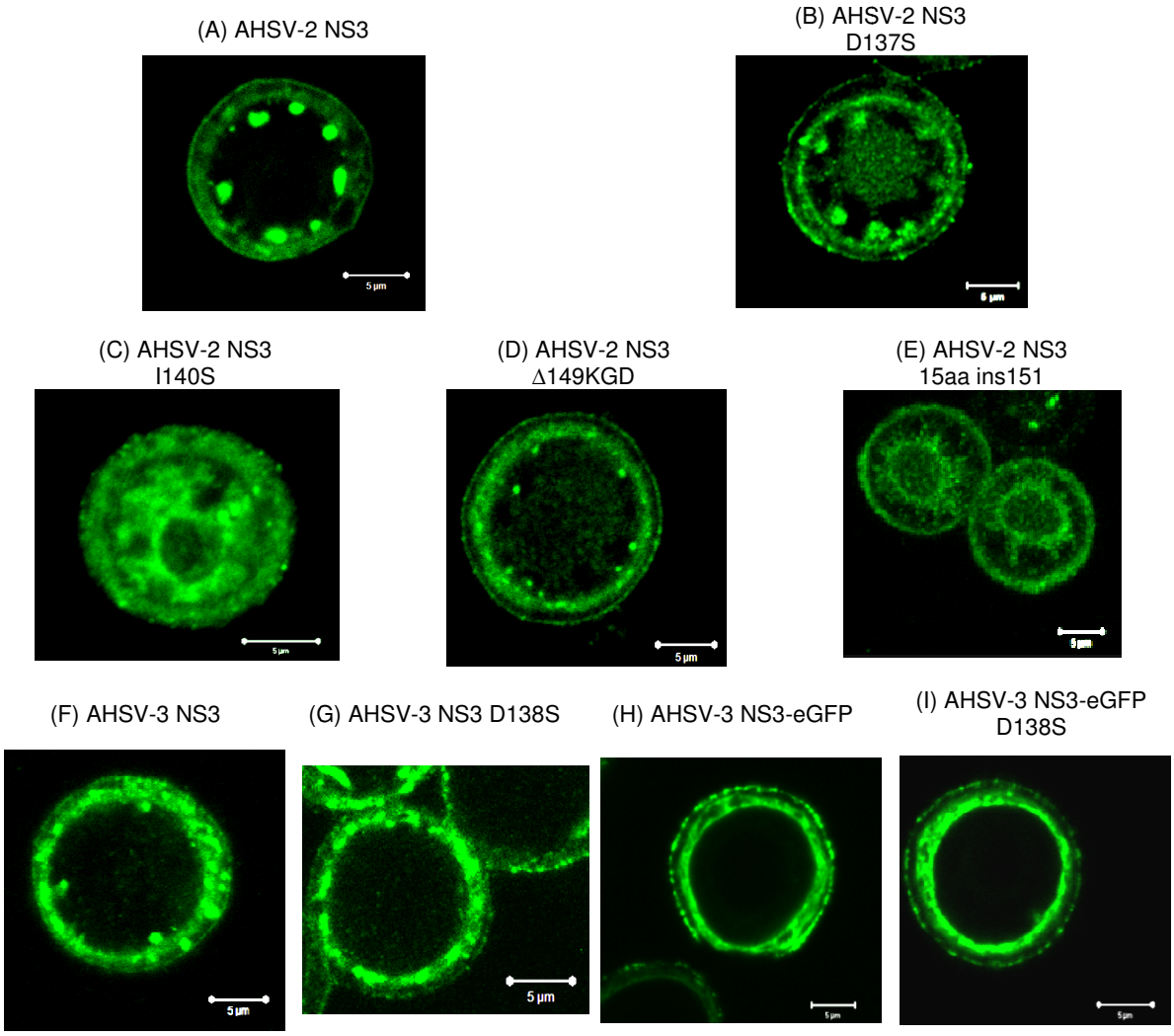

Figure 46: Confocal images of Sf9 cells infected with recombinant baculoviruses expressing versions of the NS3 protein with ISR mutations; Bac-AHSV-2 NS3 (A) and corresponding TS127IL (B); Bac-AHSV-3 NS3 (C) and TS128IL (D); Bac-AHSV-3 NS3-eGFP (E) and corresponding TS128IL (F); (Alexa-fluor 488 = Green, Magnification = 100x, Scale bar = 5 µm).

In summary, Sf9 cells were infected with recombinant baculoviruses expressing modified versions of the AHSV NS3 proteins. Cells were visualised by immunofluorescence and confocal microscopy at 24 h.p.i, while the majority of cells were still viable. This was done in order to visualise their distribution and trafficking through a Sf9 cell. The localisation patterns of all recombinant proteins are summarised in Table 13. All constructs showed a PNS (defined as punctate perinuclear and cytoplasmic) distribution and may reflect part of normal protein processing, perhaps may reflect association with the endoplasmic reticulum for folding and Golgi apparatus for modification and signalling. Addition of the eGFP tag was accompanied by the loss of INB formation in all of the constructs, not only the mutant ones. Modification to the TS motif in HD1 negated PM localisation in all three of the constructs. The specific modifications to N motif in HD2 negated PM localisation in both constructs. Thus, the specific modifications made to either of the hydrophobic domains both interfered with trafficking to the outer PM. In addition to the loss of the PM localisation, the AHSV-3 NS3 HD mutants (N and TS), also did not show the ability to form INBs. Though mutation had affected trafficking and membrane association, it remained unclear whether these changes had affected the characteristic toxic ability of the AHSV NS3 protein. Cell viability assays were employed to assess the contribution of these domains to the cytotoxic ability of NS3.

Table 13: Summary of protein localisation patterns from confocal images

Protein	INB	PNS	PM
AHSV-2 NS3	√	√	√
AHSV-3 NS3	√	√	√
AHSV-3 NS3-eGFP		√	√
AHSV-2 NS3 TS127IL	√	√	
AHSV-3 NS3 TS128IL		√	
AHSV-3 NS3-eGFP TS128IL		√	
AHSV-2 NS3 N161I	√	√	
AHSV-3 NS3 N159I		√	
AHSV-2 NS3 I140S		√	
AHSV-2 NS3 Δ149KGD	√	√	√
AHSV-2 NS3 15aa ins151		√	
AHSV-2 NS3 D137S	√	√	√
AHSV-3 NS3 D138S	√	√	√
AHSV-3 NS3-eGFP D138S		√	√

Intranuclear bodies = INB
Punctate perinuclear and cytoplasmic signal = PNS
Plasma membrane= PM

2.3.6. Cell viability assays

The AHSV NS3 protein, when expressed in a baculovirus system, has a cytotoxic effect on Sf9 cells in tissue culture. On the ultrastructural level, cells present with distorted nuclei, granular cytoplasm and completely disrupted plasma membranes (van Staden *et al.*, 1995). This phenomenon may reflect the role of NS3 in virus release and pathogenesis. In order to investigate whether the modifications to the AHSV-NS3 proteins affected this cytotoxic activity, cell viability of cells infected with recombinant baculoviruses expressing the different mutant NS3 proteins was monitored over time. Two assays were employed: a trypan blue assay and the CellTiter-Blue™ kit. Trypan blue is a vital exclusion dye that stains the cytoplasm of non-viable cells a distinct colour. The extent of cytotoxicity was quantified using light microscopy and a counting chamber and expressed as a percentage. The polyhedron promoter is activated from 18 h.p.i therefore measurements were done from 18 to 48 h.p.i. The CellTiter-Blue™ assay measures the cell viability as a function of fluorescence. Living cells can reduce resazurin to fluorescent resorufin. Non-viable cells do not reduce resazurin and no fluorescent signal is generated. The amount of fluorescence produced is proportional to the number of viable cells. Measurements were made at 24 and 48 h.p.i. The values

were expressed as percentage fluorescence relative to that of the uninfected cells (Mock). Trypan blue results will be termed “cytotoxic activity” and the results from the CellTiter-Blue™ assay will henceforth be referred to as “metabolic activity” to reduce confusion between the two sets of results, although both trypan blue and CellTiter-Blue™ assays are indicative of cell viability. Three repeats of the each experiment were performed. The average percentage cell viability was plotted against time and presented as a graph (Fig. 47 to 49). The controls used were mock infected cells or cells infected with either wildtype baculovirus or Bac-eGFP.

There was no significant difference between the cytotoxicity of the mock and wildtype baculovirus infection and both resulted in almost no cell death (Fig. 47 A). When observed under the light microscope it was noted that the mock infected cells continued to proliferate and doubled every 24 hours, whereas the wildtype baculovirus infected cells appeared to have ceased proliferation with cell counts remaining relatively close to the count at the time of infection. The CellTiter-Blue™ results indicate that the mock infected cells had no decrease in metabolic activity at 48 h.p.i. (Fig. 47 B). Rather, the total metabolic activity had increased at 48 h.p.i. relative to 24 h.p.i., this is probably due to continued cell proliferation (not shown). The wildtype baculovirus infection caused a significantly ($P=0.04$) reduced metabolic activity relative to the mock infected cells, which may reflect the altered metabolic state of infected cells (Fig. 47 B). However the metabolic activity of the wildtype baculovirus from 24 h.p.i. to 48 h.p.i. did not undergo a statistically significant change ($P=0.36$) (Fig. 47 B). Expression of the eGFP protein had a slight cytotoxic effect with a significant ($P=0.0091$) reduction in cell viability, with 83% of cells still viable at 48 h.p.i (Fig. 47 A). The additional reduction in metabolic activity from 24 h.p.i to 48 h.p.i. was 11% (Fig. 47 B).

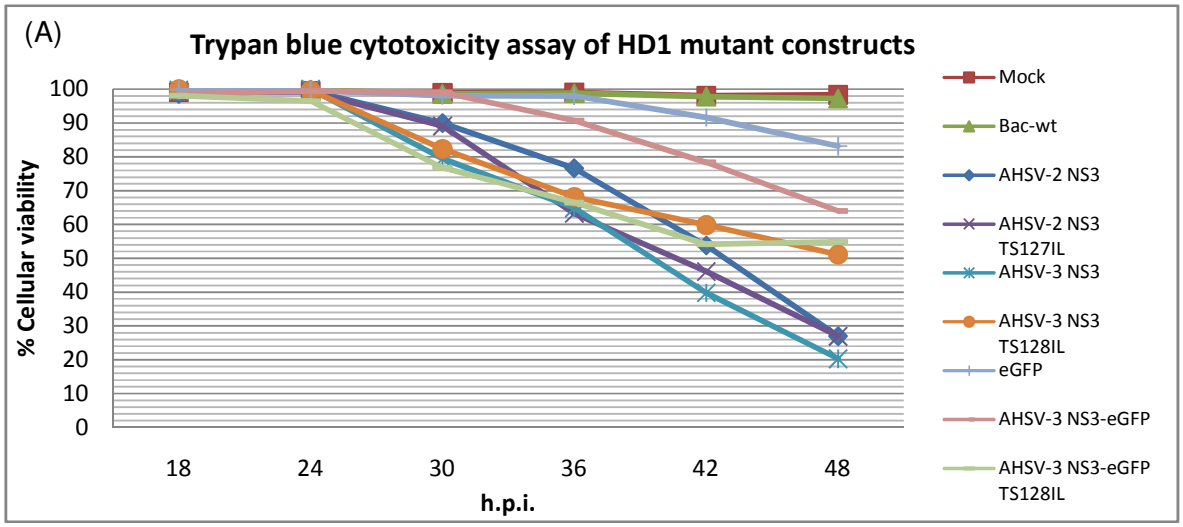

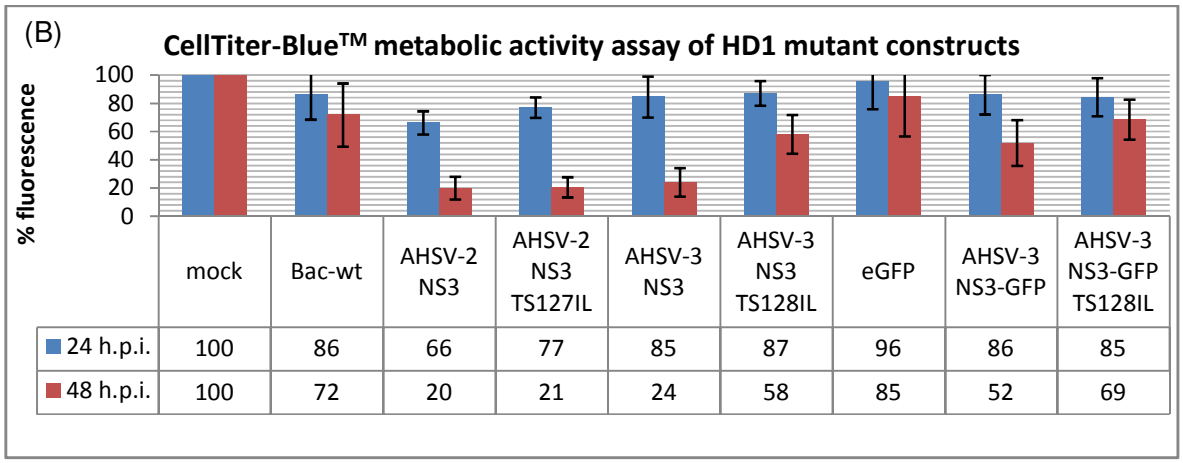

	mock	Bac-wt	AHSV-2 NS3	AHSV-2 NS3 TS127IL	AHSV-3 NS3	AHSV-3 NS3 TS128IL	eGFP	AHSV-3 NS3-GFP	AHSV-3 NS3-GFP TS128IL
24 h.p.i.	100	86	66	77	85	87	96	86	85
48 h.p.i.	100	72	20	21	24	58	85	52	69

Figure 47: Cytotoxicity assays of Sf9 cells infected with baculoviruses expressing NS3 proteins with modifications to HD1 TS; Trypan blue assay (A) and CellTiter-Blue™ assay (B). The recombinant baculoviruses used to infect cells were wildtype baculovirus, Bac-eGFP; Bac-AHSV-2 NS3; Bac-AHSV-2 NS3 TS127IL, Bac-AHSV-3 NS3; Bac-AHSV-3 NS3 TS128IL; Bac-AHSV-3 NS3-eGFP; Bac-AHSV-3 NS3-eGFP TS128IL.

The expression of the AHSV-2 NS3 and AHSV-3 NS3 proteins were both associated with increased cytotoxicity from 24 h.p.i. onward, six hours from when polyhedrin specific protein expression had been initiated. By 48 h.p.i. less than 30% of cells were still viable (Fig. 47 A). The cytotoxic effect of AHSV-2 NS3 expression at 48 hours compared to the mock infected was statistically significant ($P>0.0001$). In the corresponding time period, the AHSV-3 NS3 expression reduced cell viability to 20±9%, this change was also statistically significant ($P<0.0001$). There was no significant ($P=0.22$) difference between the cytotoxic effects of AHSV-2 NS3 and AHSV-3 NS3. The CellTiter-Blue™ assay results indicated that 48 hours following infection with recombinant baculoviruses

expressing either the AHSV-2 NS3 protein or the AHSV-3 NS3 protein, experienced a reduction in metabolic activity to below 30% (Fig. 47 B). The reductions in metabolic activity showed by AHSV-2 NS3 (P=0.0002) and the AHSV-3 NS3 (P=0.0005) were both statistically significant. There was no significant (P=0.56) difference between the effects of AHSV-2 NS3 and AHSV-3 NS3 on metabolic activity of infected cells. Thus, there was a definite relationship between the reduction in metabolic activity and level of cytotoxicity. The reduction in metabolic activity reflects the reduction in viable cell population size. The effects of expression of both AHSV-3 NS3 and AHSV-2 NS3 had similar effects on cell viability as reflected by both these sets of data (Fig. 47).

The difference in cytotoxicity between the AHSV-3 NS3 and AHSV-3 NS3-eGFP was statistically significant (P=0.0003) with the AHSV-3 NS3-eGFP showing a 40% less reduction in cell death. After 48 hours the cultures expressing the AHSV-3 NS3-eGFP presented 34% (P=0.0186) drop in metabolic activity, significantly less pronounced than that observed for AHSV-3 NS3 (Fig. 47 B). Thus both trypan blue and CellTiter-Blue^{TM} assays reflected that the AHSV-3 NS3-eGFP protein had less severe effect on cell viability as compared to the AHSV-3 NS3 protein. The effect of the eGFP tag on the AHSV-3 NS3 cytotoxic phenotype was considerable.

Modification to the HD1 TS motif had differential effects on the AHSV-2 NS3 and AHSV-3 NS3 proteins cytotoxic effect (Fig. 47). Relative to AHSV-3 NS3 expressing cells, those expressing the AHSV-3 NS3 TS128IL protein had double the amount of metabolic activity and double the amount of cells left viable at 48 h.p.i. (Fig. 47 B). Whereas the cells producing the AHSV-2 NS3 TS127IL protein showed no significant deviation from the cytotoxic or metabolic phenotype of AHSV-2 NS3 expressing in the same time-span (Fig. 47). There were no significant differences between the cytotoxic and metabolic phenotypes observed for AHSV-3 NS3-eGFP versus the AHSV-3 NS3-eGFP TS128IL (Fig. 47). Therefore, the modification to the TS motif in HD1 of NS3 only affected AHSV-3 NS3 and resulted in the reduction in the lethal phenotype.

The HD2 N motif modification caused a significant phenotypic change in the cytotoxic phenotype of AHSV-3 NS3 but not AHSV-2 NS3 (Fig. 48). Cells infected with recombinant baculoviruses expressing the AHSV-2 NS3 N161I protein did not show significant deviation from that observed for AHSV-2 NS3 after 48 hours, however there was a difference in trend between 36 and 42 h.p.i. (Fig. 48). In contrast to the AHSV-2

NS3 N161I expressing cells, after 48 hours the AHSV-3 NS3 N159I producing cells showed a significant reduction in cytotoxic activity and increased metabolic activity relative to the wild type AHSV-3 NS3 (Fig. 48). These results are similar to that observed for the NS3 HD1 TS modification baculoviruses. The modification the HD2 N of NS3 only affected AHSV-3 NS3 and resulted in the reduction of its effects on cell viability.

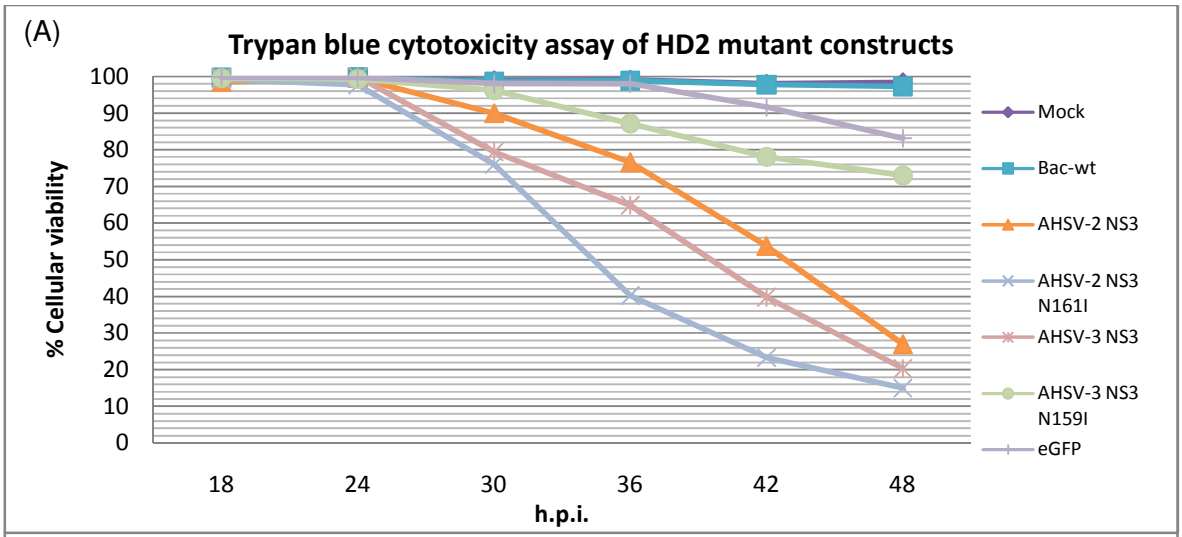

(B) CellTiter-Blue™ metabolic activity assay of HD2 mutant constructs

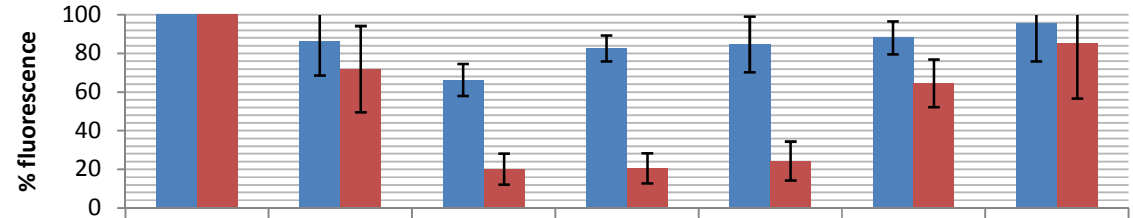

	mock	Bac-wt	AHSV-2 NS3	AHSV-2 NS3 N161I	AHSV-3 NS3	AHSV-3 NS3 N159I	eGFP
24 h.p.i.	100	86	66	83	85	88	96
48 h.p.i.	100	72	20	21	24	65	85

Figure 48: Cytotoxicity assays of Sf9 cells infected with baculoviruses expressing NS3 proteins with modifications to HD2 N; Trypan blue assay (A) and the CellTiter-Blue™ (B). The constructs evaluated were Wildtype baculovirus, Bac-eGFP; Bac-AHSV-2 NS3; Bac-AHSV-2 NS3 N161I, Bac-AHSV-3 NS3; Bac-AHSV-3 NS3 N159I.

None of the ISR modifications had major altering effects on the cytotoxic phenotype (Fig. 49). The average cytotoxicity of all of the untagged mutant constructs remained similar to those of both AHSV-2 NS3 and AHSV-3 NS3 after 48 hours. There were no

significant deviations in the metabolic activity of any of the ISR constructs relative to the AHSV-2 NS3 and AHSV-3 NS3 expressing cells. There was no significant difference between the AHSV-3 NS3-eGFP and the AHSV-3 NS3-eGFP D138S mutant construct.

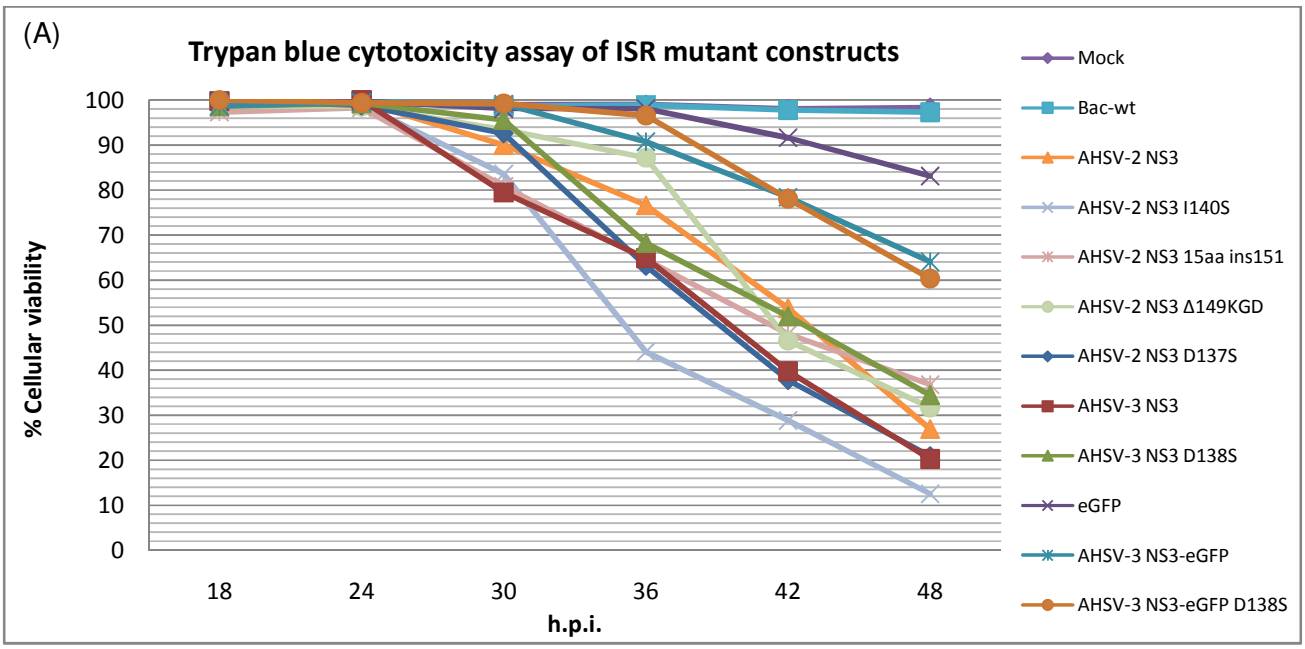

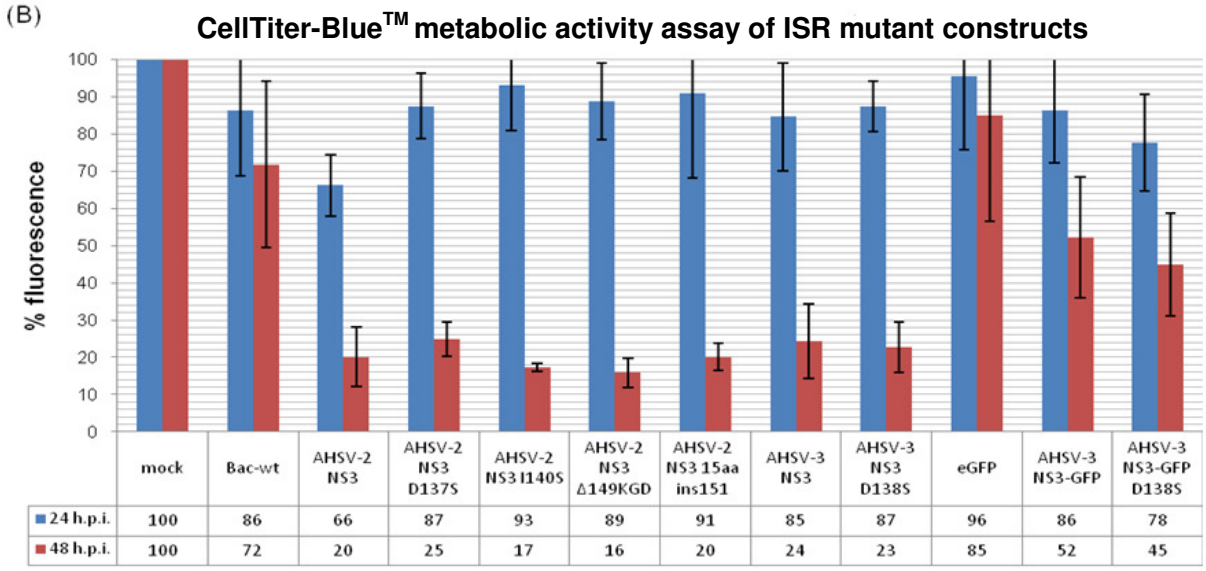

Figure 49: Cytotoxicity assays of Sf9 cells infected with baculoviruses expressing NS3 proteins with modifications to ISR; Trypan blue assay (A) and the CellTiter-Blue™ (B). The constructs evaluated were Wildtype baculovirus, Bac-eGFP; Bac-AHSV-2 NS3 and related ISR mutants: I140S, Δ149KGD, 15aa ins151, and D137S; Bac-AHSV-3 NS3; Bac-AHSV-3 NS3 D138S; Bac-AHSV-3 NS3-eGFP; Bac-AHSV-3 NS3-eGFP D138S.

In summary, there seemed to be a good correlation between the Trypan Blue cytotoxicity results and the CellTiter-Blue™ metabolic activity results. When the level of cell death increased, the ability to metabolize resazurin decreased. The AHSV-2 NS3 and AHSV-3 NS3 had similar effects on cells expressing them, both reducing percentage cell viability and metabolic activity to around below 30%. The eGFP tag on the C- terminal end of NS3 was associated with a decrease in cytotoxicity relative to the AHSV-3 NS3, as reflected by the increased percentage viability after 48 hours and an increased ability to metabolize resazurin. The HD1 TS-motif modification did not significantly affect AHSV-2 NS3 but did affect AHSV-3 NS3 and AHSV-3 NS3-eGFP, which both showed relative reductions in cytotoxicity, accompanied by increased metabolic activity. HD2 N-motif modification was associated with similar cytotoxicity for AHSV-2 NS3 and decreased cytotoxicity for AHSV-3 NS3. ISR modification did not result in significant deviations in the cytotoxic phenotype of the modified NS3 proteins. Some but not all modifications made to the AHSV NS3 protein affected the characteristic NS3 effect on cell viability.

2.4. Discussion

The influence of key motifs and residues on the three-dimensional structure of membrane proteins are difficult to study, specifically because of the difficulties in crystallising the proteins in their native conformation (Baker, 2010). Mutational approaches are employed for elucidating the functions of motifs in membrane proteins. The aim of this project was to determine the roles of previously identified motifs in the function of AHSV NS3 by site directed mutagenesis and subsequent expression of mutant proteins in a baculovirus expression. To this end, PCR based methods were used to generate mutant versions of the NS3 gene. Eight baculoviruses expressing modified versions of the AHSV NS3 protein were generated during the course of this project. Three mutants targeting the TS motif in hydrophobic domain one (HD1) of NS3 were generated, namely AHSV-2 NS3 TS127IL, AHSV-3 NS3 TS128IL and AHSV-3 NS3-eGFP TS128IL. Two of the mutants generated targeted the N residue in the second hydrophobic domain (HD2) of AHSV NS3; these were AHSV-2 NS3 N161I and AHSV-3 NS3 N159I. Three mutants were generated to study the role of motifs in the intervening spacer region (ISR) of NS3, these were AHSV-2 D137S, AHSV-3 NS3 D138S and AHSV-3 NS3-eGFP D138S. In addition to these constructs, three available mutant construct of the AHSV-2 NS3 ISR were evaluated, these were AHSV-2 NS3 I140S, AHSV-2 NS3 Δ149KGD and AHSV-2 NS3 15aa ins151. These constructs were evaluated in terms of membrane association, rough assay for cellular distribution, cellular localisation and cytotoxicity.

Two methods were employed for site-directed mutagenesis; these were the megaprimer method and the Quikchange method. The target gene was 766 bp, which means that the largest megaprimer that could be used according to the literature was about 500 bp (Barik, 1996). The size of the megaprimer itself did not seem to be the determining factor as the AHSV-2 S10 D137S had a megaprimer of 454 bp, which could be successfully used, whereas the AHSV-3 S10 TS128IL had a megaprimer of 430 bp and could not be optimized. The orientation (forward or reverse) of the megaprimer did influence the efficiency of amplification (not shown). In an attempt to identify reasons why the method could not be optimized in all cases, the literature was explored. From the literature it is evident that the success of the approach may depend on the innate differences between the megaprimer products, be it secondary structure formation (3' hairpins), GC content or the strength of binding between two strands of the double

stranded megaprimer (Barettino *et al.*, 1994; Barik, 1995; 1996; 1997a; b; 2002; Barik & Galinski, 1991; Brons-Poulsen *et al.*, 2002; Burke & Barik, 2003). The Quikchange method could also not be optimised for some of the constructs. Even though the primers were able to amplify and produce the expected products when used in combination with the general primers, when they were used together amplification did not occur. This may be due to the binding strength of the two primers to each other when used in unison. In an attempt to denature the primers, the denaturation temperature was increased, but this did not improve amplification. What worked for one construct did not necessarily work for another. Therefore, reactions needed to be individually optimised and techniques were not suitable for all instances. Cloning of the PCR products and Gateway system generation of recombinant baculoviruses were accomplished without major difficulties. Mutations were confirmed via automated Sanger sequencing and expression of the various constructs was confirmed by Western blot.

At this point it is important to keep in mind that the expression levels of the various constructs were not equal; some were barely detectable and required high levels of exposure to enable detection, these were AHSV-2 NS3 I140S and AHSV-2 NS3 15aa; levels of expression of the eGFP tagged NS3 constructs were significantly higher than for the untagged versions. These inconsistencies may indeed compromise the reliability of the data or reduce comparability between the sets of data and were considered.

Characteristics of the intervening spacer region can influence the function of their native protein. The length of the spacer region between transmembrane domains can affect the topology and the mechanism of insertion into the membrane (Goder *et al.*, 1999). Conserved residues had been identified previously and these were proposed to have possible function in the NS3 protein's processing, trafficking and function (van der Sluis, 2007). A three residue KGD motif is present only in the highly pathogenic AHSV-2 NS3 and may perhaps play a role in this phenotype (van der Sluis, 2007). The spacer may therefore be important for the protein folding, membrane association and NS3 function. It is for these reasons that the spacer length was targeted for mutational studies. Modification to the AHSV NS3 ISR had a variety of effects on the intracellular distributions of the recombinant proteins but their effects on the cytotoxicity were negligible. All modifications of the ISR caused an increase in soluble NS3. Some of the modifications resulted in the altered localisation pattern observed using confocal microscopy.

Hydrophilic regions or motifs between membrane spanning domains, like the D residue in the ISR of NS3, have been shown to be essential for pore function of viroporin proteins and may also play a role in protein folding (de Jong *et al*., 2004). Modification of the D motif in the ISR had variable effects on the AHSV-2 NS3 and AHSV-3 NS3 protein characteristics. The D138S modification to AHSV-2 NS3 was accompanied by the following characteristics: more general distribution through membrane flotation profile; no significant changes in rough fractionation profiles; confocal data showed similar distribution to that of AHSV-2 NS3 with defined INBs. The only major difference was that the AHSV-2 NS3 D137S protein presented with an increased general nucleoplasmic component. The D138S modification of AHSV-3 NS3 and AHSV-3 NS3-eGFP proteins caused no significant changes in membrane association, rough fractionations or confocal profiles. In hindsight, the change of the D residue to an S may have failed to disrupt the function of the residue in the protein, as the D and S are both hydrophilic residues. The change would not necessarily affect the proteins viroporin hydrophilic pore or hydrogen bonding required for oligomerisation or protein folding. It may be more insightful to mutate the residue to something nonpolar or hydrophobic that would disrupt hydrogen bonding ability or the hydrophilic nature of the residue.

The detection of the AHSV-2 NS3 I140S, Δ149KGD, 15aa ins151 proteins proved challenging during membrane flotation, fractionation and confocal work and a lot of variation in the results obtained were encountered. It is likely that the difficulties encountered were due to the low levels of expression found of these constructs. No major conclusions can be made from results relating to these constructs. Nevertheless, the following observations were made, some of which contradict previous data (van der Sluis, 2007). The AHSV-2 NS3 I140S, Δ149KGD, 15aa ins151 proteins all showed some shift to the soluble high-density fractions even though the majority of protein remained associated with the membrane fractions in the membrane flotation profile. Despite this shift, there was no significant change in the subcellular fractionation (N-P-S) profiles of any of these proteins. This contradicts results reported previously which stated that the AHSV-2 NS3 I140S and 15aa ins151 were limited to the soluble fractions (van der Sluis, 2007). The confocal images captured from cells expressing AHSV-2 NS3 I140S, Δ149KGD, 15aa ins151 had to be captured under high exposure because of difficulty detecting the fluorescent signal. This may have therefore increased the amount

of background fluorescence, subsequently reducing the confidence in the validity of the localisation patterns observed. It seemed as though AHSV-2 NS3 I140S and 15aa ins expression resulted in the complete loss of AHSV-2 NS3 characteristic confocal localisation patterns, with generalised distribution patterns in the cyto- and nucleoplasm. The wheel-like patterns of localisation were also observed, but only under high excitation/exposure conditions which may indicate that the signal is not specific but rather background. The AHSV-2 NS3 Δ149KGD modification did not alter the localisation pattern dramatically. There were no effects on the cytotoxic phenotype associated with AHSV-2 NS3 expression and therefore it appears that the motifs targeted in the ISR were not critical for the NS3 toxicity.

The eGFP tag is a very useful tool for the study of proteins in live cells (Ehrhardt, 2003). It has been used successfully for the study of viral protein trafficking in several instances (Chalfie, 1995; Fetzer *et al.*, 2005; Lux *et al.*, 2005; Neubauer *et al.*, 2002; Ojala *et al.*, 2004; Zhang *et al.*, 2005). The addition of the eGFP tag to the C-terminal end of the AHSV NS3 protein allowed clear visualisation of the protein by confocal imaging techniques; additionally it allowed the easy detection and quantification of the tagged proteins in solution (fractionisation and flotations). The addition of the eGFP to the AHSV-3 NS3 resulted in a phenotype that may be described as follows: maintained membrane association (from membrane flotations and subcellular fractionations), plasma membrane (PM) and punctate perinuclear and cytoplasmic (PNS) localisation, but loss in intranuclear body (INB) formation (confocal data). In addition to this the cytotoxic ability was significantly reduced (trypan blue and CellTiter-Blue^{TM}). Thus, the addition of eGFP tag did not affect PM association but negated the INB formation and cells expressing the eGFP-fusion protein exhibited reduced levels of cell death. It may well be that the inherent solubility of the eGFP tag interferes with the ability of the NS3 protein to multimerise and act as a viroporin even though it had been successfully trafficked to the PM.

Threonine and serine motifs have been shown to be involved in protein folding and oligomerisation, their highly conserved nature in the NS3 protein made them ideal targets for site directed mutagenesis (Dawson *et al.*, 2002; Gray & Matthews, 1984; van der Sluis, 2007). Modification of HD1 affected only the membrane association of AHSV-2 NS3 TS127IL, and had no effect on the AHSV-3 NS3 TS128IL or AHSV-3 NS3-eGFP TS128IL proteins' fractionation profiles. The AHSV-2 NS3 TS127IL had a general

distribution through the membrane flotation gradient in comparison to the AHSV-2 NS3, which was limited to the membrane-associated low density fractions (LDF). The association of AHSV-2 NS3 TS127IL with the LDF was not completely lost, but significantly reduced. Rough fractionation by differential centrifugation also indicated that only the AHSV-2 NS3 TS127IL protein had an altered distribution when compared to the unmutated NS3 control. The AHSV-2 NS3 TS127IL protein had no protein in the P fractions but was still associated with the N and S fractions, indicative of a loss of PM association. The membrane/lipid associated AHSV-2 NS3 TS127IL therefore must be representative of the N fraction associated membranous structures, possibly the nuclear membrane or the closely associated endoplasmic reticulum (ER).

In terms of the confocal localisation patterns, the AHSV NS3 characteristic distribution (INB, PNS and PM) was distorted with modification of the HD1 TS motif. The entire group of HD1 TS mutant construct had altered localisation patterns, which may indicate the generalised importance of the motif across serotypes. The AHSV-2 NS3 TS127IL protein lost PM localisation but retained INB and PNS. These INB and PNS bodies were less prominent than that observed for the wildtype AHSV-2 NS3. The AHSV-3 NS3 TS128IL mutation was accompanied by loss of the PM and INB localisation patterns. The AHSV-3 NS3-eGFP TS128IL distribution presented with the loss of PM localisation. Note that only the AHSV-2 NS3 TS127IL protein retained the INB formation but PM localisation was lost for all of the HD1 TS mutant constructs.

The Sf9 cell culture toxic phenomena originally described by Van Staden *et al.* in 1995 that is usually associated with NS3 expression was significantly reduced for the cultures expressing AHSV-3 NS3 TS128IL, as shown by the trypan blue assay and the CellTiter-Blue™ assay results. The AHSV-2 NS3 TS127IL showed no significant changes in toxicity when compared to the wildtype.

Modification of the HD1 TS motif therefore had different effects on phenotypes of AHSV-2 NS3 and AHSV-3 NS3 proteins. The AHSV-2 NS3 TS127IL proteins lost specific localisation characteristics, excluding the INB formation, but cytotoxic ability was retained. The AHSV-3 NS3 TS128IL proteins lost the INBs and cytotoxic ability was reduced. From the HD1 TS mutant data it may be deduced that membrane localisation of NS3 is not required for cytotoxicity.

Polar amino acids like the N residue in HD2 of NS3 have been shown to have structural roles and possibly a role in homo-oligomerisation (Choma *et al.*, 2000). Mutation of the AHSV NS3 HD2 N motif resulted in similar phenotypes to that observed for HD1 TS mutants. The AHSV-2 NS3 N161I protein was no longer limited to the membrane associated LDF fractions and had a more general distribution in the membrane flotation gradient, and it negated association with the plasma membrane associated P fraction during rough fractionations. The confocal images indicated that there was no PM distribution but some PNS but the AHSV-2 NS3 N161I proteins were concentrated in INBs (not as pronounced as those seen for AHSV-2 NS3) and the effect of this mutant on cell viability remained unaffected. The AHSV-3 NS3 N159I protein had the following phenotype: normal membrane association as is evident from membrane flotations; normal P fraction association; confocal data suggests loss of PM and INBs; cell viability assays suggest a loss in cytotoxic ability.

When the INBs were lost, the levels of cell death was reduced and when they were present the high levels of cell death persisted. The presence or absence of PM localisation did not correlate with a change in effect on cell viability in AHSV-2 NS3 constructs but did correlate in the AHSV-3 NS3. These results do not completely support the viroporin hypothesis for AHSV-2 NS3 action where the protein disrupts the integrity of the PM by specific action at thereat. For AHSV-2 NS3, there seems to be a correlation in the presence of INBs and effects on cell viability. A loss of INBs as accompanied by reduced cytotoxic ability. PM localisation may not be a prerequisite for the AHSV NS3 protein associated cell death, but the INBs are associated with this phenomenon. However, for the AHSV-3 NS3 proteins when the PM and INB localisation were both lost there was a decrease in cytotoxicity. For the AHSV-2 NS3 proteins there was a loss in visible PM localisation, however the expression levels of these proteins were low. It is also important to keep in mind that the presence of the nuclear localisation signal (NLS) may influence the phenotype observed. It may well be the small soluble component in the AHSV-2 NS3 protein population that is responsible for the persistent cytotoxicity. Further studies are required clarify the link between NS3 intracellular localisation and cytotoxicity.

Both the HD1 TS and HD2 N mutant data sets indicate that modifications to these domains are associated with a loss in PM specific localisation, for both the AHSV-2 NS3 and AHSV-3 NS3 proteins. These modifications may have affected the NS3 folding or

conformation resulting in the loss of PM specific trafficking. As mentioned in Chapter 1, folding the proteins are monitored by quality control machinery (Maggioni & Braakman, 2005). If folding errors have occurred then folding factors keep misfolded proteins in the ER (Ellgaard *et al.*, 1999). High resolution electron microscopy may allow visualisation of the NS3 protein and mutant proteins in different cellular compartments and specific organelles.

It is possible that the introduced mutations had resulted in misfolded proteins that were retained in the ER, never reaching the PM through their specific trafficking pathways. (Ellgaard *et al.*, 1999; Maggioni & Braakman, 2005). Misfolding may occur directly due to the mutation introduced or interference from macromolecular crowding and folding factors stop misfolded proteins from leaving the ER (Ellgaard *et al.*, 1999). In this case, there may have been an accumulation of protein in the ER and the INBs may be aggregates of protein bulging into the nucleus from the closely associated ER. However, the native AHSV NS3 proteins when expressed using the baculovirus system form INBs even though they are trafficked to the PM. The AHSV-3 NS3-eGFP lost only the INBs and not PM. The INBs do not seem to be an intermediate of the PM trafficking pathway or a result of its inhibition.

If there were two separate trafficking pathways responsible for the INB and the PM localisations respectively then the mutation may have affected one individually. It may well be that the baculovirus has its own trafficking pathway to the nucleus as the native virus forms polyhedra within the nucleus of *Spodoptera frugiperda* during normal infection (Kelly, 1982). However, AHSV-2 NS3 and AHSV-3 NS3 did not react in the same way to mutations targeting the motifs, specifically AHSV-3 NS3 proteins lost both INB and PM localisation and the AHSV-2 NS3 retained INBs. It seems as though the AHSV-2 NS3's lipid association was disrupted more readily by mutation than the AHSV-3 NS3. Bioinformatic studies have predicted that the AHSV-3 NS3 protein has a stronger membrane affinity than AHSV-2 NS3 (Meiring, 2009a; van der Sluis, 2007). In turn, modification to the AHSV-3 NS3 protein caused loss of INB formation more easily than it did for AHSV-2 NS3 (Meiring, 2009a). The tendency of the AHSV-2 NS3 mutant proteins to retain their nuclear localisation may be due to the presence of a NLS which is not present in AHSV-3 NS3 (Meiring, 2009a). It may be possible to attribute the localisation pattern to the NLS if one was to construct analogue mutants in a different AHSV-2 strain, one that does not have the NLS. The intrinsic characteristics of the

proteins can influence possible responses of proteins to modifications, thus generalised conclusions relating to mutagenesis cannot be made.

AHSV infection of insect vector *Culicoides* cells in tissue culture is non-cytotoxic but when the AHSV NS3 protein is expressed in tissue culture insect cells (Sf9), cells present with almost complete cell death within 48 hours. The formation of the INBs and the corresponding cytotoxicity may therefore be an artefact generated by expression of AHSV NS3 in a baculovirus expression system and not a true representation of the protein's function in AHSV release. Studies in mammalian cells using transient expression of the protein in a mammalian expression system yield almost undetectable levels of AHSV NS3 protein expression. An additional consideration is that the study of the NS3 protein using an expression system does not permit the influence of the complex interactions between it and the other virally encoded proteins. Use of the newly developed reverse genetic system for AHSV (Matsuo *et al.*, 2010) and further studies using this technology will remove doubt on the value of the data obtained in this study.

Observations indicate a relationship between loss in INB formation and reduction in cytotoxicity. It is not clear how these INBs were formed, how they act to influence cellular viability; what's more, it does not specify whether these INBs are functional units or artefacts of the expression system. The INBs may well have a role in cytotoxicity, but the mechanisms involved remain unclear. It is possible that NS3 misfolding has resulted in aggregates of protein or specific nuclear bodies had been formed, both of which have been shown to cause cell death in instances of disease. The formation of these aggregates interferes with normal cellular processes (Krieghoff-Henning & Hofmann, 2008; Zimbera *et al.*, 2004). It may also be possible that the formation of these INBs are because of the baculovirus system itself as the baculovirus is a nuclear virus and proteins are trafficked to the nucleus at later stages of the baculovirus life cycle (Volkman et al., 1976). Until the nature of these INBs have been clarified and their association with the AHSV life cycle has been shown in the right cell line further discussion will be merely speculative.

CHAPTER 3: CONCLUDING REMARKS

Concluding remarks

The study aimed at evaluating the roles of specific conserved residues in the transmembrane hydrophobic domains and intervening spacer region of nonstructural protein NS3 of African horsesickness virus in localisation, trafficking and cytotoxicity. The motifs that were targeted for study had various effects on membrane association of the proteins, as well as on their subcellular localisation, intracellular trafficking. The modifications had varying effects on the cytotoxic effect on insect cells. It is possible that the targeted motifs were required for proper folding or oligomerisation of the NS3 protein but the direct links between disruption of domains and observed phenotypes were difficult to define. Functional protein assays are the dominant focus of membrane associated proteins because of the difficulties encountered in bioinformatics studies of membrane proteins. Structural data could give insights into why mutations or additions of tags like eGFP change the characteristics of the proteins being studied (Baker, 2010). Little work has been published in this field of molecular biology and bioinformatics possibly because of the difficulties encountered when attempting to crystallize membrane proteins. Further developments of the technology may allow better understanding of the effects of site directed mutagenesis on membrane associated proteins.

An unexpected observation made during the course of this study is that the loss of INBs, and not PM association resulted in a loss of cytotoxicity. However, it is still unclear if the INBs are specific functional bodies or artefacts of the expression system. It may well be integration into intracellular membranes of the ER or Golgi that had lead to the cytotoxic phenotype that is observed with AHSV NS3 expression. Colocalisation studies or high-resolution electron microscopy studies may provide insights into specifically which cellular organelles are associated with AHSV NS3. It is not clear if the mutations that negated cytotoxicity had influenced the multimerisation of NS3, thus negating the viroporin activity at whichever organelle they may function. The INBs may well be specific functional units in the AHSV viral lifecycle, but until shown in the native viral life cycle this deduction cannot be made.

When constructing a chimera, it is important to keep in mind that the structure and function of both the eGFP and the studied protein should remain intact (Ashby *et al.*,

2004). The mutants were constructed as both NS3 eGFP chimeras and the untagged mutant proteins. The phenotypes observed for the eGFP tagged proteins showed key differences to the untagged constructs, these include reduced cytotoxicity and confocal localisation patterns. The similarities include membrane localisation and the subcellular fractionation profile. The Western blot data obtained for the membrane flotation was supported by the fluorescence data. From the confocal data it was apparent that when the plasma membrane localisation was lost in the untagged constructs mutant (e.g. AHSV-3 NS3 TS128IL), the tagged eGFP constructs (AHSV-3 NS3-eGFP TS128IL) showed the same loss. The INBs formation was lost but the other patterns of localisation remained intact, and the mutations had similar effects on the eGFP tagged and untagged AHSV-3 NS3 constructs which allows some potential usefulness to the eGFP tag. The eGFP tag could allow the realtime visualisation of the AHSV-3 NS3-eGFP protein trafficking to the PM that could be informative to the phases of NS3 processing and function over a period.

In summary, it has been established previously that the AHSV NS3 protein plays a role in viral release from infected cells through action at the PM, in this study the formation of INBs have been putatively linked to the AHSV NS3 induced cytotoxicity. The eGFP tag may be useful in studying certain aspects or characteristics of the AHSV NS3 protein but the eGFP tagged protein did not retain all of the characteristics associated with NS3 expression. The AHSV NS3 protein is a multifunctional protein, essential to the AHSV virus life cycle. An understanding of NS3 and the possible role of these INBs may provide insights into the factors that contribute to the virulence and pathogenesis of AHSV.

REFERENCES:

Agrawal, N., Dasaradhi, P. V., Mohmmed, A., Malhotra, P., Bhatnagar, R. K. & Mukherjee, S. K. (2003). RNA interference: biology, mechanism, and applications. *Microbiol Mol Biol Rev* **67**, 657-685.

Andrew, M., Whiteley, P., Janardhana, V., Lobato, Z., Gould, A. & Coupar, B. (1995). Antigen specificity of the ovine cytotoxic T lymphocyte response to bluetongue virus. *Vet Immunol Immunopathol* **47**, 311-322.

Anfinsen, C. B. (1973). Principles that govern the folding of protein chains. *Science* **181**, 223-230.

Ashby, M. C., Ibaraki, K. & Henley, J. M. (2004). It's green outside: tracking cell surface proteins with pH-sensitive GFP. *Trends Neurosci* **27**, 257-261.

Baker, M. (2010). The gatekeepers revealed. *Nature* **465**.

Balasuriya, U. B., Nadler, S. A., Wilson, W. C., Pritchard, L. I., Smythe, A. B., Savini, G., Monaco, F., De Santis, P., Zhang, N., Tabachnick, W. J. & Maclachlan, N. J. (2008). The NS3 proteins of global strains of bluetongue virus evolve into regional topotypes through negative (purifying) selection. *Vet Microbiol* **126**, 91-100.

Banerjee, A. K. & Shatkin, A. J. (1970). Transcription in vitro by reovirus-associated ribonucleic acid-dependent polymerase. *J Virol* **6**, 1-11.

Bansal, O. B., Stokes, A., Bansal, A., Bishop, D. & Roy, P. (1998). Membrane organization of bluetongue virus nonstructural glycoprotein NS3. *J Virol* **72**, 3362-3369.

Barettino, D., Feigenbutz, M., Valcarcel, R. & Stunnenberg, H. G. (1994). Improved method for PCR-mediated site-directed mutagenesis. *Nucleic Acids Res* **22**, 541-542.

Barik, S. (1995). Site-directed mutagenesis by double polymerase chain reaction. *Mol Biotechnol* **3**, 1-7.

Barik, S. (1996). Site-directed mutagenesis in vitro by megaprimer PCR. *Methods Mol Biol* **57**, 203-215.

Barik, S. (1997a). Mutagenesis and Gene Fusion by Megaprimer PCR. In *PCR cloning protocols*, pp. 173 - 182. Edited by B. A. White. Totowa, New Jersey 07512: Humana Press Inc.

Barik, S. (1997b). Mutagenesis and gene fusion by megaprimer PCR. *Methods Mol Biol* **67**, 173-182.

Barik, S. (2002). Megaprimer PCR. *Methods Mol Biol* **192**, 189-196.

Barik, S. & Galinski, M. S. (1991). "Megaprimer" method of PCR: increased template concentration improves yield. *Biotechniques* **10**, 489-490.

Baylis, M., Mellor, P. S. & Meiswinkel, R. (1999). Horse sickness and ENSO in South Africa. *Nature* **397**, 574.

Beaton, A. R., Rodriguez, J., Reddy, Y. K. & Roy, P. (2002). The membrane trafficking protein calpactin forms a complex with bluetongue virus protein NS3 and mediates virus release. *Proc Natl Acad Sci U S A* **99**, 13154-13159.

Beyleveld, M. (2007). Interaction of nonstructural protein NS3 of African horsesickness with viral and cellular proteins. MSc dissertation University of Pretoria

Bhattacharya, B., Noad, R. J. & Roy, P. (2007). Interaction between Bluetongue cirus outer capsid protein VP2 and vimentin is necessary for virus egress. *Virology journal* **4**.

Bhattacharya, B. & Roy, P. (2008). Bluetongue virus outer capsid protein VP5 interacts with membrane lipid rafts via a SNARE domain. *J Virol* **82**, 10600-10612.

Bishop, N., Horman, A. & Woodman, P. (2002). Mammalian class E Vps proteins recognize ubiquitin and act in the removal of endosomal protein-ubiquitin conjugates. *J Cell Biol* **157**, 91-101.

Bonneau, K. R., Topol, J. B., Gerry, A. C., Mullens, B. A., Velten, R. K. & MacLachlan, N. J. (2002). Variation in the NS3/NS3A gene of bluetongue viruses contained in Culicoides sonorensis collected from a single site in southern California. *Virus Res* **84**, 59-65.

Bosman, P., Bruckner, G. K. & Faul, A. (1995). African horse sickness surveillance systems and regionalisation/zoning: the case of South Africa. *Rev Sci Tech* **14**, 645-653.

Boyce, M., Wehrfritz, J., Noad, R. & Roy, P. (2004). Purified recombinant bluetongue virus VP1 exhibits RNA replicase activity. *J Virol* **78**, 3994-4002.

Bremer, C. W., Huismans, H. & Van Dijk, A. A. (1990). Characterization and cloning of the African horsesickness virus genome. *J Gen Virol* **71 (Pt 4)**, 793-799.

Brignati, M. J., Loomis, J. S., Wills, J. W. & Courtney, R. J. (2003). Membrane association of VP22, a herpes simplex virus type 1 tegument protein. *J Virol* **77**, 4888-4898.

Brodsky, J. L. & McCracken, A. A. (1999). ER protein quality control and proteasome-mediated protein degradation. *Semin Cell Dev Biol* **10**, 507-513.

Brons-Poulsen, J., Nohr, J. & Larsen, L. K. (2002). Megaprimer method for polymerase chain reaction-mediated generation of specific mutations in DNA. *Methods Mol Biol* **182**, 71-76.

Brons-Poulsen, J., Petersen, N. E., Horder, M. & Kristiansen, K. (1998). An improved PCR-based method for site directed mutagenesis using megaprimers. *Mol Cell Probes* **12**, 345-348.

Brookes, S. M., Hyatt, A. D. & Eaton, B. T. (1993). Characterization of virus inclusion bodies in bluetongue virus-infected cells. *J Gen Virol* **74 (Pt 3)**, 525-530.

Brown, D. & Breton, S. (2000). Sorting proteins to their target membranes. *Kidney Int* **57**, 816-824.

Brown, D. A. & London, E. (1998). Functions of lipid rafts in biological membranes. *Annu Rev Cell Dev Biol* **14**, 111-136.

Burke, E. & Barik, S. (2003). Megaprimer PCR: application in mutagenesis and gene fusion. *Methods Mol Biol* **226**, 525-532.

Burrage, T. G. & Laegreid, W. W. (1994). African horsesickness: pathogenesis and immunity. *Comp Immunol Microbiol Infect Dis* **17**, 275-285.

Burroughs, J. N., O'Hara, R. S., Smale, C. J., Hamblin, C., Walton, A., Armstrong, R. & Mertens, P. P. (1994). Purification and properties of virus particles, infectious subviral particles, cores and VP7 crystals of African horsesickness virus serotype 9. *J Gen Virol* **75 (Pt 8)**, 1849-1857.

Calisher, C. H. & Mertens, P. P. (1998). Taxonomy of African horse sickness viruses. *Arch Virol Suppl* **14**, 3-11.

Carrasco, L. (1995). Modification of membrane permeability by animal viruses. *Adv Virus Res* **45**, 61-112.

Carrasco, L., Otero, M. J. & Casrillo, J. L. (1989). Modification of membrane permeability by animal viruses. *Pharmac Ther* **40**, 171-212.

Celma, C. C. & Roy, P. (2009). A viral nonstructural protein regulates bluetongue virus trafficking and release. *J Virol* **83**, 6806-6816.

Chalfie, M. (1995). Green fluorescent protein. *Photochem Photobiol* **62**, 651-656.

Choma, C., Gratkowski, H., Lear, J. D. & DeGrado, W. F. (2000). Asparagine-mediated self-association of a model transmembrane helix. *Nat Struct Biol* **7**, 161-166.

Coetzer, J. A. W. & Erasmus, B. J. (1994). African Horsesickness. In *Infectious diseases of Livestock with special reference to Southern Africa*. Edited by J. A. W. Coetzer, G. R. Thomson & R. C. Tustin: Oxford University Press.

Dawson, J. P., Weinger, J. S. & Engelman, D. M. (2002). Motifs of serine and threonine can drive association of transmembrane helices. *J Mol Biol* **316**, 799-805.

de Jong, A. S., Melchers, W. J., Glaudemans, D. H., Willems, P. H. & van Kuppeveld, F. J. (2004). Mutational analysis of different regions in the coxsackievirus 2B protein:

requirements for homo-multimerization, membrane permeabilization, subcellular localization, and virus replication. *J Biol Chem* **279**, 19924-19935.

de Sa, R. O., Zellner, M. & Grubman, M. J. (1994). Phylogenetic analysis of segment 10 from African horsesickness virus and cognate genes from other orbiviruses. *Virus Res* **33**, 157-165.

De Waal, P. J. & Huismans, H. (2005). Characterization of the nucleic acid binding activity of inner core protein VP6 of African horse sickness virus. *Arch Virol* **150**, 2037-2050.

Diprose, J. M., Burroughs, J. N., Sutton, G. C., Goldsmith, A., Gouet, P., Malby, R., Overton, I., Zientara, S., Mertens, P. P., Stuart, D. I. & Grimes, J. M. (2001). Translocation portals for the substrates and products of a viral transcription complex: the bluetongue virus core. *Embo J* **20**, 7229-7239.

Diprose, J. M., Grimes, J. M., Sutton, G. C., Burroughs, J. N., Meyer, A., Maan, S., Mertens, P. P. & Stuart, D. I. (2002). The core of bluetongue virus binds double-stranded RNA. *J Virol* **76**, 9533-9536.

Doms, R. W., Lamb, R. A., Rose, J. K. & Helenius, A. (1993). Folding and assembly of viral membrane proteins. *Virology* **193**, 545-562.

Du Toit, R. M. (1944). The transmission of bluetongue and horse sickness.

Eaton, B. T. & Crameri, G. S. (1989). The site of bluetongue virus attachment to glycophorins from a number of animal erythrocytes. *J Gen Virol* **70 (Pt 12)**, 3347-3353.

Eaton, B. T., Hyatt, A. D. & Brookes, S. M. (1990). The replication of bluetongue virus. *Curr Top Microbiol Immunol* **162**, 89-118.

Eaton, B. T., Hyatt, A. D. & White, J. R. (1987). Association of bluetongue virus with the cytoskeleton. *Virology* **157**, 107-116.

Eaton, B. T., Hyatt, A. D. & White, J. R. (1988). Localization of the nonstructural protein NS1 in bluetongue virus-infected cells and its presence in virus particles. *Virology* **163**, 527-537.

Ehrhardt, D. (2003). GFP technology for live cell imaging. *Curr Opin Plant Biol* **6**, 622-628.

Ellgaard, L., Molinari, M. & Helenius, A. (1999). Setting the standards: quality control in the secretory pathway. *Science* **286**, 1882-1888.

Ellis, R. J. (2001). Macromolecular crowding: an important but neglected aspect of the intracellular environment. *Curr Opin Struct Biol* **11**, 114-119.

Els, H. J. (1973). Electron microscopy of bluetongue virus RNA. *Onderstepoort J Vet Res* **40**, 73-75.

Erasmus, B. J. (1973). the pathogenesis of African horse sickness. In *Equine-infections Diseases*, pp. 1-11. Edited by J. F. Bryans & H. Gerber. Paris Karger: Proceeding of the Third international Conference on Equine Infectious Diseases.

European Food Safety Authority, E. F. S. A. (2007). Scientific Report of the Scientific Panel on Animal Health and Welfare on request from the Commission (EFSA-Q-2006-311) and EFSA Selfmandate (EFSA-Q-2007-063) on bluetongue. *The EFSA Journal* **479**, 1-29.

Fetzer, C., Tews, B. A. & Meyers, G. (2005). The carboxy-terminal sequence of the pestivirus glycoprotein E(rns) represents an unusual type of membrane anchor. *J Virol* **79**, 11901-11913.

Fewell, S. W., Travers, K. J., Weissman, J. S. & Brodsky, J. L. (2001). The action of molecular chaperones in the early secretory pathway. *Annu Rev Genet* **35**, 149-191.

Forzan, M., Wirblich, C. & Roy, P. (2004). A capsid protein of nonenveloped Bluetongue virus exhibits membrane fusion activity. *Proc Natl Acad Sci U S A* **101**, 2100-2105.

Fra, A. M., Williamson, E., Simons, K. & Parton, R. G. (1995). De novo formation of caveolae in lymphocytes by expression of VIP21-caveolin. *Proc Natl Acad Sci U S A* **92**, 8655-8659.

French, T. J., Inumaru, S. & Roy, P. (1989). Expression of two related nonstructural proteins of bluetongue virus (BTV) type 10 in insect cells by a recombinant baculovirus: production of polyclonal ascitic fluid and characterization of the gene product in BTV-infected BHK cells. *J Virol* **63**, 3270-3278.

Fu, H., Leake, C. J., Mertens, P. P. & Mellor, P. S. (1999). The barriers to bluetongue virus infection, dissemination and transmission in the vector, Culicoides variipennis (Diptera: Ceratopogonidae). *Arch Virol* **144**, 747-761.

Fukusho, A., Ritter, G. D. & Roy, P. (1987). Variation in the bluetongue virus neutralization protein VP2. *J Gen Virol* **68 (Pt 11)**, 2967-2973.

Gard, G. P., Weir, R. P. & Walsh, S. J. (1988). Arboviruses recovered from sentinel cattle using several virus isolation methods. *Vet Microbiol* **18**, 119-125.

Ghiasi, H., Fukusho, A., Eshita, Y. & Roy, P. (1987). Identification and characterization of conserved and variable regions in the neutralization VP2 gene of bluetongue virus. *Virology* **160**, 100-109.

Gillies, S., Bullivant, S. & Bellamy, A. R. (1971). Viral RNA polymerases: electron microscopy of reovirus reaction cores. *Science* **174**, 694-696.

Goder, V., Bieri, C. & Spiess, M. (1999). Glycosylation can influence topogenesis of membrane proteins and reveals dynamic reorientation of nascent polypeptides within the translocon. *J Cell Biol* **147**, 257-266.

Gomez-Villamandos, J. C., Sanchez, C., Carrasco, L., Laviada, M. M., Bautista, M. J., Martinez-Torrecuadrada, J., Sanchez-Vizcaino, J. M. & Sierra, M. A. (1999). Pathogenesis of African horse sickness: ultrastructural study of the capillaries in experimental infection. *J Comp Pathol* **121**, 101-116.

Gouet, P., Diprose, J. M., Grimes, J. M., Malby, R., Burroughs, J. N., Zientara, S., Stuart, D. I. & Mertens, P. P. (1999). The highly ordered double-stranded RNA genome of bluetongue virus revealed by crystallography. *Cell* **97**, 481-490.

Gould, A. R. (1988). Nucleotide sequence of the Australian bluetongue virus serotype 1 RNA segment 10. *J Gen Virol* **69 (Pt 4)**, 945-949.

Gould, E. A. & Higgs, S. (2009). Impact of climate change and other factors on emerging arbovirus diseases. *Trans R Soc Trop Med Hyg* **103**, 109-121.

Gray, T. M. & Matthews, B. W. (1984). Intrahelical hydrogen bonding of serine, threonine and cysteine residues within alpha-helices and its relevance to membrane-bound proteins. *J Mol Biol* **175**, 75-81.

Grimes, J., Basak, A. K., Roy, P. & Stuart, D. (1995). The crystal structure of bluetongue virus VP7. *Nature* **373**, 167-170.

Grimes, J. M., Burroughs, J. N., Gouet, P., Diprose, J. M., Malby, R., Zientara, S., Mertens, P. P. & Stuart, D. I. (1998). The atomic structure of the bluetongue virus core. *Nature* **395**, 470-478.

Guirakhoo, F., Catalan, J. A. & Monath, T. P. (1995). Adaptation of bluetongue virus in mosquito cells results in overexpression of NS3 proteins and release of virus particles. *Arch Virol* **140**, 967-974.

Han, Z. & Harty, R. N. (2004). The NS3 protein of bluetongue virus exhibits viroporin-like properties. *J Biol Chem* **279**, 43092-43097.

Harder, T. & Simons, K. (1997). Caveolae, DIGs, and the dynamics of sphingolipid-cholesterol microdomains. *Curr Opin Cell Biol* **9**, 534-542.

Hassan, S. H., Wirblich, C., Forzan, M. & Roy, P. (2001). Expression and functional characterization of bluetongue virus VP5 protein: role in cellular permeabilization. *J Virol* **75**, 8356-8367.

Hassan, S. S. & Roy, P. (1999). Expression and functional characterization of bluetongue virus VP2 protein: role in cell entry. *J Virol* **73**, 9832-9842.

Hatherell, T.-L. (2007). An investigation into the sucellular localisation of nonstructural protein NS3 of African horsesickness virus. MSc dissertation University of Pretoria

Hegde, R. S. & Lingappa, V. R. (1997). Membrane protein biogenesis: regulated complexity at the endoplasmic reticulum. *Cell* **91**, 575-582.

Hewat, E. A., Booth, T. F., Loudon, P. T. & Roy, P. (1992a). Three-dimensional reconstruction of baculovirus expressed bluetongue virus core-like particles by cryo-electron microscopy. *Virology* **189**, 10-20.

Hewat, E. A., Booth, T. F. & Roy, P. (1992b). Structure of bluetongue virus particles by cryoelectron microscopy. *J Struct Biol* **109**, 61-69.

Hicke, L. & Dunn, R. (2003). Regulation of membrane protein transport by ubiquitin and ubiquitin-binding proteins. *Annu Rev Cell Dev Biol* **19**, 141-172.

Huismans, H. & Bremer, C. W. (1981). A comparison of an australian bluetongue virus isolate (CSIRO 19) with other bluetongue virus serotypes by cross-hybridization and cross-immune precipitation. *Onderstepoort J Vet Res* **48**, 59-67.

Huismans, H. & Cloete, M. (1987). A comparison of different cloned bluetongue virus genome segments as probes for the detection of virus-specified RNA. *Virology* **158**, 373-380.

Huismans, H. & Els, H. J. (1979). Characterization of the tubules associated with the replication of three different orbiviruses. *Virology* **92**, 397-406.

Huismans, H. & Erasmus, B. J. (1981). Identification of the serotype-specific and group-specific antigens of bluetongue virus. *Onderstepoort J Vet Res* **48**, 51-58.

Huismans, H. & Van Dijk, A. A. (1990). Bluetongue virus structural components. *Curr Top Microbiol Immunol* **162**, 21-41.

Huismans, H., van Dijk, A. A. & Bauskin, A. R. (1987a). In vitro phosphorylation and purification of a nonstructural protein of bluetongue virus with affinity for single-stranded RNA. *J Virol* **61**, 3589-3595.

Huismans, H., van Dijk, A. A. & Els, H. J. (1987b). Uncoating of parental bluetongue virus to core and subcore particles in infected L cells. *Virology* **157**, 180-188.

Hurtley, S. M., Bole, D. G., Hoover-Litty, H., Helenius, A. & Copeland, C. S. (1989). Interactions of misfolded influenza hemaglutinin with binding protein(BiP). *Journal of cell biology*, 2117-2126.

Hwang, G., Yang, Y., Chiou, J. & Li, J. K. (1992). Sequence conservation among the cognate nonstructural NS3/3A protein genes of six bluetongue viruses. *Virus Res* **23**, 151-161.

Hyatt, A. D. & Eaton, B. T. (1988). Ultrastructural distribution of the major capsid proteins within bluetongue virus and infected cells. *J Gen Virol* **69 (Pt 4)**, 805-815.

Hyatt, A. D. & Eaton, B. T. (1990). Virological applications of the grid-cell-culture technique. *Electron Microsc Rev* **3**, 1-27.

Hyatt, A. D., Eaton, B. T. & Brookes, S. M. (1989). The release of bluetongue virus from infected cells and their superinfection by progeny virus. *Virology* **173**, 21-34.

Hyatt, A. D., Gould, A. R., Coupar, B. & Eaton, B. T. (1991). Localization of the non-structural protein NS3 in bluetongue virus-infected cells. *J Gen Virol* **72**, 2263.

Hyatt, A. D., Zhao, Y. & Roy, P. (1993). Release of bluetongue virus-like particles from insect cells is mediated by BTV nonstructural protein NS3/NS3A. *Virology* **193**, 592-603.

Inumaru, S. & Roy, P. (1987). Production and characterization of the neutralization antigen VP2 of bluetongue virus serotype 10 using a baculovirus expression vector. *Virology* **157**, 472-479.

Jayaram, H., Estes, M. K. & Prasad, B. V. (2004). Emerging themes in rotavirus cell entry, genome organization, transcription and replication. *Virus Res* **101**, 67-81.

Jensen, M. J., Cheney, I. W., Thompson, L. H., Mecham, J. O., Wilson, W. C., Yamakawa, M., Roy, P. & Gorman, B. M. (1994). The smallest gene of the orbivirus, epizootic hemorrhagic disease, is expressed in virus-infected cells as two proteins and the expression differs from that of the cognate gene of bluetongue virus. *Virus Res* **32**, 353-364.

Kahlon, J., Sugiyama, K. & Roy, P. (1983). Molecular basis of bluetongue virus neutralization. *J Virol* **48**, 627-632.

Kar, A. K., Bhattacharya, B. & Roy, P. (2007). Bluetongue virus RNA binding protein NS2 is a modulator of viral replication and assembly. *BMC Mol Biol* **8**, 4.

Kar, A. K., Iwatani, N. & Roy, P. (2005). Assembly and intracellular localization of the bluetongue virus core protein VP3. *J Virol* **79**, 11487-11495.

Kar, A. K. & Roy, P. (2003). Defining the structure-function relationships of bluetongue virus helicase protein VP6. *J Virol* **77**, 11347-11356.

Kelly, D. C. (1982). Review: Baculovirus replication *J Gen Virol* **63**, 1-13.

Krieghoff-Henning, E. & Hofmann, T. G. (2008). Role of nuclear bodies in apoptosis signalling. *Biochimica et Biophysica Acta* **1783** 2185–2194.

Laegreid, W. W., Burrage, T. G., Stone-Marschat, M. & Skowronek, A. (1992a). Electron microscopic evidence for endothelial infection by African horsesickness virus. *Vet Pathol* **29**, 554-556.

Laegreid, W. W., Skowronek, A., Stone-Marschat, M. & Burrage, T. (1993). Characterization of virulence variants of African horsesickness virus. *Virology* **195**, 836-839.

Laegreid, W. W., Stone-Marschat, M., Skowronek, A. & Burrage, T. (1992b). Infection of endothelial cells by African horse sickness viruses. In: Bluetongue, African Horse Sickness, and Related Orbiviruses. T.E. Walton & B.I. Osburn (Ed), CRC Press, Florida, pp807-814.

Laude, A. J. & Prior, I. A. (2004). Plasma membrane microdomains: organization, function and trafficking. *Mol Membr Biol* **21**, 193-205.

Lawton, J. A., Estes, M. K. & Prasad, B. V. (1997). Three-dimensional visualization of mRNA release from actively transcribing rotavirus particles. *Nat Struct Biol* **4**, 118-121.

Lee, J. W. & Roy, P. (1986). Nucleotide sequence of a cDNA clone of RNA segment 10 of bluetongue virus (serotype 10). *J Gen Virol* **67 (Pt 12)**, 2833-2837.

Lippincott-Schwartz, J., Bonifacino, J. S., Yuan, L. C. & Klausner, R. D. (1988). Degradation from the endoplasmic reticulum: Disposing of newly synthesised proteins. *Cell*, 209-220.

Lippincott-Schwartz, J. & Smith, C. L. (1997). Insights into secretory and endocytic membrane traffic using green fluorescent protein chimeras. *Curr Opin Neurobiol* **7**, 631-639.

Lloyd, T. E., Atkinson, R., Wu, M. N., Zhou, Y., Penneta, G. & Bellen, H. J. (2002). Hrs regulates endosome invagination and receptor tyrosine kynase signalling in Drosophila. *Cell* **108**, 261-269.

Lord, C. C., Woolhouse, M. E. & Barnard, B. J. (1997). Transmission and distribution of virus serotypes: African horse sickness in zebra. *Epidemiol Infect* **118**, 43-50.

Lu, X., McDonald, S. M., Tortorici, M. A., Tao, Y. J., Vasquez-Del Carpio, R., Nibert, M. L., Patton, J. T. & Harrison, S. C. (2008). Mechanism for coordinated RNA packaging and genome replication by rotavirus polymerase VP1. *Structure* **16**, 1678-1688.

Luckow, V. A., Lee, S. C., Barry, G. F. & Olins, P. O. (1993). Efficient generation of infectious recombinant baculoviruses by site-specific transposon-mediated insertion of foreign genes into a baculovirus genome propagated in Escherichia coli. *J Virol* **67**, 4566-4579.

Lux, K., Goerlitz, N., Schlemminger, S., Perabo, L., Goldnau, D., Endell, J., Leike, K., Kofler, D. M., Finke, S., Hallek, M. & Buning, H. (2005). Green fluorescent protein-tagged adeno-associated virus particles allow the study of cytosolic and nuclear trafficking. *J Virol* **79**, 11776-11787.

Lymperopoulos, K., Noad, R., Tosi, S., Nethisinghe, S., Brierley, I. & Roy, P. (2006). Specific binding of Bluetongue virus NS2 to different viral plus-strand RNAs. *Virology* **353**, 17-26.

Lymperopoulos, K., Wirblich, C., Brierley, I. & Roy, P. (2003). Sequence specificity in the interaction of Bluetongue virus non-structural protein 2 (NS2) with viral RNA. *J Biol Chem* **278**, 31722-31730.

Maggioni, C. & Braakman, I. (2005). Synthesis and quality control of viral membrane proteins. *Curr Top Microbiol Immunol* **285**, 175-198.

Maree, F. F. & Huismans, H. (1997). Characterization of tubular structures composed of nonstructural protein NS1 of African horsesickness virus expressed in insect cells. *J Gen Virol* **78 (Pt 5)**, 1077-1082.

Maree, S., Durbach, S., Maree, F. F., Vreede, F. & Huismans, H. (1998). Expression of the major core structural proteins VP3 and VP7 of African horse sickness virus, and production of core-like particles. *Arch Virol Suppl* **14**, 203-209.

Martin, L. A., Meyer, A. J., O'Hara, R. S., Fu, H., Mellor, P. S., Knowles, N. J. & Mertens, P. P. (1998). Phylogenetic analysis of African horse sickness virus segment 10: sequence variation, virulence characteristics and cell exit. *Arch Virol Suppl* **14**, 281.

Martinez-Costas, J., Sutton, G., Ramadevi, N. & Roy, P. (1998). Guanylyltransferase and RNA 5'-triphosphatase activities of the purified expressed VP4 protein of bluetongue virus. *J Mol Biol* **280**, 859-866.

Matsuo, E., Celma, C. C. P. & Roy, P. (2010). A reverse genetics system of African horse sickness virus reveals existence of primary replication. *FEBS Letters*.

McDonald, S. M., Tao, Y. J. & Patton, J. T. (2009). The ins and outs of four-tunneled Reoviridae RNA-dependent RNA polymerases. *Curr Opin Struct Biol* **19**, 775-782.

Meiring, T. L. (2009a). Role of African horsesickness virus protein NS3 in cytotoxicity and virus induced cytopathology. PhD thesis University of Pretoria

Meiring, T. L., Huismans, H. & Staden, V. v. (2009b). Genome segment reassortment identifies non-structural protein NS3 as a key protein in African horsesickness virus release and alteration of membrane permeability. *Arch Virol* **154**, 263–271.

Meiswinkel, R. & Paweska, J. T. (2003). Evidence for a new field *Culicoides* vector of African horse sickness in South Africa. *Preventive Veterinary Medicine* **60**, 243-253.

Mellor, P. S. (1993). African horse sickness: transmission and epidemiology. *Vet Res* **24**, 199-212.

Mellor, P. S. & Boorman, J. (1995). The transmission and geographical spread of African horse sickness and bluetongue viruses. *Ann Trop Med Parasitol* **89**, 1-15.

Mellor, P. S. & Hamblin, C. (2004). African horse sickness. *Vet Res* **35**, 445-466.

Mellor, P. S. & Leake, C. J. (2000). Climatic and geographic influences on arboviral infections and vectors. *Rev Sci Tech* **19**, 41-54.

Mertens, P. (2004). The dsRNA viruses. *Virus Res* **101**, 3-13.

Mertens, P. P., Burroughs, J. N. & Anderson, J. (1987). Purification and properties of virus particles, infectious subviral particles, and cores of bluetongue virus serotypes 1 and 4. *Virology* **157**, 375-386.

Mertens, P. P. & Diprose, J. (2004). The bluetongue virus core: a nano-scale transcription machine. *Virus Res* **101**, 29-43.

Mertens, P. P. & Sangar, D. V. (1985). Analysis of the terminal sequences of the genome segments of four orbiviruses. *Virology* **140**, 55-67.

Modrof, J., Lymperopoulos, K. & Roy, P. (2005). Phosphorylation of bluetongue virus nonstructural protein 2 is essential for formation of viral inclusion bodies. *J Virol* **79**, 10023-10031.

Moss, S. R., Jones, L. D. & Nuttall, P. A. (1992). Comparison of the nonstructural protein, NS3, of tick-borne and insect-borne orbiviruses. *Virology* **187**, 841-844.

Mullens, B. A. & Holbrook, F. R. (1991). Temperature effects on the gonotrophic cycle of Culicoides variipennis (Diptera: Ceratopogonidae). *J Am Mosq Control Assoc* **7**, 588-591.

Nakata, T., Sobue, K. & Hirokawa, N. (1990). Conformational change and localization of calpactin I complex involved in exocytosis as revealed by quick-freeze, deep-etch electron microscopy and immunocytochemistry. *J Cell Biol* **110**, 13-25.

Nason, E. L., Rothagel, R., Mukherjee, S. K., Kar, A. K., Forzan, M., Prasad, B. V. & Roy, P. (2004). Interactions between the inner and outer capsids of bluetongue virus. *J Virol* **78**, 8059-8067.

Neubauer, A., Rudolph, J., Brandmuller, C., Just, F. T. & Osterrieder, N. (2002). The equine herpesvirus 1 UL34 gene product is involved in an early step in virus egress and can be efficiently replaced by a UL34-GFP fusion protein. *Virology* **300**, 189-204.

O'Hara, R. S., Meyer, A. J., Burroughs, J. N., Pullen, L., Martin, L. A. & Mertens, P. P. (1998). Development of a mouse model system, coding assignments and

identification of the genome segments controlling virulence of African horse sickness virus serotypes 3 and 8. *Arch Virol Suppl* **14**, 259-279.

Oellermann, R. A. (1970). Plaque formation by African horsesickness virus and characterization of its RNA. *Onderstepoort J Vet Res* **37**, 137-143.

Oellermann, R. A., Els, H. J. & Erasmus, B. J. (1970). Characterization of African horsesickness virus. *Arch Gesamte Virusforsch* **29**, 163-174.

Ojala, K., Tikka, P. J., Kautto, L., Kapyla, P., Marjomaki, V. & Oker-Blom, C. (2004). Expression and trafficking of fluorescent viral membrane proteins in baculovirus-transduced BHK cells. *J Biotechnol* **114**, 165-175.

Owens, R. J., Limn, C. & Roy, P. (2004). Role of an arbovirus nonstructural protein in cellular pathogenesis and virus release. *J Virol* **78**, 6649-6656.

Patton, J. T., Vasquez-Del Carpio, R., Tortorici, M. A. & Taraporewala, Z. F. (2007). Coupling of rotavirus genome replication and capsid assembly. *Adv Virus Res* **69**, 167-201.

Paweska, J. T., Prinsloo, S. & Venter, G. J. (2003). Oral susceptibility of South African *Culicoides* species to live-attenuated serotype-specific vaccine strains of African horse sickness virus (AHSV). *Medical and Veterinary Entomology* **17**, 436-447.

Paweska, J. T., Venter, G. J. & Mellor, P. S. (2002). Vector competence of South African Culicoides species for bluetongue virus serotype 1 (BTV-1) with special reference to the effect of temperature on the rate of virus replication in C. imicola and C. bolitinos. *Med Vet Entomol* **16**, 10-21.

Pierce, C. M., Balasuriya, U. B. & MacLachlan, N. J. (1998). Phylogenetic analysis of the S10 gene of field and laboratory strains of bluetongue virus from the United States. *Virus Res* **55**, 15-27.

Polo, S., Sigismund, S., Faretta, M., Guidi, M., Capua, M. R., Bossi, G., Chen, H., De Camilli, P. & Di Fiore, P. P. (2002). A single motif responsible for ubiquitin recognistion and monoubiquitination in endocytic proteins. *Nature* **416**, 451-455.

Pornillos, O., Garrus, J. E. & Sundquist, W. I. (2002). Mechanisms of enveloped RNA virus budding. *Trends Cell Biol* **12**, 569-579.

Prasad, B. V., Yamaguchi, S. & Roy, P. (1992). Three-dimensional structure of single-shelled bluetongue virus. *J Virol* **66**, 2135-2142.

Purse, B. V., Mellor, P. S., Rogers, D. J., Samuel, A. R., Mertens, P. P. & Baylis, M. (2005). Climate change and the recent emergence of bluetongue in Europe. *Nat Rev Microbiol* **3**, 171-181.

Quan, M., van Vuuren, M., Howell, P. G., Groenewald, D. & Guthrie, A. J. (2008). Molecular epidemiology of the African horse sickness virus S10 gene. *J Gen Virol* **89**, 1159-1168.

Raiborg, C., Bache, K. G., Gillooly, D. J., Madshus, I. H., Stang, E. & Stenmark, H. (2002). Hrs sorts ubiquinated proteins into clathrin-coated microdomains of early endosomes. *Nat Cell Biol* **4**, 394-398.

Raiborg, C., Rusten, T. E. & Stenmark, H. (2003). Protein sorting into multivesicular endosomes. *Curr Opin Cell Biol* **15**, 446-455.

Ramadevi, N., Burroughs, N. J., Mertens, P. P., Jones, I. M. & Roy, P. (1998). Capping and methylation of mRNA by purified recombinant VP4 protein of bluetongue virus. *Proc Natl Acad Sci U S A* **95**, 13537-13542.

Ramadevi, N. & Roy, P. (1998). Bluetongue virus core protein VP4 has nucleoside triphosphate phosphohydrolase activity. *J Gen Virol* **79 (Pt 10)**, 2475-2480.

Rao, C. D., Kiuchi, A. & Roy, P. (1983). Homologous terminal sequences of the genome double-stranded RNAs of bluetongue virus. *J Virol* **46**, 378-383.

Rothberg, K. G., Heuser, J. E., Donzell, W. C., Ying, Y. S., Glenney, J. R. & Anderson, R. G. (1992). Caveolin, a protein component of caveolae membrane coats. *Cell* **68**, 673-682.

Roy, P. (1989). Bluetongue virus genetics and genome structure. *Virus Res* **13**, 179-206.

Roy, P. (1990). Use of baculovirus expression vectors: development of diagnostic reagents, vaccines and morphological counterparts of bluetongue virus. *FEMS Microbiol Immunol* **2**, 223-234.

Roy, P. (2005). Bluetongue virus proteins and particles and their role in virus entry, assembly, and release. *Adv Virus Res* **64**, 69-123.

Roy, P. (2008). Functional mapping of Bluetongue virus proteins and their interactions with host proteins during virus replication. *Cell Biochem Biophys* **50,** 143-157.

Roy, P., Bishop, D. H., Howard, S., Aitchison, H. & Erasmus, B. (1996). Recombinant baculovirus-synthesized African horsesickness virus (AHSV) outer-capsid protein VP2 provides protection against virulent AHSV challenge. *J Gen Virol* **77 (Pt 9)**, 2053-2057.

Roy, P., Fukusho, A., Ritter, G. D. & Lyon, D. (1988). Evidence for genetic relationship between RNA and DNA viruses from the sequence homology of a putative polymerase gene of bluetongue virus with that of vaccinia virus: conservation of RNA polymerase genes from diverse species. *Nucleic Acids Res* **16**, 11759-11767.

Sailleau, C., Moulay, S. & Zientara, S. (1997). Nucleotide sequence comparison of the segments S10 of the nine African horsesickness virus serotypes. *Arch Virol* **142**, 965-978.

Salaun, C., James, D. J. & Chamberlain, L. H. (2004). Lipid rafts and the regulation of exocytosis. *Traffic* **5**, 255-264.

Sarafian, T., Pradel, L. A., Henry, J. P., Aunis, D. & Bader, M. F. (1991). The participation of annexin II (calpactin I) in calcium-evoked exocytosis requires protein kinase C. *J Cell Biol* **114**, 1135-1147.

SciEdCentral (1995). Primer Designer, 5.1 edn: Scientific & Educational Software.

Shi, S. C., Katz, a., D.J., Schnell, J. D., Sutanto, M., Emr, S. D. & Hicke, L. (2002). Epsins and Vps27p/Hrs contain ubiquitin-binding domains that function in receptor endocytosis. *Nat Cell Biol* **4**, 389-393.

Simons, K. & Ikonen, E. (1997). Functional rafts in cell membranes. *Nature* **387**, 569-572.

Skowronek, A. J., LaFranco, L., Stone-Marschat, M. A., Burrage, T. G., Rebar, A. H. & Laegreid, W. W. (1995). Clinical pathology and hemostatic abnormalities in experimental African horsesickness. *Vet Pathol* **32**, 112-121.

Stauber, N., Martinez-Costas, J., Sutton, G., Monastyrskaya, K. & Roy, P. (1997). Bluetongue virus VP6 protein binds ATP and exhibits an RNA-dependent ATPase function and a helicase activity that catalyze the unwinding of double-stranded RNA substrates. *J Virol* **71**, 7220-7226.

Stoltz, M. A., van der Merwe, C. F., Coetzee, J. & Huismans, H. (1996). Subcellular localization of the nonstructural protein NS3 of African horsesickness virus. *Onderstepoort J Vet Res* **63**, 57.

Sutton, G., Grimes, J. M., Stuart, D. I. & Roy, P. (2007). Bluetongue virus VP4 is an RNA-capping assembly line. *Nat Struct Mol Biol*.

Tabachnick, W. J. (2004). Culicoides and the global epidemiology of bluetongue virus infection. *Veterinaria Italiana, (3), 2004* **40**, 145-150.

Tao, Y., Farsetta, D. L., Nibert, M. L. & Harrison, S. C. (2002). RNA synthesis in a cage--structural studies of reovirus polymerase lambda3. *Cell* **111**, 733-745.

Thomas, C. P., Booth, T. F. & Roy, P. (1990). Synthesis of bluetongue virus-encoded phosphoprotein and formation of inclusion bodies by recombinant baculovirus in insect cells: it binds the single-stranded RNA species. *J Gen Virol* **71**, 2073-2083.

Tomley, F. M. & Shirley, M. W. (2009). Livestock infectious diseases and zoonoses. *Philos Trans R Soc Lond B Biol Sci* **364**, 2637-2642.

Urakawa, T., Ritter, D. G. & Roy, P. (1989). Expression of largest RNA segment and synthesis of VP1 protein of bluetongue virus in insect cells by recombinant baculovirus: association of VP1 protein with RNA polymerase activity. *Nucleic Acids Res* **17**, 7395-7401.

Urakawa, T. & Roy, P. (1988). Bluetongue virus tubules made in insect cells by recombinant baculoviruses: expression of the NS1 gene of bluetongue virus serotype 10. *J Virol* **62**, 3919-3927.

van der Sluis, R. (2007). Comparison and functional analysis of different domains of the cytotoxic protein NS3 of five orbiviruses. MSc dissertation University of Pretoria

Van Dijk, A. A. & Huismans, H. (1988). In vitro transcription and translation of bluetongue virus mRNA. *J Gen Virol* **69 (Pt 3)**, 573-581.

van Meer, G. (1989). Lipid traffic in animal cells. *Annu Rev Cell Biol* **5**, 247-275.

van Niekerk, M., Freeman, M., Paweska, J. T., Howell, P. G., Guthrie, A. J., Potgieter, A. C., van Staden, V. & Huismans, H. (2003). Variation in the NS3 gene and protein in South African isolates of bluetongue and equine encephalosis viruses. *J Gen Virol* **84**, 581-590.

Van Niekerk, M., Smit, C. C., Fick, W. C., van Staden, V. & Huismans, H. (2001a). Membrane association of African horsesickness virus nonstructural protein NS3 determines its cytotoxicity. *Virology* **279**, 499-508.

van Niekerk, M., van Staden, V., van Dijk, A. A. & Huismans, H. (2001b). Variation of African horsesickness virus nonstructural protein NS3 in southern Africa. *J Gen Virol* **82**, 149-158.

van Staden, V., Smit, C. C., Stoltz, M. A., Maree, F. F. & Huismans, H. (1998). Characterization of two African horse sickness virus nonstructural proteins, NS1 and NS3. *Arch Virol Suppl* **14**, 251-258.

van Staden, V., Stoltz, M. A. & Huismans, H. (1995). Expression of nonstructural protein NS3 of African horsesickness virus (AHSV): evidence for a cytotoxic effect of NS3 in insect cells, and characterization of the gene products in AHSV infected Vero cells. *Arch Virol* **140**, 289.

van Staden, V., Theron, J., Greyling, B. J., Huismans, H. & Nel, L. H. (1991). A comparison of the nucleotide sequences of cognate NS2 genes of three different orbiviruses. *Virology* **185**, 500-504.

Venter, G. J., Graham, S. D. & Hamblin, C. (2000). African horse sickness epidemiology: vector competence of south african Culicoides species for virus serotypes 3, 5 and 8. *Med Vet Entomol* **14**, 245-250.

Venter, G. J., Koekemoer, J. J. & Paweska, J. T. (2006). Investigations on outbreaks of African horse sickness in the surveillance zone in South Africa. *Rev Sci Tech* **25**, 1097-1109.

Verwoerd, D. W. (1969). Purification and characterization of bluetongue virus. *Virology* **38**, 203-212.

Verwoerd, D. W., Els, H. J., De Villiers, E. M. & Huismans, H. (1972). Structure of the bluetongue virus capsid. *J Virol* **10**, 783-794.

Verwoerd, D. W. & Huismans, H. (1972). Studies on the in vitro and the in vivo transcription of the bluetongue virus genome. *Onderstepoort J Vet Res* **39**, 185-191.

Verwoerd, D. W., Huismans, H. & Erasmus, B. J. (1979). Orbiviruses. In *Comprehensive Virology*, pp. 285 - 345.: Plenum Publishing Corporation.

Verwoerd, D. W., Louw, H. & Oellermann, R. A. (1970). Characterization of bluetongue virus ribonucleic acid. *J Virol* **5**, 1-7.

Volkman, L. E., Summers, M. D. & Hsieh, C. H. (1976). Occluded and nonoccluded nuclear polyhedrosis virus grown in Trichoplusia ni: comparative neutralization comparative infectivity, and in vitro growth studies. *J Virol* **19**, 820-832.

Wirblich, C., Bhattacharya, B. & Roy, P. (2006). Nonstructural protein 3 of bluetongue virus assists virus release by recruiting ESCRT-I protein Tsg101. *J Virol* **80**, 460-473.

Wittmann, E. J., Mello, P. S. & Baylis, M. (2002). Effect of temperature on the transmission of orbiviruses by the biting midge, Culicoides sonorensis. *Med Vet Entomol* **16**, 147-156.

Wu, X., Chen, S. Y., Iwata, H., Compans, R. W. & Roy, P. (1992). Multiple glycoproteins synthesized by the smallest RNA segment (S10) of bluetongue virus. *J Virol* **66**, 7104-7112.

Yasuda, J. (2005). HIV budding and Tsg101. *Uirusu* **55**, 281-286.

Zhang, G., Gurtu, V. & Kain, S. R. (1996). An enhanced green fluorescent protein allows sensitive detection of gene transfer in mammalian cells. *Biochem Biophys Res Commun* **227**, 707-711.

Zhang, S. C., Zhang, G., Yang, L., Chisholm, J. & Sanfacon, H. (2005). Evidence that insertion of Tomato ringspot nepovirus NTB-VPg protein in endoplasmic reticulum membranes is directed by two domains: a C-terminal transmembrane helix and an N-terminal amphipathic helix. *J Virol* **79**, 11752-11765.

Zimbera, A., Nguyenb, Q. D. & Gespachb, C. (2004). Nuclear bodies and compartments: functional roles and cellular signalling in health and disease. *Cellular Signalling* **16** 1085– 1104.

APPENDIX A:
Multiple sequence alignment

Nucleotide sequence alignments of the mutant S10 gene segments constructed with each of the specific mutations enclosed in a □. In these sequence alignments, the ▪ represents similarity to the reference sequence and ▬ represents sections where there is no corresponding sequence (for example where there is a deletion). The consensus sequence and indication of percentage homology is also given.